Oxford Brookes University

PhD Thesis

The Role of Lysosomes in Radiation Induced Genomic Instability

A thesis submitted in partial fulfilment of the requirements of Oxford Brookes University for the degree of Doctor of Philosophy

Author:
Scott James Bright

Supervisor:
Prof. Munira Kadhim

October 2013

acknowledgements

Initially I would like to extend my deepest gratitude to the genomic instability research group. In particular Kim Chapman and Deborah Bowler who have been the most supportive group members anyone could ask for, as well as Dr. Ammar Al-Mayah who's comedy and optimism kept me going. I am thankful to Dr. Sue Vaughan for her input. I would also like to thank Dr. Sarah Irons who has played an instrumental hand in making me a scientist. Finally I would like to express my sincerest thanks to my supervisor, Prof. Munira Kadhim, who has expertly guided me through this PhD, without her knowledge and support this would not have been possible. Failure was never an option!

The team at the Radiation Oncology and Biology unit within Oxford University, past and present, in particular Dr. Mark Hill, Dr Jamie Thompson and Luke Bird. Thank you for your help in experiments both practical and guidance for the future.

A huge thank you has to be extended to my friends for keeping me going and realising there is a life outside a PhD, in no particular order Neil Hargreaves for de-stressing running sessions Morgan Rogers for his tough love and top bloke status, Simon Gamble for his floor and what will be an amazing holiday, Richard "Monty" Fox for his helpful suggestions in every aspect of life, and Jamie Mallet for liking my leather jacket. Team Europe also deserve credit for an inspiring summer in New York in particular Dr. Tina Koch, you beat me. I would also like to thank Charlotte Evans who for the vast majority of my PhD showed nothing but support and optimism for the future.

Finally without my family,in particular Mum, Dad and James, I would never have reached this stage, there unwavering support in a number of ways is undeniably the reason for any success I may achieve. This thesis is dedicated to you!

THANK YOU!

Published Work and Presentations

Presentations

2010: Presentation to the Association for Radiation Research; Identifying molecular signalling communication between irradiated cells and their microenvironment

2011: Presentation to the International Congress of Radiation Research; The role of lysosomes in radiation induced genomic instability.

2012: Presentation to the 5th international Systems Biology Workshop; Radiation induced sub-cellular alterations and potential for non-targeted effects

Published Work

2014: "A potential mechanism for Reactive Oxygen species in lysosomal permeabilization following X-irradiation" Manuscript in preparation

2014: "Exosome involvement in radiation induced non-targeted effects: Exosome characterisation" Manuscript in preparation

Abbreviations

Abbreviation	Description
A-Smase	Acid Sphingomylinase
AO	Acridine orange
A.U.	Arbitrary units
BE	Radiation induced-bystander effects
BSA	Bovine serum albumin
CIN	Chromosomal instability
°C	degrees Celsius
CHO	Chinese hamster ovary (cells)
CM-H2DCFDA	5-(and-6)-chloromethyl-2',7'-dichlorodihydrofluorescein diacetate
(k)Da	(kilo) Dalton
dH2O	Distilled water
DMSO	Dimethyl Sulfoxide
DNA	Deoxyribonucleic Acid
DSB	DNA double strand breaks
Mt DNA	mitochondrial DNA
EDTA	Ethylenediaminetetraacetic acid
EGTA	Ethylene glycol tetraacetic acid

Abbreviation	Description
ER	Endoplasmic reticulum
FITC	Fluorescein isothiocyanate
FCS	Foetal calf serum
GJIC	Gap junction inter-cellular communication
GI	Radiation induced-genomic instability
Gy	Gray
HBSS	Hank's balanced salt solution
HR	Homologous recombination
HSP	Heat shock protein
Hr	Hour
ICRP	International Commission on Radiological Protection
IL	Interleukin
IR	Ionizing Radiation
KCl	Potassium chloride
LAMP	Lysosome associated membrane protein
LAPF	Lysosome-associated and apoptosis-inducing protein containing PH and FYVE domains
LET	Linear Energy Transfer

Abbreviation	Description
M	Molar
M6P	Mannose-6-phoshate
MPR	Mannose-6-phoshate receptor
MEM	Minimum Essential Medium
mg	Milligram
miRNA	MicroRNA
ml	Millilitre
mm	Millimetre
mM	Millimolar
MW	Molecular weight
mRNA	messenger RNA
µg	Microgram
µl	Microlitre
µm	Micrometer
ng	Nanogram
NaCl	Sodium chloride
NHEJ	Non-homologous end joining

Abbreviation	Description
nm	Nanometre
NO	Nitric oxide
NTE	non-targeted effects
OH	Hydroxyl group
p	p-value
PBS	Phosphate Buffered Saline
PD	Population doubling
RNA	Ribonucleic acid
rpm	Revolutions per minute
ROI	Region of interest
ROS	Reactive oxygen species
SCE	sister chromatid exchanges
SEM	Standard error of mean
TGF-beta	Transforming growth factor-beta
TNF-alpha	Tumour necrosis factor-alpha
UV	Ultra violet

Abstract

Our understanding of ionizing radiation and its associated biological effects has recently undergone a paradigm shift from a DNA-centric model to one inclusive of non-targeted effects (NTE), so called for the lack of direct radiation interaction with DNA. Two effects encompassed within the NTE paradigm are termed genomic instability (GI) and bystander effects (BE). GI can be described as an increase in rate of genetic alterations many cell generations after the initial radiation exposure. BE can be defined as the manifestation of radiation like effects in un-irradiated cells that have communicated with cells that have been irradiated either through inter-signalling utilising gap junctions or the secretion of a soluble diffusion signalling factor.

The exact mechanisms that underlie these processes are still under investigation but a wealth of evidence suggests that a number of mechanisms are involved. These include; cytokine signalling, oxidative stress, inflammation and sub-cellular alterations, in addition to factors such as genetic background and radiation quality/dose.

This study was designed to investigate lysosomal involvement in radiation induced NTE, whether it be downstream of one of the above mentioned mechanisms, or independent of their involvement. To this end the primary human fibroblast cell line, HF19, was exposed to X-rays at therapeutic and diagnostic doses of 2 and 0.1 Gy respectively. Bystander groups were also established by media transfer techniques. Cells were analysed over the first 24 hours and then at 1 and 20 population doublings, initially for detection of GI and BE and thus confirm the suitability of the system. The lysosomes were then analysed for permeability and their distribution within the cell. Oxidative stress was also measured in a bid to correlate this event with lysosomal perturbations. Finally lysosomal contents, in particular DNaseIIα, were analysed for their cellular location along with analysis of nuclear membrane permeability which we surmised would facilitate the redistribution of lysosomal enzymes.

The results demonstrated that HF19 cells were susceptible to the induction of GI and BE. The latter was noted within the first hour following irradiation in both 0.1 and 2 Gy bystander groups. High levels of chromosomal instability were also induced in both 0.1 and 2 Gy directly irradiated groups, 1 population doubling after exposure. Chromosomal instability was still noted

at 20 population doublings mainly in the 2 Gy although the 0.1 Gy group did show elevated levels. A similar pattern was observed in the bystander group. However we were unable to detect sustained production of the bystander signal at 20 population doublings.

Lysosomal properties were also characterised and measured at corresponding time points; large alterations were observed in the first 24 hours following irradiation, furthermore, the lysosomes appeared more permeable at 20 population doublings especially in bystander groups, however, these changes did not correlate with increases in oxidative stress. As a result we further examined cells for changes in the distribution of lysosomal enzymes, in particular DNaseIIα, however no significant changes were observed. Nuclear permeability was additionally investigated as to whether increased permeability facilitated enzyme redistribution; however permeability appeared reduced rather than increased.

In summary, our investigations have demonstrated and confirmed that HF19 cells are susceptible to the induction of GI and BE following low LET X-ray exposure. The results suggest that the mechanism of radiation induced GI and BE responses can be correlated with alterations in lysosomal membrane permeability which appears independent of oxidative stress. We also demonstrated that if lysosomes are involved in NTE it is unlikely to be through direct action of DNaseIIα but rather from enzymes such as acid sphingomylinase. To conclude, radiation was able to alter lysosomes and nuclear permeability at delayed time points which was correlated with GI , however it appears DNaseIIα is not involved. It also appears that an early effect of the bystander signal may have antioxidant property.

Contents

List of Figures

Chapter 1

Introduction

1.1 Ionizing Radiation

Ionizing radiation (IR) is a continual presence in our environment, natural background sources add to man made radiation from sources such as medical diagnostics and treatment (Hall and Giaccia, 2006). The defining characteristic of ionizing radiation is its ability to ionize molecules, by depositing large amounts of energy in a localized area. The energy dissipated per IR event is about 33 eV (electron volts) (Hall and Giaccia, 2006), which is enough to disturb chemical structures important in biology, such as covalent bonds. Ionizing radiation can be broadly subdivided into electromagnetic radiation and particulate radiation (Hall and Giaccia, 2006) based on their linear energy transfer (LET) properties. Electromagnetic radiations consist of X- and γ-rays, and are usually classed as low LET radiation sources. They share very similar physical and chemical properties and activities, the division is primarily dictated by wavelength and their mode of production.

Particulate radiations involve particles moving with enough energy to be ionizing, these are usually classed as high LET (Hall and Giaccia, 2006). They include electrons, protons, neutrons and α-particles. Structurally, α-particles are helium nuclei consisting of two protons and two neutrons and have a net positive charge. The decay of radon gas results in the emission of α-particles and is the major source of background radiation in the environment. Estimations

suggest 10,000 to 20,000 cases of lung cancer in the United States per annum are in part caused by the inhalation of decaying radon (Hall and Giaccia, 2006).

A number of units exist to quantify radiation, the Gray (Gy) quantifies the absorbed dose *i.e.* the energy deposited per unit mass (1 Gy = 1 Joule/Kg). As described earlier however, different radiation qualities have different LET's and therefore will be more or less sparsely ionizing. To account for this the effective dose can be calculated, measured in Sievert (Sv). One Gy is equal to 1 Sv for low LET sparsely ionizing radiation such as X-rays. A weighting factor is applied for densely ionizing radiations such as α-particles, in this case 20 (therefore 1 Gy = 20 Sv) (Wakeford, 2004).

The action of radiation at a biological level can be either direct or indirect, this is partly related to the LET of the radiation dose in question. Direct action is associated mostly with high LET radiation such as α-particles. In this instance the radiation source interacts directly with a sensitive target, such as DNA (Baverstock and Belyakov, 2010). Alternatively radiation may act indirectly, this method of action is mostly associated with low LET electromagnetic radiation. In mechanistic terms, radiation interacts with other atoms in the cell in particular, water, which induces cellular damage mediated by reaction products such as secondary electrons or reactive oxygen species (ROS), a type of free radical.

Free radicals are atoms carrying an unpaired orbital electron in their outer shell, as a result the spin states within the atom are not balanced and the chemical species are highly reactive. Certain radicals such as the hydroxyl radical are common after IR, radicals such as this can diffuse small distances within the cell allowing them to damage a range of cell components. Estimates suggest that two thirds of X-ray damage is caused through an indirect action and the hydroxyl radical (Hall and Giaccia, 2006).

1.2 Biological Effects of Ionizing Radiation

Ionizing radiation is effective at inducing biological effects, primarily because of the non-random nature of energy deposition *i.e.* energy is deposited in tracks. Low LET radiation is able to retain its energy more effectively than high LET because it interacts with far fewer atoms,

however it is able to produce secondary electrons which have a short diffusion distance of nanometres and produce dense clusters of ionization. High LET deposits its energy much more readily and is therefore more densely ionizing. However both are relatively clustered on the scale of DNA, it is this clustering of aberrations that result in complex DNA damage and efficiency in producing biological effects.

The process of inducing a biological effect can be viewed as the summation of 3 stages. Initially physical processes occur whereby the radiation interacts with molecules and atoms either exciting or ionizing them, the latter being of greatest importance with regard to biological effects. There are three main mechanisms in which this occurs or how X-rays can be absorbed and transfer its energy, namely Compton scattering, the photoelectric effect and pair production (Hall and Giaccia, 2006). Which one occurs depends on the energy of the incident photon. Compton scattering is the most prevalent at X-ray doses associated with radiotherapy (Hall and Giaccia, 2006). In this case the incident photon deposits a proportion of its energy in a planetary electron of the atom. The resulting effect is the production of a fast electron, which itself might travel to cause further ionization events (Hall and Giaccia, 2006); the incident photon continues with reduced energy. The photoelectric effect is more predominant at low dose diagnostic radiology (Hall and Giaccia, 2006). In this instance the photon donates its entire energy to a tightly bound electron. The resulting effect is the ejection of the electron from the atom, which in many cases will react with nearby atoms (Hall and Giaccia, 2006). The vacant position is filled by an outer shell electron of an electron external to the atom. The change in energy levels usually results in the emission of a photon of X-ray characteristic. Pair production is most applicable to very high energy photons (Hall and Giaccia, 2006). These photons interact with atomic nuclei with the production an electron and accompanying positron. Again the electron is likely to cause further ionization events while the positron is annihilated (Hall and Giaccia, 2006).

As a result and subsequent to the interaction of radiation with matter, chemical processes take place, where reactive species generated from ionization events react with neighbouring chemicals. These chemical reactions lead to biological alterations; the cell responds to this and thus a biological response is induced; these effects may be present for seconds, or the lifespan of the organism.

1.2.1 Types of Effects

Cytoplasmic Effects

Ionizing radiation is capable of affecting the whole cell, including cytoplasmic structures. One major method of action is through the production of ROS, and their subsequent interaction with nearby structures and proteins. Proteins that react with certain species are able to alter signal transduction pathways, in particular nitrosylation of Ras (Valerie et al., 2007b) and oxidation of Tyr-phosphatase (Hutchison, 1985) can enhance the ERK1/2 pathway.

Mitochondria can also be affected by ionizing radiation, due to their relatively large proportion of cell volume. Additionally their role in respiration makes them the major ROS producer in the cell. Alterations in redox reactions as a result of perturbed mitochondria leads to a disturbed redox environment. Electrons are leaked from the electron transport chain as a result of their normal operation; this leads to the production of superoxide ($O_2^{\cdot}$); although potentially dangerous to the cell, it is important in signal transduction. However radiation causes an excess leakage, and consequently an excess of $O_2^{\cdot}$. The cell is unable to buffer excessive production of ROS, and they therefore are able to react with cell components. As they are produced by the mitochondria, they may react with mitochondrial (mt) DNA creating mutations and aberrant mitochondria unable to fulfil their role. One common and stable deletion has been characterized by Prithivirajsingh et al. (2004) and Chen et al. (2011), in this instance a large portion of mtDNA is lost, that codes for subunits of the ATPase and other enzymes, resulting in reduced mitochondrial function and further ROS production.

Radiation is also able to alter lipid membranes such as the plasma membrane. Lipid peroxides can be formed as a result of IR exposure, usually affecting polyunsaturated fats (PUFA) the resulting effect is a chain reaction usually damaging numerous lipids until the chain is stopped by another radical. The resulting effect creates a less fluid membrane with increased permeability to small ions and reduced functionality of transport pumps (Lehnert, 2008), this fundamentally reduces the cells ability to maintain homeostasis. There is also evidence to suggest that the plasma membrane is involved in signalling following irradiation, causing genetic changes (Nagasawa et al., 2002) and apoptotic signalling through sphingomylin pathways (Pena et al., 2000;

Paris et al., 2001).

Nuclear/DNA Damage

Ionizing radiation has a detrimental effect on DNA (Hall and Giaccia, 2006; Iliakis et al., 2003), resulting in numerous types of chromosomal aberrations. Simple damage such as single strand breaks (SSB) and damage to individual bases are amongst the most abundant following radiation. The occurrence of injury maybe through a direct ionization event where the radiation track physically interacts with the individual DNA base. Alternatively other molecules within the cell such as water are ionized and the products of such events then react with DNA to cause an aberration (Hall and Giaccia, 2006). In fact the majority of cellular DNA damage is caused by this indirect mechanism (Hall and Giaccia, 2006; Alberts et al., 2008).

Of more importance to the cell is the double strand break (DSB) (Han et al., 2010), due to the ability of radiation to deposit large amounts of energy in confined spaces that leads to clustered DNA damage and the appearance of DSB (Hall and Giaccia, 2006). The clustered damage may consist of multiple DSB with base damage and SSB which all occur within the vicinity of the DSB (Frankenberg-Schwager et al., 2008). Due to the complexity of some lesions, they are unrepairable and as a consequence are lethal.

In other situations proteins can sometimes be cross linked with DNA; events such as this will structurally affect DNA processing at the level of replication, transcription and repair (Lehnert, 2008).

1.2.2 Repair Pathways

Cells receive numerous insults every day that lead to DNA damage; in order to deal with such events the cell has a number of repair pathways. A number of these pathways are implicated in the repair of radiation induced DNA damage. For sites of base damage and SSB the primary pathway is base excision repair (BER); for more complex lesions such as DSB the cell employs homologous recombination (HR) and non-homologous end joining (NHEJ) (Goodarzi and Jeggo, 2013; Tapio and Jacob, 2007; Dianov and Parsons, 2006).

Base Excision Repair

When radiation affects individual bases, the primary repair pathway used by the cell is base excision repair (BER) (Chaudhry, 2007). Following damage recognition, DNA glycosylases, each of which recognize specific base alterations, cleave the bond that links the base to the sugar phosphate backbone of the DNA molecule, this leaves an apurinic or apyrimidinic site (Robertson et al., 2009). The sugar is subsequently removed by an enzyme called AP (apurinic or apyrimidinic) endonuclease, this is then followed by the addition of a new base by a DNA polymerase which goes on to replace a section of DNA on the damaged strand. The final nick on the strand is then sealed by the action of DNA ligase completing the repair process (Robertson et al., 2009; Alberts et al., 2008; Chaudhry, 2007).

Homologous Recombination

Homologous recombination (HR) is the predominant repair mechanism of double strand breaks in S phase and G2. It relies on the ability of the damaged chromatid to interact with the undamaged chromatid (Sallmyr et al., 2008; Goodarzi and Jeggo, 2013). Initially endonucleases cleave one strand of the broken DNA in the 5' to 3' direction. The resulting single strand regions invades the homologous region of the sister chromatid which has been unwound to facilitate the strand invasion, with subsequent formation of the D-loop (Alberts et al., 2008; Murray et al., 2012). Once matched up a DNA polymerase elongates the single stranded DNA using the sister chromatid as a template. The strands then disengage and a ligase enzyme reattaches them to make a complete chromatid, finally the double helix is restored. Important proteins in the process include BRCA1 & 2 as well as RAD51 (Alberts et al., 2008).

Non-homologous end joining

Non-homologous end joining (NHEJ) largely occurs in G1 phase of the cell cycle, when sister chromatids are inaccessible to each other (Pastwa and Blasiak, 2003). Once the break is detected the protein ATM phosphorylates the histone H2AX which is followed by the binding of the Ku heterodimer (Ku70/Ku80) to each end of the DSB (Frankenberg-Schwager et al., 2008; Mahaney

et al., 2009; Pastwa and Blasiak, 2003; Pastwa and Malinowski, 2007). The Ku heterodimer acts as an anchoring site for DNA-PKcs. Once these have bound they form a bridge like structure across the break. The protein complex is then phosphorylated which recruits DNA ligase IV and XRCC4. The ends are subsequently ligated together and the protein complex is disassembled (Frankenberg-Schwager et al., 2008; Mahaney et al., 2009; Pastwa and Blasiak, 2003; Pastwa and Malinowski, 2007).

1.2.3 Cell Death

If the cell sustains an overwhelming level of damage it may simply die or stop dividing. There are a number of ways in which this occurs.

Apoptosis & Necrosis

There are many pathways and protein interactions that lead to apoptosis involving numerous stages and various regulators, however, all result in the organised dismantling of the cell to remove it from the system.

Apoptosis is perhaps the most characterised form of cell death, it has been extensively researched in relation to natural processes and as a response to certain stimuli such as IR (Belyakov et al., 1999; Elmore, 2007; Furlong et al., 2013). Apoptosis can be triggered through two main pathways either extrinsically (through death receptor signalling) or intrinsically (orchestrated through mitochondria) (Elmore, 2007) (Figure 1.1). Both routes share the concluding stages of the process converging on the cleavage of procaspase-3, with ensuing DNA fragmentation and other apoptotic related phenotypes; any remaining debris is cleared by the host immune system as a result of secreted signals (Antunes et al., 2001; Elmore, 2007).

In certain situations where the cell has received extensive damage, it simply dies following no organised process (Lindholm et al., 2010), this is termed necrosis. This can be detrimental and induce inflammation (Alberts et al., 2008), whereas apoptosis can be beneficial, in that it prevents the cell continuing with the possibility of mutation and transformation (Elmore, 2007). Necrosis can be identified through morphological changes such as oncosis (a gain in cell volume).

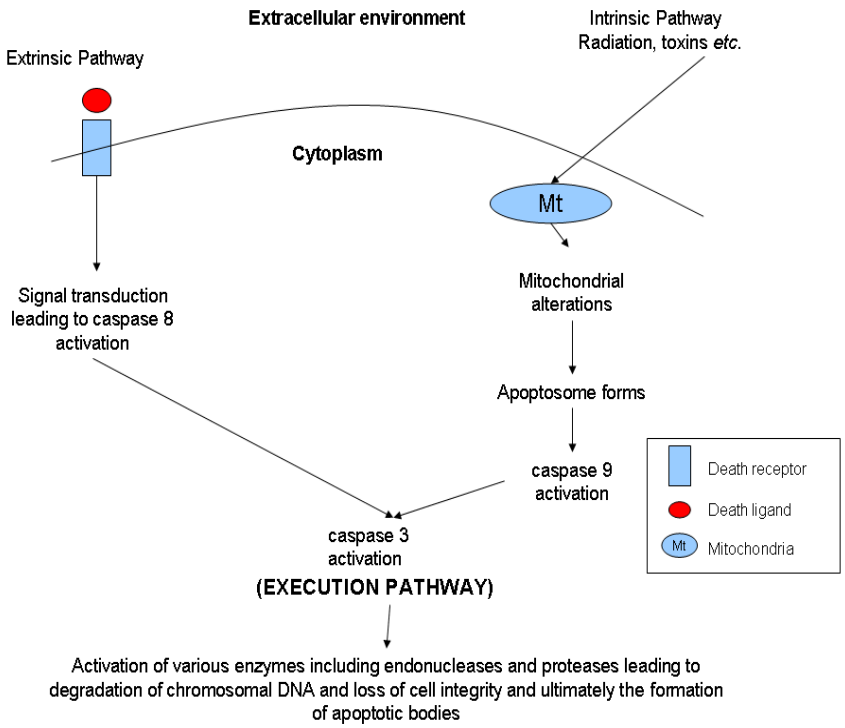

Figure 1.1: **Routes of apoptosis.** Although a gross simplification of the process, the two main routes originate either externally or internally but ultimately end in the activation of execution caspases. The cell is dismantled from within leaving apoptotic bodies, membrane bound fragments containing various parts of the cell.

Other alterations occur such as swelling of organelles. It was originally thought this process had no orchestrated process (Kroemer et al., 2009). However recent research has shown death domain receptors for instance TNFR1, can in fact induce necrosis particularly in the absence of caspase inhibitors (Kroemer et al., 2009). This newly discovered orchestrated necrosis has been termed by some researchers as necroptosis. The mediators of necrosis involve mitochondrial changes including mitochondrial membrane permeabilization. Alterations in nuclear membrane structure and cyctosolic calcium concentration (Kroemer et al., 2009). Lipid degradation is also common, this is linked to lipases such as sphingomylinase which has strong links to the lysosome, a sub-cellular organelle.(Kroemer et al., 2009)

Autophagic Cell Death

Autophagy is a process of self-digestion where the cell targets certain components for degradation and then recycles them for other needs (Shen and Codogno, 2011; Levine and Yuan, 2005),

because of this it is important in homeostasis of the cell. The process of autophagy can be further subdivided, however the general principles remain the same. The components targeted for destruction are sequestered into vesicles, and the contents are ultimately broken down by lysosomal enzymes (Oczypok et al., 2013; Shen and Codogno, 2011; Eskelinen and Saftig, 2009).

Autophagic cell death involves the early degradation of organelles and preservation of the cytoskeleton until later stages. This is morphologically distinct when compared to apoptosis which occurs in the opposite order (Czaja, 2011; Shen and Codogno, 2011). There still seems to be active debate as to whether the increased autophagy markers indicate cell death with autophagy or cell death because of autophagy (Shen and Codogno, 2011; Levine and Yuan, 2005). There is genetic evidence indicating a reduction in cell death with RNAi methods targeting certain autophagy genes such as Atg5, Atg 7 and beclin 1 (Yu et al., 2004; Shimizu et al., 2004), however these studies involved cells lacking the ability to undergo apoptosis. Other explanations put forward for the increased level of autophagic markers by Levine and Yuan (2005) include autophagy as a mechanism of cell survival in stressful situations providing essential material for cell survival, alternatively it is suggested that autophagy maybe performing a self-clearance mechanism, whereby the cell digests itself instead of leaving it for phagocytic cells (Levine and Yuan, 2005).

Senescence

Cellular senescence is in an irreversible arrest to the cell cycle (Hall and Giaccia, 2006). Although not actually dead the senescent cell is no longer able to divide and therefore pass on genetic alterations that it may have acquired. The process is thought to heavily rely on p53 and rentinoblastoma proteins (Hall and Giaccia, 2006). Although senescent, these cells still contribute to the micro-environment by secretion of growth factors and other signalling molecules (Hall and Giaccia, 2006).

Mitotic Cell Death/Mitotic Catastrophe

The most common type of cell death following irradiation is mitotic cell death or mitotic catastrophe (Hall and Giaccia, 2006). As the cell progresses into mitosis cells die as a result of damaged chromosomes and aberrant mitosis. There is still much debate as to the actual mechanisms and outcomes of the process. In fact Kimura et al. (2013) states that mitotic catastrophe is more of a precursor to processes mentioned before such as apoptosis and necrosis. Some characteristics that are associated with mitotic cell death include multiple nuclei in massive cells, containing uncondensed chromosomes and mitosis restitution (Hall and Giaccia, 2006; Kroemer et al., 2009). Cells undergo mitotic cell death following premature entry into mitosis. Some molecular mechanisms have been identified including an increased level of nuclear cyclin B1 (Castedo et al., 2004a). An intact DNA damage checkpoint is essential for avoiding mitotic catastrophe. Proteins such as RAD 1 help identify DNA adducts a series of enzymatic reactions results in signal transduction to Chk2 which halts the cell cycle and mitotic catastrophe, in fact the inhibition of Chk2 has been found to facilitate mitotic catastrophe (Castedo et al., 2004b).

1.2.4 Targeted Effects of IR

Radiation can act in a targeted manner *i.e.* its effects are caused by the radiation interacting with specific targets within the cell; this is referred to as the target theory. The primary target is usually nuclear DNA (Savage, 1993; Ottolenghi et al., 1999; Morgan, 2003). Evidence for nuclear DNA as a target comes from a number of studies summarized by Hall and Giaccia (2006) looking at the incorporation of radioactive thymidine. The radiation source comes from short range α-particles resulting in a localized dose to the nucleus and DNA held within. Other experiments looking at modification of cell lethality through alterations in radiation type, oxygen concentration and dose rate appear to correlate with chromosomal aberrations, implicating damaged chromosomes in the process (Meijer et al., 1999; Chapman et al., 2008).

The cell has limited options following irradiation. It can enter into programmed cell death or necrosis or attempt to repair any damage. Should the repair process fail in some way leading to a mis-repaired aberration, that aberration is fixed and inherited by the progeny of

the irradiated cell (Mahaney et al., 2009; Morgan, 2003). In this instance cytogenetic analysis should reveal homogeneous damage *i.e.* the damage present is transmitted to all the progeny and is therefore clonal. This is observed in leukaemia development following radiotherapy where a clonal reciprocal translocation between chromosome 4 and 11 leads to acute myeloid leukaemia (Inoue et al., 1985).

The most frequent types of direct damage include: base alterations, DNA-DNA or DNA-protein cross links, DNA single strand breaks (SSB) and double strand breaks (DSB) (Hall and Giaccia, 2006; Chang, 2006). Probably the most important event is the induction of DSB, either by direct or indirect action of IR; this can lead to the appearance of chromosomal and chromatid aberrations (Vasireddy et al., 2010; Bryant et al., 2010; Bryant, 1984; Frankenberg-Schwager et al., 2008). The aberrations induced can be classified into stable aberrations such as reciprocal translocations, which are usually non-lethal, and unstable aberrations such as the formation of dicentric chromosomes which usually result in cell death (Hall and Giaccia, 2006).

The target theory describes very well the above types of damage and how they are induced, but is inconsistent with work conducted in the last two decades that describes radiation-like effects in un-irradiated cells, referred to as the bystander effect (BE) (Morgan, 2003). In radiation biology BE has come to be defined as the manifestation of radiation-like effects in cells that have not been directly irradiated but have been able to communicate with those that have (Morgan and Sowa, 2009; Morgan, 2003). Delayed non-clonal aberrations termed genomic instability (GI), have also been observed; this can be defined as the presence of a range of potentially detrimental effects observed in the progeny of an irradiated cell, arising many cell divisions after the initial insult (Morgan et al., 1996; Kadhim et al., 1992).

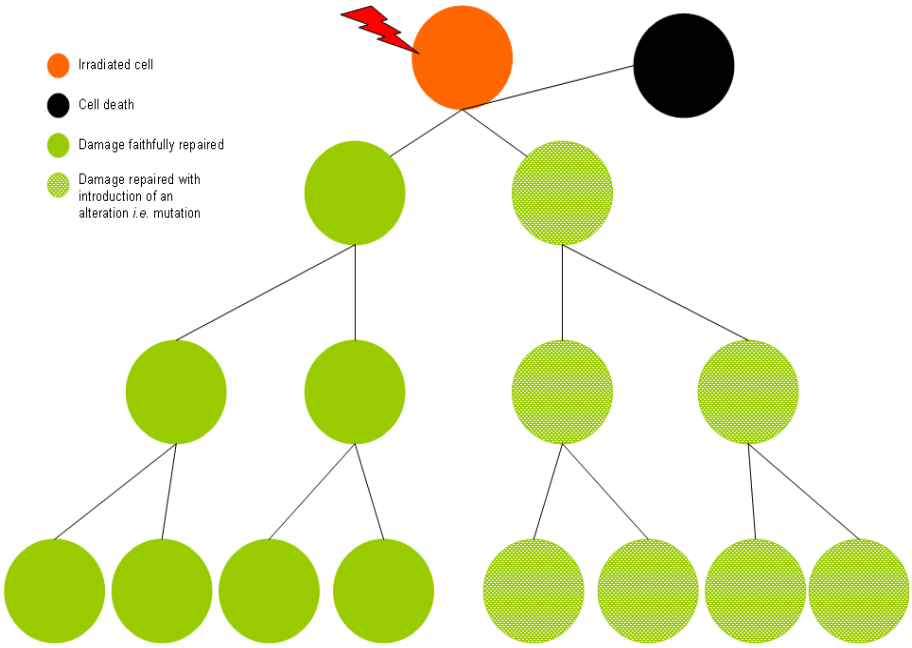

Figure 1.2: **The classical paradigm of radiation biology:** A parent cell (orange) is irradiated, mutations are acquired and passed onto the progeny (hashed green), damage could be repaired (green), or cells enter apoptosis/necrosis or any other form of cell death (black and red) due to overwhelming damage.

1.3 Non-Targeted Effects

1.3.1 Bystander Effects

Bystander effects (BE), as described above occur in cells that have no history of encountering any form of damaging agent (Figure 1.3), this is a significant finding and has implications directly relating to human exposure. Rzeszowska-Wolny et al. (2009); Preston (2004); Prise et al. (2003); Nagasawa and Little (1992) were some of the first to report BE; sister chromatid exchanges (SCE) were noted in 30% of a Chinese hamster ovary (CHO) cell population although only 1% came into contact with IR. The gross chromosomal aberrations observed were thought to be induced by ROS. Due to the nature of the aberrations Nagasawa and Little (1992) observed they concluded that a recombinational process was occurring. Further validation of the BE came from a study using a charged particle microbeam where a defined number of cells were irradiated with a lethal dose of 20 α-particles per cell (Zhou et al., 2000). This was similar to work by conducted by Deshpande et al. (1996) who demonstrated excessive sister chromatid formation compared to expected levels, although no mechanism is postulated other than an extra-nuclear one. The exclusive analysis of bystander cells showed a 3 to 4 fold increase in mutations. Since then BE have been demonstrated in different cell lines with different biological endpoints such as chromosomal aberrations, mutagenesis, micronucleus formation, sister chromatid exchanges (SCE) and cell death, reviewed by Morgan (2003).

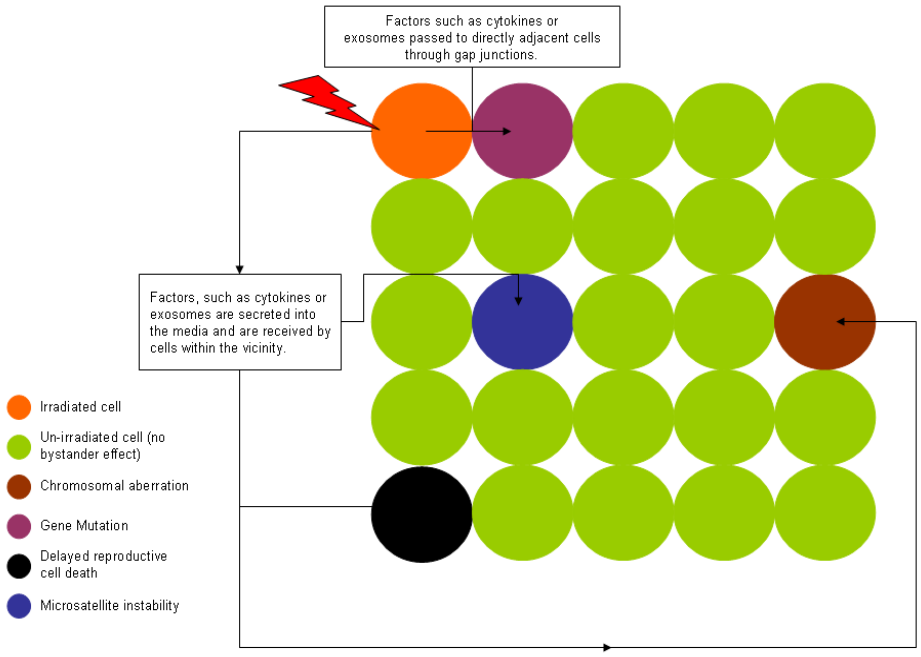

Figure 1.3: **Schematic of bystander effect:** Damaged cells appear adjacent to and spatially removed from the insulted cell. A signal can be passed through gap junctions that directly link adjacent cells. Alternatively a signal maybe secreted into the extracellular environment to be endocytosed by a cell at a distant site.

One of the most notable properties of the BE is the deviation from linearity. Much of the work has demonstrated that the phenomenon is induced maximally at low doses (Prise et al., 2003). Exposure to low dose high LET radiation (α-particles) was able to induce BE (Hickman et al., 1994) and this was further supported by work from Lehnert and Goodwin (1997) and Lehnert et al. (1997) who also demonstrated that low doses of α-particles induced SCEs. Low LET X-rays have also induced BE at doses between 0.01 and 0.5 Gy, where significant levels of cytotoxicity were induced predominantly as a result of the BE (Seymour and Mothersill, 2000). The BE also fails to show a dose response *i.e.* it is either induced or there is no effect (Zhou et al., 2001). In light of this, it has been suggested current risk management is ineffective at managing these relatively newly documented effects, and our current perception of risk to radiation exposure is not accurate (Shore, 2009). It is important to emphasize that BE are not induced in every situation and is very much dependant on the cell type communicating and receiving the signal as well as other factors, as reported by Sowa et al. (2010) who observed

no DNA damage and no reduction in clonogenic survival in human skin fibroblasts and human colon carcinoma cells after exposure to high and low LET bystander media.

Mechanisms of the Bystander Effect

The evidence above demonstrates that the target theory of radiation biology is not all encompassing, with respect to the fact that direct DNA damage is not essential for the induction of typical radiation damage (Baverstock and Belyakov, 2010). Various experimental designs involving differing communication environments have led to the postulation of two mechanisms of radiation induced BE. Firstly, research using the Columbia charged particle microbeam and grid shielding experiments (grids used to shield part of a cell population, while the remainder is exposed) suggested that cell concentration and therefore cell to cell contact through gap junction intercellular communication (GJIC) is important (Lorimore et al., 1998; Wu et al., 1999; Smilenov et al., 2006). Secondly, media transfer experiments (involving the transfer of media from irradiated cells to a bystander population) and co-culture experiments (irradiated cells are cultured with bystander cells without physical contact) induced a wide range of cellular aberrations, through a media soluble factor (Mothersill and Seymour, 1997; Lyng et al., 2000; Bowler et al., 2006).

Gap Junction Intercellular Communication (GJIC)

Gap junctions form communication networks with neighbouring cells. They are formed from connexin proteins that form channels to make a link between two cells (Telford and Bridgman, 1995). These channels allow the passage of molecules such as cyclic adenosine monophosphate (cAMP), that potentially have the ability to alter metabolic and signalling events in the cell (Ballarini et al., 2006). In order to examine their role in BE, chemicals such as lindane and octanol were used as general inhibitors of GJIC (Autsavapromporn et al., 2013; Azzam et al., 1998; Persaud et al., 2005; Zhou et al., 2000). It was found that these inhibitors greatly reduced the bystander effect in a number of ways including down regulation of p53, mutant yield and apoptosis (Autsavapromporn et al., 2013; Azzam et al., 1998; Persaud et al., 2005; Zhou et al., 2000). Further justification of the role of GJIC comes from genetically altered cell lines

which effectively remove any communication between cells via gap junctions. Using this model Zhou et al. (2001) demonstrated that AL cells (dominant negative for connexin 43) showed no mutagenic BE.

Soluble diffusion factors

As mentioned above BE can be induced through a media soluble factor. Medium transfer experiments with a variety of end-points, have shown, that irradiated cells secrete a factor, or factors, that are capable of inducing BE (Han et al., 2007; Sokolov et al., 2005; Smilenov et al., 2006; Persaud et al., 2005; Azzam et al., 2004). Although the majority of these factors are still unidentified, the cellular responses have been well documented. In studies by Lyng et al. (2000), γ-rays induced a calcium pulse in un-irradiated cells 1-2 minutes after incubation with medium from irradiated cells. This was followed by changes in mitochondrial membrane permeability 30 to 120 minutes later, and subsequently accompanied the induction of ROS. The addition of an antioxidant reduced the bystander factor associated-cell killing thereby implicating redox reactions in the process.

Mothersill and Seymour (1997), provided more detail on BE, through medium transfer experiments following γ-ray exposure. They found that epithelial cells are able to secrete a cytotoxic factor into the medium that could kill un-irradiated cells, but no such effect was seen in fibroblasts and as a result the effect was said to be dependent on cell type. Their results have also demonstrated that medium irradiated in the absence of cells, showed no such effect. They found the bystander response was independent of dose between 0.5 to 5 Gy, but that the effect was proportional to the amount of cells irradiated, *i.e.* the greater the number of cells, the greater secretion of bystander factor(s) and ultimately an increased number of damaged cells.

In addition to the BE being induced by a secreted soluble factor, Nagar et al. (2003a,b) have demonstrated that a secreted factor is able to induce a response termed death inducing effect. The GM10115 cell line (mouse cells plus human chromosome 4) was cultured in medium from stable and unstable clones of the above cell line. After incubation with the medium from various clones it was noted that incubation for 24 or 48 hours was able to induce complete cytotoxicity. It is possible that this effect shares some kind of overlap with BE.

Types of Bystander Signal

The modalities of signal transduction are discussed above, yet there is no confirmed mechanism that applies to all circumstances (Sowa et al., 2010). Various processes and targets have been identified, of which one is the induction of cyclooxygenase-2 (COX-2) (Hei, 2006). It is up-regulated more than 3 fold in normal human lung fibroblast bystander populations (Zhou et al., 2005) and as a result is thought to be involved in bystander responses. COX-2 is an enzyme which functions to produce prostaglandins, which act in the inflammatory response (Laufer et al., 2003). Inflammatory responses in general have links to BE and GI (Lorimore and Wright, 2003). In studies by Zhou et al. (2001), when an inhibitor of COX-2 was introduced, the bystander mutational effect was greatly reduced although it still remained slightly above control levels. In the same study, insulin growth factor binding protein-3 (IGFBP3) was consistently reduced by about 7 fold. Such a reduction leads to greater binding of insulin to cell surface receptors. Consequently signalling events such as the mitogen-activated protein kinase (MAPK) and extracellular signal related kinase (ERK) are initiated; activation of the latter is an important event prior to COX-2 expression. Again inhibition of ERK reduced the BE therefore suggesting it has a role in the signalling process.

Cytokines have also been shown in some cases to have mechanistic links to BE induction (Temme and Bauer, 2013; Schaue et al., 2012; Dickey et al., 2009; Han et al., 2010). Cytokines are heavily involved in immunity and inflammation and exert their function locally and systemically, binding to cell surface receptors triggering internal signal cascades that can alter gene expression and other metabolic processes (Alberts et al., 2008). An important characteristic in their action that links to experimental observations is their pleiotropy or ability to exert different effects on different cells (Ozaki and Leonard, 2002).

The cytokine TGF-β1 is important in the induction of cell proliferation (Han et al., 2010), its up-regulation after irradiation stimulated cell division in bystander cells and subsequently increased the number of DSBs as individual cells lacked the time to repair aberrations correctly. This study has built on past work all pointing towards cytokine signalling having a role in BE. Media transfer experiments demonstrated results similar to the above showing that the presence of TGF-β1 and nitrogen oxide (NO) elevated γH2AX foci, and that when these signals

were inactivated the effect was negated (Dickey et al., 2009). Other cytokines implicated in BE include IL6, IL8, MCP-1 and RANTES (Dieriks et al., 2010), which were all identified at increased levels in the growth medium of irradiated cells after exposure to X-rays (2 Gy). Zhou et al. (2008) showed a role for TNF-α and IL-1β both of which are involved in COX-2 expression in normal human fibroblasts via NFκB. Inhibition of TNF-α, IL-1β and NF-κB have all been linked to a reduction in COX-2 and nitric oxide synthase (iNOS) and simultaneously a reduction in BE. These results support a hypothesis that in certain cases, part of the damage in bystander cells is a consequence of cytokine signalling.

As well as cytokine signalling, oxidative stress via reactive oxygen species (ROS) and nitrogen oxides (NO) are all implicated in bystander responses (Law et al., 2010; Kashino et al., 2007; Shankar et al., 2006; Persaud et al., 2005; Shao et al., 2004). In the case of ROS they are very short lived therefore their production is either close to their site of action, or the production mechanism is activated for an extended period of time.

Oxidative stress, in the form of superoxide and hydrogen peroxide produced by oxidase enzymes, was shown to be able to stimulate a number, of p53 damage response pathways and micronucleus formation through GJIC signalling (Azzam et al., 2002). Further analysis of the p53 protein showed it was activated due to phosphorylation at serine 15, this provided confirmation that p53 was up-regulated in response to DNA damage. This effect was at least in part mediated by GJIC as gap junction inhibitors reduced the BE (Azzam et al., 2002).

Wu et al. (1999) supports oxidative stress as a possible mechanism for BE, observations noted a doubling in spontaneous mutation frequency with significant increases in mutations at the CD59 locus. After four cytoplasmic traversals (the traversal of one α-particle through the cytoplasm of a target cell *i.e.* no direct interaction with the nucleus), a two to three-fold increase was seen. On addition of the free radical scavenger, dimethyl sulfoxide (DMSO), the mutation frequency was reduced indicating that the mutagenicity of cytoplasmic irradiation depends upon intracellular generation of ROS.

In summary, a core component of bystander signalling involves cytokines such as TNF-α and TGF-β1. Upon binding to cell surface receptors numerous intra-cellular signalling cascades are triggered such as MAPK pathways leading to the activation of transcription factor NF-κB which

in turn increases expression of pro-inflammatory proteins such as COX-2 and iNOS, yielding the products prostaglandin and NO respectively. The ultimate products are likely to be the clastogenic factors that are involved in the initiation of the BE. Although this presents a simple picture of the process, BE expression is actually dependant on cell line, cell density, radiation type and radiation dose (Morgan, 2003). Consequently the overall bystander process is likely to involve multiple signalling pathways and events and not one simple signal molecule and cascade.

Bystander effect *in vivo*

Fundamental evidence for BE *in vivo* exists from the study of α-particle irradiation of the liver of Chinese hamsters (Brooks et al., 1983). Radioactive particles were deposited in the liver of hamsters where cells closest to the particle received the highest dose; however cytogenetic analysis demonstrated an increased frequency of aberrations but no correlation was established in relation to radiation quality, dose and frequency of damage. As a result, researchers concluded that although the whole organ was not exposed, it was all at a risk of damage. Experiments using models of human skin in an *in vivo* set-up used a charged particle microbeam to irradiate a fraction of the experimental tissue. Analysis of cells up to 1mm showed significant increases in apoptosis and micronuclei formation (Belyakov et al., 2005).

More recently Mancuso et al. (2008) showed irradiation of mouse bodies led to a high incidence of medulloblastoma in the shielded cerebellum. Gap junction intracellular communication (GJIC) was thought to have a role as its inhibition reduced the effect of tumour initiation and DSBs. Other researchers report clastogenic factors *in vivo* that are responsible for BE induction. These have been observed in humans following accidental exposure to acute doses of radiation, for example blood extracted from A-bomb survivors cultured with cell cultures demonstrated aberrations in bystander cells (Morgan, 2003; Williams, 2008).

It is also important to note clinical *in vivo* effects, which are usually referred to as abscopal effects. Abscopal effects are BE following the clinical treatment of tumours, where factors secreted from irradiated cells are observed to act at a distant site within the same subject. An example of this was recently observed in the treatment of an individual receiving radiotherapy

the treatment of Chronic Lymphocytic Leukaemia (CLL). Irradiation of diseased tissue in the axilla resulted in tumour regression at a distant site although the factor wasn't identified (Lakshmanagowda et al., 2009).

1.3.2 Genomic Instability

Radiation Induced Genomic Instability

Genomic instability is a term that describes an increased rate in acquisition of genomic modifications, which can appear at delayed time points in the progeny of the irradiated cell. Figure 1.4 shows some possible cellular fates associated with GI. Kadhim et al. (1992) were some of the first to report radiation induced GI, when they observed karyotypic abnormalities in 40-60% of murine stem cells exposed to doses of α-particles that provided, on average, 1 hit/cell. This observation grossly exceeds the observation of gene mutations at similar doses, and suggests that it is unlikely to be a single mutation in a gene or gene family that results in the instability phenotype. However it is speculated that genes from critical pathways are involved, possibly through an epigenetic mechanism (Aypar et al., 2011).

Between 1996 and 2001 Watson provided numerous examples of GI, initially Watson et al. (1996) demonstrated *in vivo*, the expression of non-clonal chromosomal instability (CIN) after irradiating murine stem cells with α-particles: the presence of CIN persisted for a year. In 1997 Watson et al. (1997) linked the quantity of superoxide, a ROS, produced with the level of CIN observed. Further research in 2000 (Watson et al., 2000) led to the demonstration of *in vivo* CIN in the progeny of non-irradiated stem cells helping to establish a link between BE, GI and IR (Watson et al., 2000). Chromosomal instability was displayed in CBA mice, a relatively radiosensitive strain, after whole body exposure to X-rays or 0.5 Gy neutron irradiation. Bone marrow cells showed 17% and 5% stable and unstable aberrations respectively (Watson et al., 2001). Ultimately the authors concluded that CIN can be induced *in vitro* and after transplantation be passed on *in vivo*, in some cases persisting for the lifetime of the animal in question. More recently Tanaka et al. (2008) published data on the induction of CIN, including dicentric or centric chromosomes and micronuclei. Aberrations were found to be present after

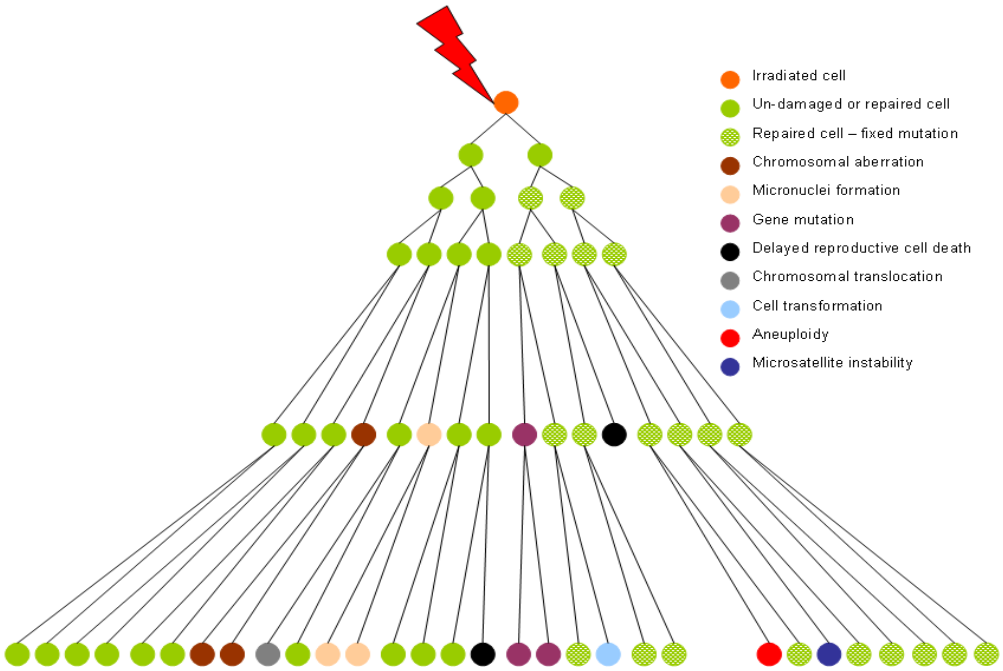

Figure 1.4: **Genomic Instability:** A representation of the delayed responses observed after irradiation. Different aberrations may appear in the descendants of an irradiated cell many cell divisions after the initial insult.

continuous γ-ray exposure for 400 days at doses of 20mGy/day to 200 mGy/day with differences in induction observed between dose rates. However, similarly to BE, GI is not universally induced (Hamasaki et al., 2009). T-lymphocytes recovered from A-bomb survivors have to date not shown a significant induction of non-clonal chromosomal damage (Kodama et al., 2005). This irregularity in GI response could be due to several factors such as radiation type and dose, genetic predisposition and cell/tissue type.

Factors influencing genomic instability

As stated above, many factors influence the type and extent of GI such as radiation type and dose rate, cell line and genetic differences. The most studied is the difference between high and low LET radiation induced instability with α-particles and γ-rays respectively. Chapman et al. (2008) reviewed the differing effects of radiation type and dose: they reported that low LET X-rays were seen to have varying effects at different doses. For example a general damage response

was seen at all doses but persisted up to 18 hours after exposure to 0.1 Gy. Delayed effects were seen in irradiated and bystander populations after 1 Gy irradiation, but had disappeared after 18 hours in irradiated groups but remained high in bystander groups. After exposure to 0.01 Gy an increase in DSB appeared, however this was exclusive to this dose. At the delayed time point (in excess of 10 population doublings) GI was absent from all groups except 0.01 Gy. After high LET radiation (α-particle) exposure at 0.5 Gy, significant damage was seen in all cultures, the delayed effect was increased after 24 Hr in a bystander population, however it was decreased in the direct group indicating active repair processes. After twenty eight days following irradiation, GI was present as a persistent and significant increase in DNA damage (Chapman et al., 2008).

Kadhim et al. (1994) have demonstrated differences in genetic susceptibility to radiation-induced instability in five individual human bone marrow samples. Each individual sample showed a wide range in the number of aberrations after irradiation. The results demonstrated a tier-like effect, some cells being highly sensitive, others moderately sensitive and a subset slightly sensitive or insensitive. The genotype of the cell line in question has also been further implicated in GI manifestation *in vitro*. Mothersill and Seymour (1997) examined the effect of medium from irradiated epithelium and fibroblasts on bystander cells. Medium from irradiated epithelium was able to induce a significant toxic effect on fibroblasts, but the effect was not reciprocated when irradiated fibroblast medium was incubated with epithelial cells. Genotype was also to play a role in GI responses in studies by Kadhim et al. (1998). They showed GI could be induced in one primary human fibroblast, HF19 but not in the similar line HF12 cell line. This finding can be correlated with a study by Watson et al. (1997) which linked levels of ROS to show quantitative differences related to genetic background. More recently there have been large inter-disciplinary collaborative teams looking at radiosensitivity and its link to genetics. Barnett et al. (2012) published data regarding single nucleotide polymorphisms (SNP's): they found no association between the SNP within the TGF-β gene locus and toxicity.

Furthermore, the dose rate has important implications for GI as observed in V-79 Chinese hamster cells. When subjected to 0.5 Gy γ-rays at dose rates of 0.48 Gy/min (acute exposure) and 0.0485 Gy/min (chronic exposure) the appearance of micronuclei (MN) was measured at 20 doublings in both acute and chronic exposures. The frequency of MN in the chronic population

cells was high and remained so for 40-60 generations, while acute irradiation showed a reduction in MN formation after 20 generations (Antoshchina et al., 2005).

Mechanism of GI

At present there is no all encompassing mechanism that describes the mechanistic processes involved in initiating, perpetuating and sustaining GI (Morgan, 2003). However certain patterns have been identified in its induction that suggest possible mechanisms. For example, GI appears at much higher frequencies than standard gene mutations at a single locus indicating that these aberrations are unlikely to be involved in GI (reviewed by Lorimore et al. (2003). There is mounting evidence associating epigenetic factors where changes in DNA methylation, histone modification and RNA-associated silencing could cause the biological changes associated with GI (Kovalchuk and Baulch, 2008). Pogribny et al. (2005) examined the effect of low dose IR on inducing DNA lesions and alterations of global genome methylation, specifically trimethylation of histone H4 lys20 in an *in vivo* murine model leading to gene activation. Following fractionated whole body irradiation with 0.5 Gy X-ray, murine thymus showed a significant reduction in methylation at histone H4 lys20. It was also observed that *de novo* methyltransferase 1 (DNMT1) was reduced as well as DNMT3b but only in males, highlighting gender as a potential influencing factor. Methyl binding proteins such as MePC2 were reduced by 20%; such observations were accompanied by the formation of γH2AX foci highlighting DNA double strand breaks. Koturbash et al. (2006a,b) also documented epigenetic mechanisms involved in transgenerational effects and BE *in vivo*. Initial work looked at the levels of cytosine methylation in the offspring of exposed parents. Upon examination it appeared that there was a loss of global genome methylation in the thymus on cytosine residues, the same reduction in DNMT1 (as above) was also noted combined with DNA strand breaks (Koturbash et al., 2006a). Unilateral exposure of mice to X-rays showed a suppression of methylation in irradiated cells but no such effect in bystander cells. However DNMT3a/b appeared to be down regulated whilst DNMT1 was up-regulated in bystander cells (Koturbash et al., 2006b). Interestingly two methyl binding proteins known to be involved in transcriptional silencing, MePC2 and MBD2, were also up-regulated in bystander cells; additionally all these effects were accompanied by DNA damage. As well as providing evidence for an epigenetic role, the study also linked GI and

BE. Taken together these studies demonstrate that radiation can induce DNA damage whilst altering the normal epigenetic processes that occur within the cell.

There is also much evidence relating to oxidative stress as a causative agent of GI in particular non-clonal chromosomal instability. Chronic oxidative stress (less than 30 hours, 1 hour per day) induced instability and at a significantly higher rate, than acute (more than 2 hour exposure) oxidative stress. Another scenario is proposed that implicates nicotinamide adenine dinucleotide phosphate (NADPH) oxidase, the major end product of which is superoxide (Babior, 1999). NADPH oxidase can be activated to produce large amounts of the free radical to initiate signalling cascades, it can then be secreted into the local extracellular environment to oxidise adjacent cells or proteins, the latter would be consistent with mediating the bystander response. The detrimental action of ROS could implicate them in damaging sub-cellular organelles, for example lysosomes and mitochondria; this process may play a role in radiation induced non-targeted effects.

The process of inflammation has also been implicated in radiation induced genomic instability (Lorimore et al., 2003; Aivaliotis et al., 2012). Lorimore et al. (2001) suggests that inflammation may have a role in the induction of GI, as it was noted that macrophage activation persisted long after the initial radiation insult *in vivo* and that associated actions of macrophage activation such as NO and superoxide production maybe therefore be involved in GI induction. Alternatively Aivaliotis et al. (2012) suggest that an increase in growth promoting cytokines may induce DSB through replicative stress. Inflammation can also induce the formation of an extremely reactive free radical species called peroxynitrite anion (ONOO), This can cause various adducts in DNA such as base alterations and strand breaks (Valko et al., 2006). Finally the DNA damage response (DDR) has been implicated when Cianfarani et al. (1998) demonstrated in addition to inflammatory cytokines a simultaneous increase in p53 activation. Chromosomal instability in the form of chromosomal aberrations which was attributed to inflammatory processes.

A link between bystander effects and genomic instability

The disaster at Chernobyl has provided an opportunity for the investigation of *in vivo* radiation induced BE and GI. It was found that GI was present at an increased frequency in thyroid carcinoma cells that were adjacent to cells exposed to the radiation (Williams, 2008). The observations implicate a role for BE inducing GI and eventually radiation carcinogenesis. There is also evidence for a link between BE and GI *in vitro*, demonstrated through numerous experimental studies. In all cases cellular communication between irradiated and un-irradiated cells either through secreted soluble factors or GJIC led to induction of GI. Grid shielding experiments, where the majority of unshielded cells died, showed levels of CIN remained the same irrespective of the grid being in place or not (Lorimore et al., 1998). This indicated that most of the cells demonstrating CIN have a non-irradiated background resulting in the conclusion that the induction of this damage was caused by intercellular communication *i.e.* a bystander mechanism.

The two NTE's responses also share many common characteristics *e.g.* micronuclei formation, delayed lethal mutation/reproductive cell death and induced chromosomal rearrangements. Additionally the up-regulation of oxidative stress in bystander cells is similar to that observed in radiation-induced GI (Kovalchuk and Baulch, 2008; Ponnaiya et al., 2011).

1.3.3 Sub-cellular organelles and non-targeted effects (NTE's)

With advancing technology and ever increasing resources to investigate radiation induced GI and BE, various laboratories have started to investigate the sub-cellular environment and in particular organelles like the mitochondria. Recently Yoshida et al. (2012) demonstrated that IR was able to cause mitochondrial dysfunction hours after the radiation insult which led to increased oxidative stress at delayed time points and it was thus hypothesised that mitochondria play a role in GI. Similarly, media bystander studies undertaken by Lyng et al. (2000) have been shown to alter mitochondrial membrane permeability and thus support their role in GI. However, there has been very little work on other organelles such as the lysosome. Coates et al. (2001) suggests that radiation could alter the lysosomal system in a way that disturbs enzyme

location. We therefore wanted to investigate this organelle further to ascertain its possible role in radiation induced GI.

1.4 Lysosomes

Lysosomes are membrane bound organelles present throughout all eukaryotic nucleated cells (Holtzman, 1989; Saftig, 2005), they have a lowered pH compared to the cytoplasm maintained at pH 5 by the action of ATP powered proton pumps (Mindell, 2012; Saftig, 2005). The enzymes held within the lumen are soluble and work optimally in the acidic conditions (Luzio et al., 2007; Mindell, 2012). Their primary function is to act as a terminus for macromolecules that have been targeted for degradation. They contain a number of enzymes, collectively known as acid hydrolases that are able to degrade components such as proteins, carbohydrates, lipids and DNA (Alberts et al., 2008; Saftig, 2005).

1.4.1 Lysosome Morphology

Lysosomes are defined by their functional properties rather than their structural appearance, although there are some characteristics which help in the identification and classification. They are normally spherical or ovoid in appearance and have a simple lipid membrane layer. They normally occupy a certain intracellular location dependant on the cell line (Saftig, 2005); in many cases this is perinuclear. Lysosomal size also varies depending on cell line, for example in hepatocytes they can appear sub-micron, however in macrophages they can exceed several microns. Both size and number can be affected markedly by the presence of un-degraded material in the lysosomes (Saftig, 2005). At the ultrastructural level, lysosomes have been shown to possess an electron dense lumen with an electron poor inner halo and a small electron dense outer ring apparent after staining with osmium tetroxide and uranyl acetate (Saftig, 2005; Holtzman, 1989).

1.4.2 Lysosome Biogenesis

The actual origin of the lysosome in terms of how and where the membrane is constructed, is still somewhat unknown (Lacombe et al., 2013). There are two main theories: The first states that the lysosomal membrane starts off as a budding vesicle from the Golgi body (GB). In this circumstance proteins destined for lysosomes are processed in the GB and emerge at the trans Golgi network where they bud off in vesicles that go on to become primary lysosomes (Saftig, 2005; Pitt, 1975). The alternative proposed route of lysosome biogenesis is the Golgi associated Endoplasmic Reticulum (ER) from which Lysosomes arise *i.e.* the GERL model. In this instance the membrane originates from the smooth ER (SER), and proteins and enzymes are transported from the rough ER (RER) to the SER where they by-pass the GB (Pitt, 1975).

There has been minimal work carried out on the formation of lysosomal membranes; most research has concentrated on the subsequent trafficking of proteins to the lysosomes, and the roles they play therein.

Lysosomal hydrolases and membrane proteins that are newly synthesized have to be directly targeted to the lysosome. The most well studied mechanism of specific trafficking is through mannose-6-phoshate (M6P) and its receptor (MPR). Upon delivery of the acid hydrolases to the cis Golgi network they are tagged with a M6P at a specific polypeptide signal patch (Holtzman, 1989; Saftig, 2005). As they travel through the Golgi they bind transmembrane MPRs located at the trans Golgi network. Proteins such as adaptor protein-1 (AP1) and Golgi-localized, γ-ear-containing, ADP ribosylation factor-binding proteins (GGAs) (Mullins and Bonifacino, 2001; Luzio et al., 2007; Lbke et al., 2009) are also involved the process. A vesicle containing the hydrolases buds off as a result of clathrin binding to the cytosolic side of the MPR (Lbke et al., 2009; Luzio et al., 2007). Once the vesicle buds the pH drops to around 6 which causes the dissociation of the hydrolases from their receptors (Alberts et al., 2008). The receptors are transported back to the Golgi where they are recycled; however in some circumstances hydrolases are packaged incorrectly and sent to the extracellular space (Alberts et al., 2008). In this case MPR are also directed to the plasma membrane where they recapture enzymes and target them to lysosomes through endocytosis (Saftig, 2005).

Membrane proteins do not necessarily follow the same mechanism. Activator protein-3 is one protein that has been shown to help target membrane proteins to lysosomes, in the case of LAMPs 1 and 2 they were shown to associate to AP-3 membrane domains (Peden et al., 2004).

1.4.3 Lysosomal Functions

As mentioned above the lysosome is the terminal site of intracellular degradation, for a range of targets including endocytosed proteins, whole organelles or even phagocytosed bacteria.

Endocytosed material is transported in vesicles called endosomes (Saftig, 2005; Holtzman, 1989; Pitt, 1975). Often cell surface receptors such as epidermal growth factor (EGF) and its associated receptor (EGFR) are internalized and delivered to lysosomes for breakdown and recycling. Live cell imaging and correlative microscopy has recently shown that endosomes can transiently or fully fuse with lysosomes to form a hybrid organelle (Bright et al., 2005). The process is considered to work in a stepwise fashion involving 3 stages (reviewed by Luzio et al. (2007)).

1. Tethering: Initially a physical link between lysosomes and endosomes is made. The proteins involved are unknown, however the mammalian homotypic fusion and vacuole protein sorting (HOPS) complex in association with Rab7 is thought likely to be involved.

2. Formation of the trans SNARE complex: The formation of a SNAREpin from 4 SNAREs is essential in the next step, anchoring membranes together.

3. Membrane Fusion: The two membranes become sufficiently close so that their membranes merge into one.

As well as degrading components of extracellular origin such as growth factors and their receptors, lysosomes also degrade intracellular material such as organelles and other macromolecules in a process called autophagy. However, it is now thought that autophagy and lysosomes have a much greater role than quality control and degradation (Mehrpour et al., 2010).

Autophagy encompasses a number of sub-processes, macroautophagy (the formation of a membrane around a target that is subsequently engulfed by a lysosome), microautophagy (parts of the cytoplasm are directly taken into the lysosomal lumen) and chaperone mediated au-

tophagy (heat shock proteins accompany a targeted protein to the lysosome for degradation). Autophagy and lysosomal degradation occurs continually at a basal level to remove mis-folded or oxidized proteins, and in times of starvation it has been shown that proteolysis is undertaken to provide a food source (Lacombe et al., 2013). Autophagy and lysosomal breakdown is also thought to have an anti-aging role due to the removal of damaged mitochondria that may release ROS (Mehrpour et al., 2010; Czaja, 2011). The limitation of ROS and release of harmful proteins through autophagy and lysosomal degradation can also be considered as important in the prevention of transformation by limiting the activation of oncogenic pathways and therefore tumour development and progression (Chen and Karantza-Wadsworth, 2009; Mehrpour et al., 2010).

Roles for lysosomes and autophagy have been implicated in both innate and adaptive immunity. Innate immunological processes involve identification of intracellular bacteria and are packed into autophagosomes and destroyed by lysosomes. During adaptive immunological responses lysosomes break them down to yield antigenic peptides that are then used for presentation to CD-4 positive cells (Eskelinen and Saftig, 2009). Lysosomes have also been linked to apoptosis and cell death as they remove damaging agents from the cell system and therefore prevent the signal cascades leading to apoptosis (Werneburg et al., 2004; Chen and Karantza-Wadsworth, 2009). A number of protein interactions have also been documented that relate the two processes. All these functions make lysosomes a terminal point for the regulation of a number of important events and can therefore be said to act in cellular homeostasis (Mehrpour et al., 2010; Eskelinen and Saftig, 2009)

1.4.4 Proteome of the Lysosome

The lysosomal proteome consists of 3 domains, the integral membrane fraction, the membrane associated fraction and luminal acid hydrolases (Lbke et al., 2009). The latter have been well characterized and there are now thought to be in excess of 60 enzymes and associated soluble proteins (Sleat et al., 2008; Lbke et al., 2009). These enzymes are capable of degrading a number of key macromolecules including DNA, RNA, proteins, lipids and carbohydrates (Holtzman, 1989; Saftig, 2005). One of key interest is lysosomal DNase additionally known as DNaseIIα,

which is expressed in all lysosomes; it acts to degrade DNA.

In the integral membrane there are thought to be 215 proteins, of which many have known functions. Twenty have an unidentified function while another 35 were identified to function in vesicular trafficking of proteins such as Rabs and SNAREs (Bagshaw et al., 2005). The most abundant lysosomal membrane proteins include LAMP 1 and 2, LIMPII, various subunits of the ATPase-proton pump, acid phosphatase and numerous Rabs such as Rab 7. One of the proteins with an unidentified function has now been confirmed as Arl8b a lysosome specific ADP ribosylation factor. Its function has been shown to affect the microtubule-dependent movement of lysosomes from the perinuclear area to the cell periphery (Bagshaw et al., 2006).

1.4.5 Lysosomes involved in disease

There are now 40 characterized lysosomal storage disorders, which mostly relate to a deficiency in acid hydrolases (Wei et al., 2008). There is little published data on the susceptibility of these cell lines to radiation. As a result a substrate that would normally have been broken down accumulates in the lysosome to toxic levels causing ultrastuctural alterations. Most cases demonstrate neuronal degeneration (Walkley, 2007) upon pathological examination. An example include Niemann Pick disease type C (NPC): this disease usually occurs from a mutation in the gene coding for sphingomyelin, this leads to the accumulation of glycosphingolipids and the eventual toxic quantities of unesterified cholesterol. As a result, neuronal cells suffer structural and functional damage.

Interestingly, endoplasmic reticulum (ER) and oxidative stresses are associated with neurodegenerative and non-neurodegenerative lysosomal storage diseases. This effect was also demonstrated in normal control fibroblasts when the lysosome was disturbed by addition of ammonium chloride (Wei et al., 2008). These results suggest that there is communication between the ER and lysosomes and that disruption to normal lysosomal conditions can induce oxidative and ER stress that lead to apoptosis (Wei et al., 2008), similar to some of the proposed mechanisms in BE and GI in particular chromosomal damage and apoptosis stimulated by ROS.

1.4.6 Lysosomal Damage and Cellular Injury

The lysosome could be perceived as a possible hazard to the cell, as it contains a range of enzymes that can effectively degrade the cell. de Duve was the first to suggest malfunction of the lysosome could lead to intracellular damage and possible cell death (Pitt, 1975; Saftig, 2005). The effect that is most likely to apply to this project is an altered permeability in the lysosomal membrane that leads to the subsequent release of acid hydrolases. This effect was first demonstrated by Weissman et al. (1963) working on streptococcal haemolytic toxins O and S. Observations showed they caused the release of enzymes from the lysosome. The process was also observed where photo-oxidative stress in the membrane of a lysosome was able to induce a leaky state and the release of numerous enzymes including lysosomal DNase (Allison and Paton, 1965). It is thought that the induction of free radicals through photo-oxidative reactions and lipid peroxidation leads to membrane damage (Allison and Paton, 1965) and the introduction of sub-lethal and lethal chromosomal aberrations. There are striking similarities when compared to aberrations observed in radiation induced CIN. Chemical agents (Younes et al., 1983) have been used to show that lipid peroxidation results in leakage of lysosomal membranes although in the system they were using no correlation could be made with cellular damage. Allison (1966) has also proposed that this is the possible induction mechanism for cancer associated with a damaging agent such as IR or chemical carcinogens.

The signalling cytokine TNF-α, which is known to be involved in the BE (Desai et al., 2013), has also been shown to induce cellular damage through a number of downstream signalling events. One has been noted as lysosomal membrane permeabilization and the release of enzymes such as cathepsin B. Werneburg et al. (2004) found that TNF-α mediated lysosomal membrane permeabilization is dependent on intra-lysosomal cathepsin B receiving an activation signal. The model suggested is TNF-α mediated activation of factor associated with neutral sphingomyelinase activation (FAN); the resulting signalling cascade activates caspase-8 which in turn activates Bid and leads to lysosomal permeabilization, the ultimate effect of these combined events is apoptosis and tissue injury.

Sphingomyelinase and the signalling events it is involved in are also thought to be a possible influencing factor in the BE seen in human primary fibroblasts. The enzyme, which is defi-

cient in Niemann-Pick type C (NPC), is found as a luminal acid hydrolase and in the plasma membrane and has been shown to be activated by radiation. Shao et al. (2004) stated that membrane bound sphingomyelinase was able to induce the production of NO through the stimulated expression of NO synthase which in turn generated a BE. It is thus possible to speculate that lysosomal sphingomyelinase reacts with the sphingomyelin in the lysosomal membrane to produce a bystander or a GI signal following IR.

1.4.7 Lysosomal Response to Ionizing Radiation Exposure

De Rey et al. (1976) investigated the lysosome response to X-ray exposure in rat epidermis. They noted up-regulated levels of the active lysosomal enzyme acid phosphatase which was also linked to tissue keratinisation. They also suggested that lysosomes can participate in the destruction of other intracellular membranes that is characteristic of the differentiation process. Roth et al. (1962) were some of the first to identify a redistribution of lysosome enzymes from the mitochondrial fraction to the supernatant fraction after whole body X-irradiation. This was latter confirmed by Snyder and Eklund (1978) who identified that doses up to 200 rads (2 Gy) caused a redistribution 24 hours after irradiation, although there was no increased expression of the enzymes measured. The redistribution of lysosomal enzymes is thought to be a result of an effect on the lysosomal membrane. Lipid peroxidation induced after exposure to IR has been suggested as a cause (Desai et al., 1964). By mimicking a downstream effect of IR, namely oxidative stress, through the introduction of ischemia in neuronal monkey cells (Tsukada et al., 2001) showed alterations in DNaseIIα location. A massive increase in immunoreactivity both in the cytoplasm and nucleus showed that DNaseIIα was able to leak from lysosomes and translocate to the nucleus in a gradual manner. Damage to the lysosomal membrane was confirmed by electron microscopy and thought to be a result of the protease μ-calpain. This effect resulted in necrosis 5 days after the cells were placed under the ischemic conditions. It is possible to speculate that this same delayed effect seen in GI maybe responsible in part to DNaseIIα. Alternative processes such as signalling through hormones or cytokines, TNF-α discussed above, have been proposed.

1.5 Other Organelles and Damage

Other organelles implicated in cellular damage include the mitochondria, which are the primary site of cellular respiration (Alberts et al., 2008), and play a major role in apoptosis and cell signalling (Valerie et al., 2007a). Radiation-induced GI has been demonstrated in conjunction with evidence of mitochondrial dysfunction, ultimately resulting in increased levels of the reactive oxygen species H_2O_2, this in turn contributed to increased mutation frequency and gene amplification (Dayal et al., 2009). The cell nucleus, although not directly involved, has some part to play in the transmission of a signal from the cytoplasm to the DNA; if DNaseIIα is involved in the appearance of CIN then its translocation into the nucleus is either through a damaged pore/membrane or a specific trafficking/targeting mechanism. The effects of age and oxidative stress have been shown to damage nuclear pores allowing the entry of 70kDa dextran (D'Angelo et al., 2009); in relation to DNaseIIα such damage would permit entry of the enzyme since it is 45 kDa in size.

1.6 Aims of Thesis

The objective of this study is to investigate a potential role for lysosomes in the induction of genomic instability and bystander effects in HF19, a primary human fibroblast cell line. Cells are analysed at early and delayed time points to examine the induction of genomic instability. Bystander conditions are established by media transfer techniques and examined at the same time points as the direct irradiated cells. In addition we aim to detect alterations in sub-cellular organelles. Finally we aim to find a potential cause of GI/BE attributable to these alterations particularly in the lysosomal compartment. We will therefore examine the downstream effects of lysosomal alterations such as enzyme redistribution particularly the enzyme DNaseIIα for its sub-cellular location.

In order to fulfil these aims, the objectives of this project will be:

1. Establish X-ray dose and time points at which GI/BE is induced.

2. Assess lysosomal parameters following X-ray exposure including permeability and distribution, and ROS as a potential cause of lysosomal changes.

3. Investigate nuclear permeability and lysosomal enzyme location

Chapter 2

Materials and Methods

2.1 Materials

2.1.1 Cell Line

HF19, a primary non-transformed human fibroblast was used for all studies. It originates from the lung of a female foetus with an approximate cell cycle of 36 hours and a 46XX genotype. The cells grow as an adherent monolayer in a culturing flask when supplied with minimum essential medium (MEM) with Earles salts, supplemented with 2mM L-glutamine, 50,000 units Penicillin, 0.1 mg/ml Streptomycin and 15% foetal bovine sera (FBS). They were maintained in a humidified 37°C incubator at, 5% CO_2. Once the cells have adhered, they display a fusiform (spindle like) morphology, that can be viewed under an inverted light microscope.

2.1.2 Other Materials

Table 2.1: Materials and associated catalogue numbers for materials purchased.

Item	Company	Cat No
HF19 MEM Media	Gibco	21090
HF19 MEM Media (Phenol red free)	Gibco	51200
L-Glutamine	Gibco	25030
Penicillin/Streptomycin	Sigma	P0781
Trypsin	Gibco	15090
Ethylenediaminetetraacetic acid (EDTA)	Sigma	E8008
Phosphate buffered saline (PBS)	Gibco	14190
erythrosin B	Sigma	E9259
Sodium chloride (NaCl)	Sigma	S5886
Potassium chloride (KCl)	Sigma	P5405
Sodium hydroxide (NaOH)	Sigma	221465
Dimethyl sulfoxide (DMSO)	Sigma	D2650
Phosphate Buffer	VWR	363112p
Giemsa	Gurr/VWR	350864X
Entellan mounting media	VWR	1.07961.0100
6 well plate	Falcon	353502
demecolcine	Sigma	D0125
Methanol	Fisher	M/4000/17
Glacial Acetic Acid	Fisher	A/0400/PB17
fine tip mini pipette	Alpha Labaratories	LW4231
Xylene	Fisher	X/0250/17
Vectasheild	Vector Laboratories	H-1200
Normal melting point agarose (NMPA)	Sigma	A9539
Low melting point agarose (LMPA)	Fisher	BP165
Tris-HCl	Sigma	T1503
Triton-X 100	Sigma	T9284

Item	Company	Cat No
SYBR Gold	Molecular Probes/Invitrogen	S11494
Black 6 well Plate	Griener bio-one	655086
5-(and-6)-chloromethyl-2',7'-dichlorodihydrofluorescein diacetate (CM-H2DCFDA)	Molecular Probes/Invitrogen	C6827
FITC-Dextran	Molecular Probes/Invitrogen	FD40S
Matek Dish (No. 0 cover glass)	MatTek Corporation	P35G-0-14-C
Digitonin	Sigma	101105536
Acridine Orange	Sigma	A6014
DNAse Ab	Abcam	ab8119
secondary Ab Dnase	Molecular Probes/Invitrogen	A21428
Bovine serum albumin (BSA)	Sigma	A8412
Goat Serum	Gibco	16210-064
Magnesium Acetate Tetrahydrate	Sigma	M5661
HEPES	Sigma	H3375
Potassium Acetate	Sigma	P1190

2.1.3 Solutions & Buffers

Method	Buffer
Comet Assay	
Lysis Buffer	2.5 M NaCl, 100 mM EDTA (pH 8.0), 10 mM Tris-HCl (pH 7.6), 1% Triton X-100, pH to 10
Electrophoresis	0.3 M NaOH, 1 mM EDTA, pH to 13
Neutralising	0.4 M Tris-HCl, pH to 7.5
Nuclear Membrane Perm.	
Permiabilization	20mM HEPES, 110mM potassium acetate, 10 mM magnesium acetate, 0.5mM EGTA, 250 mM sucrose, 40 μg/ml Digitonin pH to 7.3 -7.4
Washing buffer	20mM HEPES, 110mM potassium acetate, 10 mM magnesium acetate, 0.5mM EGTA, 250 mM sucrose pH to 7.3 -7.4
Transfer Buffer	20mM HEPES, 110mM potassium acetate, 4 mM magnesium acetate, 5 mM sodium acetate, 0.5 mM EGTA, 250 mM sucrose pH to 7.3 -7.4
Staining	40 kDa dextran at 0.2 mg/ml in transfer
Immunohistochemistry	
Blocking	10 % Goat Serum, 1 % BSA, 0.3 % Triton-X 100 in PBS

2.2 Methods

2.2.1 Routine Cell Culture

Recovering Stocks from Liquid Nitrogen

Cryovials containing 1 ml of cell suspension in 10% DMSO were removed from liquid nitrogen and hand warmed until thawed. The cell suspension was then transferred using a 1 ml pipette to a 25cm^2 flask (T25) containing prewarmed growth medium (as detailed above) or a 75cm^2 culture flask (T75) also containing prewarmed growth medium if the cell suspension was in excess of 2 million cells/ml. The flask was incubated (37°C, 5% CO_2) to enable cell adherence. After 4 hours, success of cell attachment and cell viability was checked using an Olympus inverted phase contrast field microscope. In the event of low or no cell adherence, the flask contents were safely disposed and a new cell sample was set up from liquid nitrogen. Flasks were incubated for a further 24 hours.

HF19 Maintenance & Sub-culturing

HF19 cells were routinely sub-cultured in MEM supplemented with 2 mM L-glutamine, 50,000 units Penicillin, 0.1 mg/ml Streptomycin and 75ml/15 % foetal bovine sera (FBS). Media was stored at 4°C, before use it was allowed to warm to 37°C in a water bath. Flasks were split from one flask into 2 or escalated from a T25 to a T75. Sub-culture usually took place between 48 to 72 hours following the previous sub-culture. If cells had not reached a minimum of 80% confluence the media was changed to remove metabolic waste and replaced with fresh media warmed to 37°C.

Once the monolayer had reached a minimum of 80 % confluence they were sub-cultured. The current growth media was removed and discarded (unless required for bystander experiments). The monolayer was subsequently washed in PBS twice, after the last wash was removed 0.5, 2 or 4 mls of 0.025% trypsin in 0.01 % EDTA and PBS was added to T25, T75 or 175 cm^2 tissue culture flasks (T175), respectively. The monolayer was bathed in the trypsin-EDTA solution

for approximately 10 seconds after which it was removed. The tissue culture flask was then checked under an inverted light microscope at 40x magnification to ensure appropriate cell detachment. Any remaining trypsin-EDTA was inactivated by the addition of fresh media. The cell suspension was gently pipetted to break up any cell aggregates and then seeded into a new tissue culture flask or discarded. One passage was marked as passing after each sub-culture, and culture flasks were used for no more than 2 passages before transferring cells to a new flask.

Cell Counts Using the Viability Stain, Erythrosin B

Firstly an erythrosin B stock solution was made containing 0.4 g erythrosin B; 0.81 g sodium chloride, 0.06 g monobasic potassium phosphate, and 100ml Hanks balanced salt solution, HBSS. The solution was mixed with a magnetic stirrer while in a glass beaker containing water which was bought to the boil. While at a high temperature, a small amount of sodium hydroxide was added until all components had dissolved. After cooling the working solution was made, by adding 1 ml of stock solution to 4 ml of dH_2O. Both stock and working solutions were stored in a refrigerator at 4°C.

To perform the cell count a 100 μL aliquot of erythrosin B was placed into 1.5 ml eppendorfs, the same volume of cell suspension was added to the eppendorf. After mixing 10μL was removed and loaded onto a Neubauer Haemocytometer (haemocytometer) sealed with a coverslip. Each haemocytometer has two counting chambers both of which have a scored grid. Each grid has 4 large 1 x 1 mm squares made up of 16 smaller squares. When the coverslip is in place, it sits 0.1 mm above the haemocytometer. Therefore the total volume of each individual large square is $1 \times 1 \times 0.1 = 0.1\text{mm}^3$ or 1μL. Each of the 4 large squares per chamber were counted. To calculate the number of cells per mL of cell suspension the following formula was used.

$$\frac{(N^1 + N^2 + N^3 + N^4)}{4} \times 2 \times 10^4 = cells/ml$$

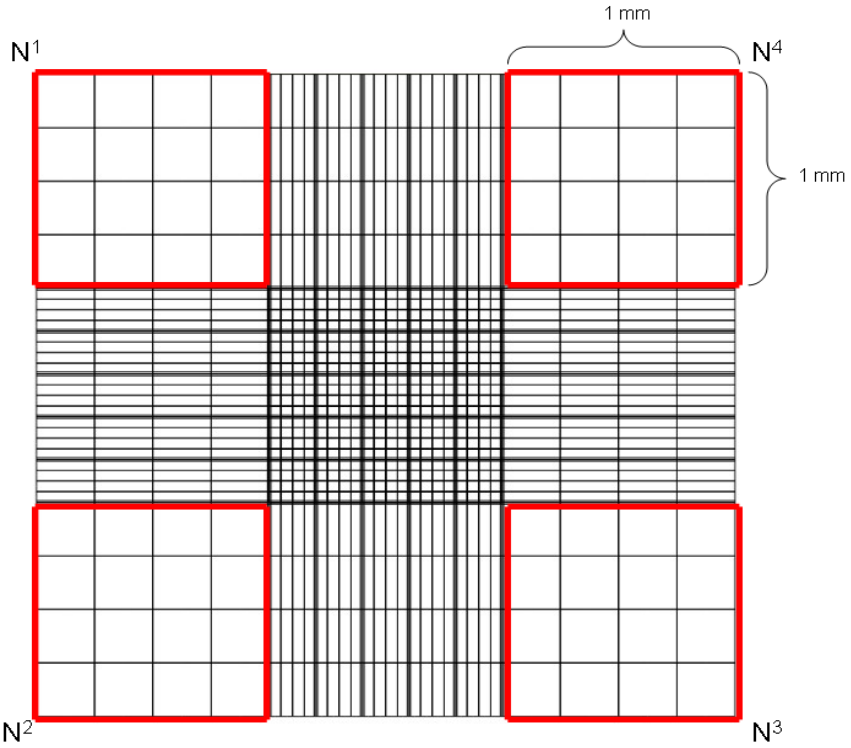

Figure 2.1: **A schematic of the haemocytometer, the red outline shows the 4 large squares used for cell counting**

Cryopreservation of cells in Liquid Nitrogen

The tissue culture flasks were allowed to grow to 100% confluence after which the used growth medium was removed and discarded. The cells were collected in a 15 ml Falcon tube as previously described and centrifuged (Jouan B4) at 1200 revolutions per minute (rpm) for 10 minutes. Supernatant was poured off and the pellet re-suspended in a volume of freezing media to give a cell density of between 1.5×10^6 and 2×10^6 in 1ml. The freezing media was prepared from 90% culture media supplemented with 10 % DMSO. Aliquots of 1 ml were then distributed between labelled cryovials. Cryovials were then moved to -20°C for 2 hours and then placed overnight at -80°C, finally the cells were moved into liquid nitrogen for long term storage.

2.2.2 Cell Irradiations

Cell irradiations were performed at the Gray Institute for Radiation Oncology & Biology, Department of Oncology, University of Oxford, utilising MXR321 X-ray machine operating at 250

kV. The nature of X-ray irradiation results in all cells being irradiated. All irradiations were carried out in tissue culture flasks or tissue culture plates. Doses of 0.1 Gy, relevant to diagnostic procedures or 2 Gy relevant to therapeutic procedures, were used at dose rates of 0.59 and 0.58 Gy/Min respectively.

2.2.3 Exposure of Bystander Cells to Irradiated Cell Conditioned Media (ICCM)

Bystander recipient cells and donor cells were grown in identical fashion to directly irradiated cells. Donor cells were irradiated wherever possible with directly irradiated cells. Throughout the radiation exposure the bystander cells were removed from the incubator and held at room temperature to replicate all conditions encountered by the irradiated cells. The irradiated donor cells were left under standard culture conditions for 4 hours, at which time the media was aspirated and filtered through a 0.22μm filter that was pre-treated with 1% BSA in PBS. Four hours was chosen as this is an established procedure within the laboratory that has proven to be suitable in the past. The treatment with BSA was conducted in order to inhibit any protein binding capacity inherent in the filter. The media from the un-irradiated bystander population was removed and discarded, the bystander cells were washed once with pre-warmed PBS and the filtrated media was applied. After 24 hours incubation with the bystander media, it was removed and routine cell culture methods were applied.

A secondary bystander group was created at a delayed time point (Figure 2.2). In this instance media was taken from direct groups (0, 0.1 and 2 Gy) at 20 population doublings and added to additionally cultured control flasks. The media was taken through the same filtering and addition process as above.

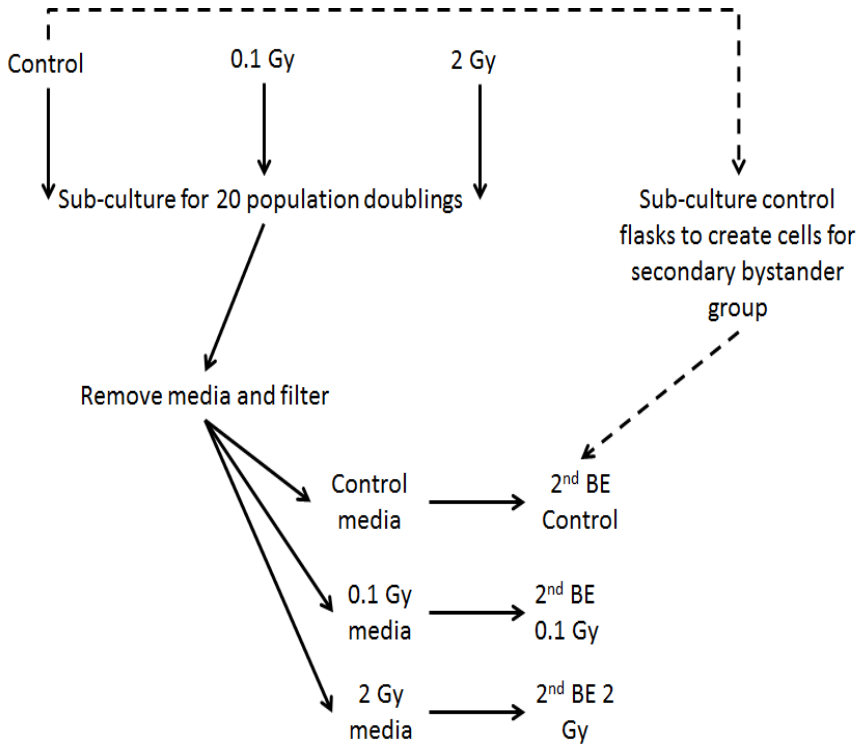

Figure 2.2: **A secondary bystander group was created by taking media at 20 PD from direct groups and added to additional cultured control cells.**

2.2.4 Single Cell Gel Electrophoresis (Comet Assay)

The comet assay is a quick, reliable and quantitative method to measure DNA damage including SSB, DSB and base damage in individual cells. The comet assay was performed in alkaline conditions to measure total DNA damage. Standard microscope slides were dipped in 1 % normal melting point agarose (NMPA) the excess was wiped from the back and the slides were air dried overnight, they were then stored in a microscope box. Also prior to cell harvesting, the alkaline lysis buffer, alkaline electrophoresis buffer and neutralization buffers were made (Table 2.1) all were chilled to 4°C.

On the day of harvest, the cells were trypsinized and collected in fresh media, cell counts were performed. An aliquot of 20,000 cells per group were put into 1.5 ml eppendorf and placed immediately on ice. When all samples had been collected the cell suspension was mixed with 200μL of 1% low melting point agarose (LMPA). The NMPA pre-coated slides were placed on an ice chilled metal plate and 200μL of the LMPA cell suspension mixture was pipetted on to

the chilled slide, a 22 x 50 mm glass cover slip was placed on top to flatten and spread the LMPA cell suspension across the whole slide. Each slide was left for 5 to 10 minutes to allow complete setting, after which the cover slips were removed and the slides put into alkaline lysis buffer, 1 % Triton-X and 1 % DMSO were added 30 minutes prior. Lysis was carried out at 4°C in the dark, lysis time ranged from 16 to 20 hours but was always consistent within groups.

After lysis treatment the slides were equilibrated in the alkaline electrophoresis buffer in a horizontal tank. Subsequently, the slides under went electrophoresis for 30 minutes in the dark at 19 V, 300 mA. Finally the slides were removed from the tank and neutralized with 3 x 10 minute washes with neutralization buffer. Any remaining buffer was removed with 4 washes of dH_2O. Slides were stained with a 1:10,000 dilution of SYBR Gold in dH_2O for 5 minutes in the dark. Finally the slides were dried overnight at 25°C overnight and analysed using Komet 5.5 Image Analysis Software (Kinetic Imaging Technology/Andor, Germany).

2.2.5 Chromosomal Analysis

Chromosomes become structurally and numerically distinct only during the metaphase stage of the cell cycle (mitosis) and mitotic inhibitors are used to collect cells at this stage for cytogenetic analysis. The most common mitotic arresting agents are colchicines, a natural alkaloid found in autumn crocus that prevents microtubule formation. Demecolcine solution is most commonly used for this purpose. It works by disrupting the mitotic spindle fibres, thereby freeing the chromosomes from the metaphase plate, allowing them to spread out inside the cell. The absence of spindle fibres also blocks anaphase, so the mitotic index is effectively increased.

Harvesting HF19 metaphases

Predefined time points for the harvesting of cells were set at 1 and 20 population doublings. Each flask was harvested when it had reached 70-80% confluence and was seen to be undergoing cell division via the inverted light microscope (presence of rounded cells). Demecolcine was added to yield a final concentration of 0.02μg/ml for each 1 ml of cell suspension; the flasks were then incubated for 1.5 hours at 37°C and 5% CO_2. During this period, a hypotonic potassium

chloride (KCl) solution was prepared; 0.55 g potassium chloride (analysis grade) was added to 100 ml ultra pure water (Millipore water, quality 18 MWcm) and kept in a 37°C water bath. A 3:1 fixative was also prepared by mixing 25ml glacial acetic acid and 75 ml methanol. After the 1.5 Hr incubation time, the confluent flasks were transferred to the Class II microbiological safety cabinet.

For each flask: the media was removed and kept in a labelled universal tube. The flasks were washed with 5 ml PBS, which was also added to the universal bottle. A second wash of 5 ml PBS was conducted to remove any last traces of media, and discarded. Cells detached with 2 ml (0.25%) trypsin which was also added to universal contents. The flask was examined on an inverted microscope to ensure detachment of the cells, 10 ml of the universal contents (saved media, PBS and trypsin) was used to collect the cells and added back to the remaining contents. Once all the cells had been collected, the samples were centrifuged at 1200 rpm in a Jouan B4 centrifuge at room temperature for 10 minutes. After centrifugation the cells were visible as a pellet at the bottom of each universal.

For each universal: The supernatant was discarded, and the pellet re-suspended by flicking the conical part of the tube vigorously, this was done thoroughly to avoid clumping at later stages. Once re-suspended, 1 ml of warmed KCl was added using a glass Pasteur pipette, with agitation. A further 3-4 ml was added, the tubes were subsequently incubated for 20 minutes at room temperature. Each universal was then poured into a 15 ml falcon tube and volume made up to 10 ml with KCl. Following the 20 minute incubation, three drops of fixative were added, and the tube inverted twice. The tubes were then centrifuged at 1000 rpm for 10 minutes after which the supernatant was discarded and the pellet was re-suspended. Using a new glass Pasteur pipette, 1 ml of the 3:1 fixative was added whilst the tube was flicked. 9 ml of 3:1 fixative was added to make a total volume of 10 ml, the tubes were incubated for a further 10 minutes at room temperature. The tubes were then centrifuged at 1200 rpm at room temperature for 10 minutes, the supernatant was once more discarded, and the pellet re-suspended by flicking. 1 ml of fixative was added whilst flicking, and was made up to a total volume of 10 ml. It was left for a final period of 30 minutes, and then centrifuged at 1200 rpm for 10 minutes at room temperature. The supernatant was discarded for the final time and filled to approximately 10 ml with 3:1 fixative and stored at -20^{0}C.

Chromosome Preparations from Fixed Cell Suspension

Falcon tubes containing the cell suspension were removed from the freezer and allowed to warm to room temperature after which time they were centrifuged at 1000 rpm for 10 minutes at room temperature. In an Astecaire cabinet, microscope slides were removed from degreasing solution (50% Diethyl-ether & 50% ethanol and wiped with a Kimwipe tissue). After centrifugation the supernatant was removed and the pellet re-suspended in approximately 1 ml of 3:1 fixative to achieve a suitable cell concentration. One of the clean microscope slides was taken and placed on a glass chamber so as to raise it from the bench level. Using a plastic Pasteur pipette, a drop of cell suspension was dropped onto the slide from a height of approximately 15 cm. Once the suspension had started to dry on the slide a series of concentric rainbow coloured rings appeared (Newtons rings), at this point the slide was waved back and forwards to aid the drying process. The process was repeated so that there was roughly four drops of suspension per slide. The whole process was then repeated for each group. Each slide was viewed under low objective (x20) of an Axiostar microscope, if metaphases were present and lying flat *i.e.* no white halo, more slides were prepared.

Staining Chromosomal Slide Preparations

The slides were allowed to air dry over night and were then subjected to Giemsa solid staining. A phosphate buffer was prepared using 1 tablet (pH 6.8) in 1 L of dH_2O. Giemsa was prepared by mixing 4 mls of the stain with 60 mls of the phosphate buffer in a coplin jar. Two more coplin jars were filled with the phosphate buffer. Slides were then stained for 3 minutes in the Giemsa/buffer solution and then agitated briefly in the second and third coplin jars of buffer. Finally, they were moved to a slide rack and left for a minimum of 12 hours before mounting.

Mounting Stained Chromosomal Slide Preparations

Prior to mounting, the stained slides were placed in xylene for 20 minutes to an hour in an Astecaire 3000E cabinet to aid mounting and remove excess stain. They were then laid onto filter paper and 2 drops of entellan mounting media were dropped onto the slide, followed

immediately by a glass cover slip (22 x 55 mm). Any air bubbles under the cover slip were worked out by applying pressure with forceps. Any excess entellan was blotted away with filter paper, and the slides were dried overnight, after which they were analysed.

Analysis of Metaphase Preparations

The experimental slides were analysed using a Zeiss Axioskop light microscope with a 100X oil immersion objective. At least 50 metaphases were scored for each group.

2.2.6 Lysosomal Membrane Permeability

Lysosomal permeability was measured using acridine orange (AO) uptake and relocation methods both adapted from Nicolini et al. (1979) & Rundquist et al. (1984). HF19 cells were grown on 13 mm 0 thickness covers slips in 35 mm petri dishes at a density of 1.6 $\times 10^5$ cells per dish. All cells were stained for 15 minutes with 5 μg/ml of (AO) under standard culture conditions. The method is based upon the metachromatic properties of AO, where at high concentrations it fluoresces red and at lower concentrations it fluoresces green. Acridine orange freely diffuses across the cell membrane, and is sequestered into lysosomes at high concentrations. The residual dye remains in the cytoplasm at lower concentrations where it fluoresces green.

Acridine Orange Relocation

Acridine orange relocation requires pre-loading of the cells (*i.e.* the cells are stained prior to treatment). It is then possible to monitor an increase in green fluorescence as lysosomes (red) become more permeable and leak AO into the cell cytoplasm (green). Experimental time points measured using AO relocation methods were 30 minutes and 1 hour. In this instance cells were loaded with 5μg/ml AO at ROB for 15 minutes under standard culture conditions. Following staining, cells were washed twice with PBS and fresh media was applied. They were subsequently irradiated and then prepared for imaging at the appropriate time point.

Acridine Orange Uptake

Acridine orange uptake focuses on the principle that at delayed time points following treatment rupture will have already occurred and therefore instead of monitoring the transition from red to green it looks at total red fluorescence as an indicator of permeability. For time points from 4 hours on this method was employed. Fifteen minutes prior to the time point cells were loaded with 5μg/ml AO for 15 minutes. Individual cover slips were washed 4 times with PBS and prepared for imaging.

Imaging Lysosomal Membrane Permeability using Acridine Orange Uptake/Relocation Methods

As stated previously cells were grown on ethanol sterilised cover slips in 35 mm petri dishes, for at least 24 hours prior to testing. After cell loading with AO individual cover slips were washed 4 times in warmed PBS (37°C), and then mounted in warmed PBS onto a slide. The cover slips were slightly raised from the slide surface by two parallel pieces of tape running horizontally across the slide approximately 10 mm apart. These were sealed in place by one piece of tape running vertically along the slide touching one edge of the cover slip. The cells were imaged using a 488 nm argon laser and a 505-550 BP filter (for green fluorescence) and a 615 LP filter for red fluorescence on a Zeiss LSM 510 meta upright laser scanning confocal microscope.

Analysis of Lysosomal Dispersion

Images obtained from AO and uptake experiments were also used in the analysis of lysosomal dispersion. Images processed from uptake/relocation experiments were subsequently opened using Image J. Selections were made using the threshold tool on transmission images. The selection was then converted to a binary mask. The binary mask was then reduced in size using the erode tool with a new selection being made with every other erosion, this created a number of concentric rings migrating to the centre of the cell. A band was made around each ring using the make band tool to create a region of interest. Each band was added to the ROI manager and measured for fluorescence intensity.

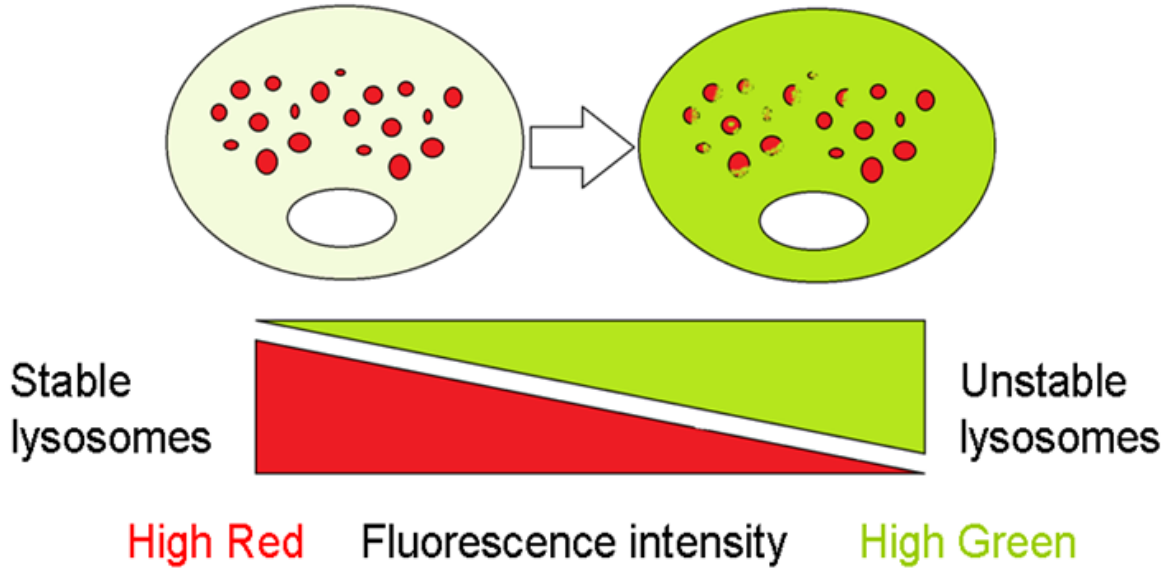

Figure 2.3: **The principle of AO uptake and relocation methods to asses lysosomal stability.** AO accumulates in lysosomes where it fluoresces red due to its high concentration. When AO is at low concentrations it fluoresces green. The AO relocation is based on AO being sequestered into lysosomes prior to treatment, after treatment lysosomal membrane permeabilization is induced causing the leakage of AO from the lysosome. A reduction in concentration of AO with the result of an increase in green fluorescence when compared to control. The AO uptake method is based on already treated cells being able to sequester less AO into lysosomes and therefore have reduced red fluorescence when compared to the control

2.2.7 Measurement of Reactive Oxygen Species

The general ROS marker CM-H_2DCFDA (2',7'dichlorodihydrofluorescein diacetate) was used to measure intracellular ROS levels after optimization in HF19. HF19 cells were seeded into black 96 well plates and measured using the Tecan Infinite F200 pro plate reader (Ex:488/Em:535). Cells were seeded at 7000 cells/well at 20 - 24 hours prior to measurement. The dye was prepared immediately before use. The dye was made into a stock solution of 1 mM in pure ethanol, it was subsequently diluted in warmed PBS (37°C) and used at a final concentration of 5 μM.

Media was removed from the wells to be tested and replaced with the PBS containing dye. Cells were incubated for 30 minutes under standard culture conditions. After 30 minutes the PBS containing dye was removed and replaced with fresh media, cells were allowed a 30 minute recovery period under standard culture conditions and then measured using the plate reader with filters of 488EX/525EM.

2.2.8 Immunohistochemistry

Cells were seeded between 20 and 24 hours prior to analysis at a density of 2×10^5 per 35 mm dish. At the appropriate time point the cells were fixed with ice cold methanol for 5 minutes at room temperature. Immediately following fixation the cells were quickly washed with PBS three times followed by three washes lasting 10 minutes whilst on a rocking table. The cells were blocked with 10% goat serum, 1%BSA and 0.3% Triton-X 100 in PBS at room temperature for 1 hour. The cells were then incubated with a 1:1500 dilution of the DNase antibody in blocking solution overnight at 4°C. The primary antibody solution was poured away and the cells were washed as above. The slide was then stained with a secondary antibody conjugated to alexafluor555 at 1:400 dilution in blocking solution for 1 hour at room temperature. The cells were washed as above with PBS and finally quickly washed with dH_2O. Finally the coverslips were mounted on top of slides with a 50:50 mixture of fluoromount G and vectasheild with DAPI, they were fixed in place with valap.

2.2.9 Nuclear Membrane Permeability

To assess nuclear membrane permeability we used a dextran translocation method adapted from Grote and Ferrando-May (2006). Prior to experimentation digitonin was dissolved in dH_2O at 20 mg/ml. This was heated to 95°C for 10 minutes, after cooling to room temperature it was spun at 14,000 *g* for 5 minutes. Finally it was aliquoted and stored at -20°C. For each batch (*i.e.* each quantity dissolved in H_2O) optimum incubation times have to be calculated.

HF19 cells were seeded into Mattek dishes 20 to 24 hours prior to examination at a density of 200,000 per dish. When ready for analysis the desired group was removed from standard culture conditions. The media was removed and the cells were quickly washed with chilled PBS. From this point onwards all steps were conducted on ice; also each respective buffer was ice cold. Firstly cells were permeabilized in permeabilization buffer plus digitonin for 1 minute (time determined in optimization). After 1 minute this was removed by pipette, and permeabilization minus digitonin was added for 1 minute. A further 2 washes followed for 5 and 10 minutes in permeabilization buffer minus digitonin. After the final wash the cells were equilibrated in

transfer buffer for 5 minutes. After the equilibration the cells were bathed in transfer buffer containing FITC-dextran 0.2 mg/ml. The dish was allowed 5 minutes to stabilise at room temperature and then imaged using a Zeiss LSM meta confocal microscope (Ex:488 nm, Em: BP 505-550). Images were analysed using Image J, a region of interest was drawn around the nucleus and the cell fluorescence was measured.

2.2.10 Statistics

Samples and slides were coded and analysed in a blind fashion (*i.e.* slides were coded by a colleague in the research group). Raw data from all experimental groups was used to compare and calculate p values. Standard error of mean was calculated to generate Y error bars for all experimental groups. For cytogenetic results; data was subjected to Fishers exact test. Data was examined for normality, if found to be normal data was subjected to 2 tailed t-test. If non-normal data was analysed with Mann-Whitney test (SPSS).

Chapter 3

Investigating the susceptibility of HF19 cells to the induction of genomic instability in directly irradiated and bystander populations

3.1 Introduction

The initial biological consequences of IR include DNA strand breaks (Scully and Xie, 2013). These can be produced by direct interaction between the track of radiation and the DNA strand resulting in ionization and an alteration in molecular structure. They are termed direct effects (Hall and Giaccia, 2006; Scully and Xie, 2013). Alternatively the radiation can interact with a less critical structure such as water, the interaction will also cause an ionization event and result in the emission of a secondary electron (Hall and Giaccia, 2006), which itself is ionizing. The secondary electron is then free to interact with a target such as DNA inducing strand breaks and alterations, these type of interactions are termed indirect effects (Hall and Giaccia, 2006).

In many cases the cell is able to correctly repair this damage and the vast majority has been repaired 24 hours following irradiation exposure. However radiation is also able to induce

the genomic instability (GI) response. Genomic instability can be a delayed, long lasting effect following ionizing radiation exposure. It can manifest in a number of ways such as chromosomal instability, delayed reproductive cell death amongst others (Morgan, 2003; Azzam et al., 2002; Kadhim et al., 1992). The cause of radiation induced GI and why it persists over time is as yet unknown, although a number of studies have pointed at various signalling pathways such as cytokines or ROS (Irons et al., 2012; Temme and Bauer, 2013; Dickey et al., 2009; Limoli and Giedzinski, 2003; Azzam et al., 2003; Liu et al., 2012). More recently the role of epigenetics has been involved, where abnormal DNA methylation patterns similar to those seen in cancer cells were noted in the progeny of irradiated cells (Merrifield and Kovalchuk, 2013; Aypar et al., 2011).

As well as occurring in irradiated cells and their descendants GI also affects bystander cells. These are cells that have received no direct radiation exposure, but have communicated with cells that have been irradiated (Morgan et al., 2002). There are two ways in which this can occur; firstly an irradiated cell directly adjacent to a un-irradiated cell can communicate through gap junctions. The passage of signalling molecules through these result in the occurrence of radiation-like effects in the un-irradiated cell (Kandouz and Batist, 2010; Azzam et al., 2003; Autsavapromporn et al., 2013). Secondly, irradiated cells may secrete various signalling molecules into the extracellular environment. These molecules can be transferred in the media to un-irradiated bystander cells, leading to the occurrence of radiation like effects (Lehnert and Goodwin, 1997; Zhou et al., 2005). Bystander effects and GI can be linked through common factors such as increased oxidative stress and increases in various cytokines (Merrifield and Kovalchuk, 2013; Watson et al., 2000; Kadhim et al., 2004).

There are also unanswered questions regarding low dose effects. There are two classifications of low dose according to Pacific Northwest National Laboratory (2012).

1. . . . the level of radiation that we are exposed to from natural background radiation excluding medical exposures

2. . . . a dose below which it is not possible to detect adverse health effects. This level has been set by the ICRP to be at 20 rads, 20,000 mrads, or 0.2 Gy, 200 mGy. Others suggest that this level is much lower and may be as low as 1 rad.

Many of the above effects depend on the genotype of the cell being studied, the radiation type and the dose (Kadhim et al., 1998; Irons et al., 2012; Kovalchuk and Baulch, 2008). Therefore in this study we looked at CIN in directly irradiated and bystander groups at therapeutic and diagnostic doses of 2 and 0.1 Gy respectively. Chromosomal instability was also assessed in bystander groups at the same time points. An additional group was also setup where media was taken from irradiated groups at delayed time points and added to fresh cells in order to see if induction of bystander effects can occur at delayed time points.

3.2 Materials & Methods

3.2.1 Cell culture

HF19 cells were removed from liquid nitrogen and placed in standard culture conditions as described in section 2.2.1. They were grown for at least 3 passages before experimentation.

3.2.2 Experimental Design

Cells were either irradiated/sham-irradiated in flasks or 6 well plates depending on the end point. For the comet assay, cells were seeded between 20 and 24 hours prior to irradiation at a density of 2×10^5 in a 6 well plate. The comet assay samples were taken at 1/2, 1, 4, 8, 12 and 24 hours following exposure. The time started as soon as cells were exposed to radiation or the bystander media. Cells were grown in T75 flasks for chromosomal analysis at a density of 1.5×10^6. Cells were irradiated using the MXR-321 X-ray source. Following irradiation cells were returned to standard culture conditions as soon as possible. Bystander groups were established 4 hours after irradiation *i.e.* irradiated cells were incubated for 4 hours following irradiation; the media was then removed filtered and added to un-treated cells to create each respective bystander group for both tissue culture flasks and 6 well plates. Direct groups were incubated for 24 hours after exposure at which point they were sub-cultured. Bystander groups were sub-cultured 24 hours after the addition of the donor media. At 20 population doublings (PD), approximately 12 passages, a secondary bystander group was established. Media was taken from the direct irradiated cells and added to control cells in order to test if the bystander signal is still active at delayed times.

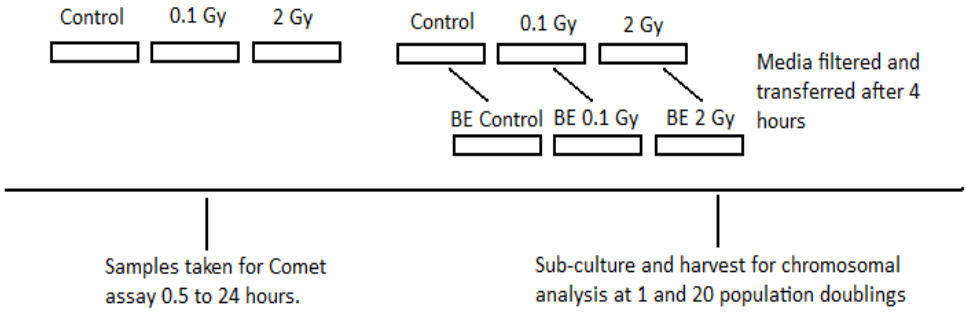

Figure 3.1: **Experimental design to investigate GI and BE induction in HF19 following exposure to X-rays** Direct and bystander groups were established and examined for early DNA damage with the comet assay over a 24 hour period. The cells were maintained for another 20 population doublings and examined for chromosomal instability as well as DNA damage again with the comet assay.

3.2.3 Chromosomal Analysis

Samples were taken at 1 and 20 population doublings, from direct and bystander groups exposed to 0, 0.1 or 2 Gy. At 20 population doublings a secondary bystander group was established to examine the longevity of signal production, media was taken from 0, 0.1 and 2 Gy and added to un-treated cells. The procedure was described in section 2.2.5; briefly cells were suspended in metaphase using the microtubule inhibitor demecolcine. The cells were collected in 75 mM potassium chloride solution for 20 minutes. They then underwent a series of fixation steps with Carnoys fixative (25% glacial acetic acid:75% methanol). Finally the suspension was dropped onto clean microscope slides and stained for analysis. Fifty metaphases were scored per group.

3.2.4 Comet assay

Samples were taken at 1/2, 1, 2, 4, 8, 12 and 24 hours as well as 20 population doublings. Described in section 2.2.4 the comet assay was used to measure total DNA damage. Briefly, cells were harvested and 20,000 cells were re-suspended in LMPA and aliquoted onto an ice cold slide precoated with NMPA. The slides were then placed under an electrophoretic field allowing the fragmented DNA to run in the agarose. The slides were then scored using a fluorescent

microscope and Komet 5.5 software. Four hundred comets were scored from 2 separate but parallel experiments.

3.3 Results

In order to examine the susceptibility of HF19 to the induction of GI we examined total DNA damage, and chromosomal aberrations were measured. Cells were exposed to 0.1 or 2 Gy, bystander groups were also established by media transfer (Section 2.2.3). Chromosomal aberrations were scored, as well as % tail DNA damage as measured by the alkaline comet assay, at early (0 - 24 hours and 1 PD) and delayed (20 PD) time points. Percentage tail DNA was chosen as an appropriate measure for the comet assay.

3.3.1 Early damage induced by X-ray exposure: Comet Analysis

To evaluate cellular response and sensitivity of HF19 cells to IR, in particular X-rays at diagnostic (0.1 Gy) and therapeutic doses (2 Gy) we used the alkaline comet assay after the radiation insult. In all experiments percentage tail DNA was used as a measure of DNA damage, results were statistically analysed using Mann-Whitney U test. Percentage tail DNA is an appropriate measure of DNA damage as it shows good linearity with dose, it also allows visualisation and comparison between establishments, example comets can be seen in Figure 3.7. Data is displayed initially as median tail DNA (Figure **??**) to highlight the average increase in magnitude of damage. Data is also displayed in box plots representing the entire population of cells to highlight the varying distributions of damage (Figure 3.3).

HF19 response to 0.1 Gy direct irradiation

HF19 cells exposed to 0.1 Gy showed significant induction of DNA damage over the first 24 hours following exposure (Figure 3.2). Initially at 30 minutes, tail DNA peaks at 11.14% $\pm$ 0.54 which was significantly increased compared to control levels 3.69% $\pm$ 0.27 ($p \leq 0.001$). It is also interesting to look at the distribution of the damage (Figure 3.3), a number of cells demonstrating tail DNA up to 60% indicating these cells were likely to be undergoing apoptosis or necrosis. After 1 hour the median tail DNA had dramatically fallen to 1.79% $\pm$ 0.23 compared to the control at 2.84% $\pm$ 0.23 ($p \leq 0.001$) indicating active DNA repair. As time progresses through 4 and 8 hours DNA damage was shown to have increased to significant levels ($p \leq .001$

and p $\leq$.01 respectively). Eventually at 12 hours, DNA damage had returned completely to control levels and this was maintained until the 24 hour time point. At 12 hours the level was still slightly elevated (4.31% $\pm$ 0.34) compared to control (3.99% $\pm$ 0.22) however this was not significant. When examining Figure 3.3 it is still possible to observe the increased distribution of damage; At 24 hours the median tail DNA (3.30% $\pm$ 0.26) was much more in line with the control value (3.86% $\pm$ 0.19) and the distribution of damage similar to that of control groups indicating the cellular DNA had been repaired. Example comets can be observed in Figure 3.7.

HF19 response to 2 Gy direct irradiation

The response after exposure to 2 Gy X-ray correlates with published data regarding DNA repair kinetics. There was a large increase in DNA damage at 1/2 hour (28.20% $\pm$ 0.59) this was observed to slightly decrease at 1 hour by approximately 5% to 23.64.0% $\pm$ 0.69 (Figure 3.2). At both time points (1/2 and 1 hour) the percentage of damage was observed to be between 40 - 50% tail DNA (both are significant at p $\leq$ 0.001), as shown in Figure 3.3. At 4 hours, levels had dramatically reduced, however they remained significantly elevated above control (p $\leq$ 0.001), It is clear to observe when viewing Figure 3.3 come that there were a number of cells demonstrating large levels of tail DNA. At 8 hours tail DNA had reduced further and there were less cells showing extensive DNA damage, this pattern was repeated until 24 hours at which point DNA damage was significantly reduced. Example comets can be observed in Figure 3.7.

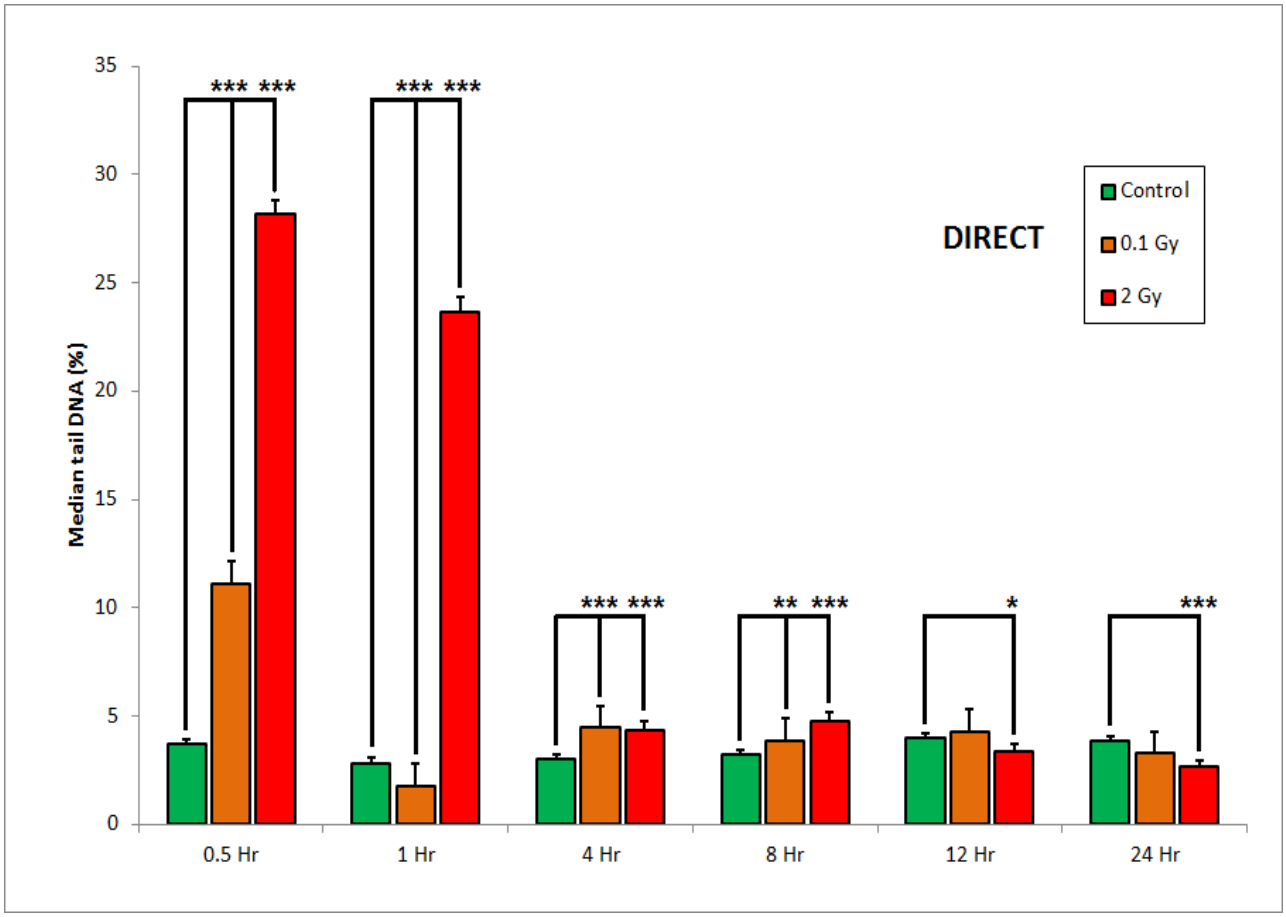

Figure 3.2: **DNA damage measured by comet assay (% tail DNA) 30 minutes to 24 hours following irradiation.** Thirty minutes following irradiation there were large increases in DNA damage, even apparent at 0.1 Gy. At one hour 0.1 Gy damage had returned to control levels, although cells exposed to 2 Gy were still shown to have elevated damage. Levels remained elevated across the 24 hour period in cells exposed to 2 Gy and remained significantly elevated until 24 hours. Between 8 and 12 hours DNA damage had returned to control levels with no significant difference until 24 hours (*=≤0.05, **=≤0.001 ***=≤0.0001).

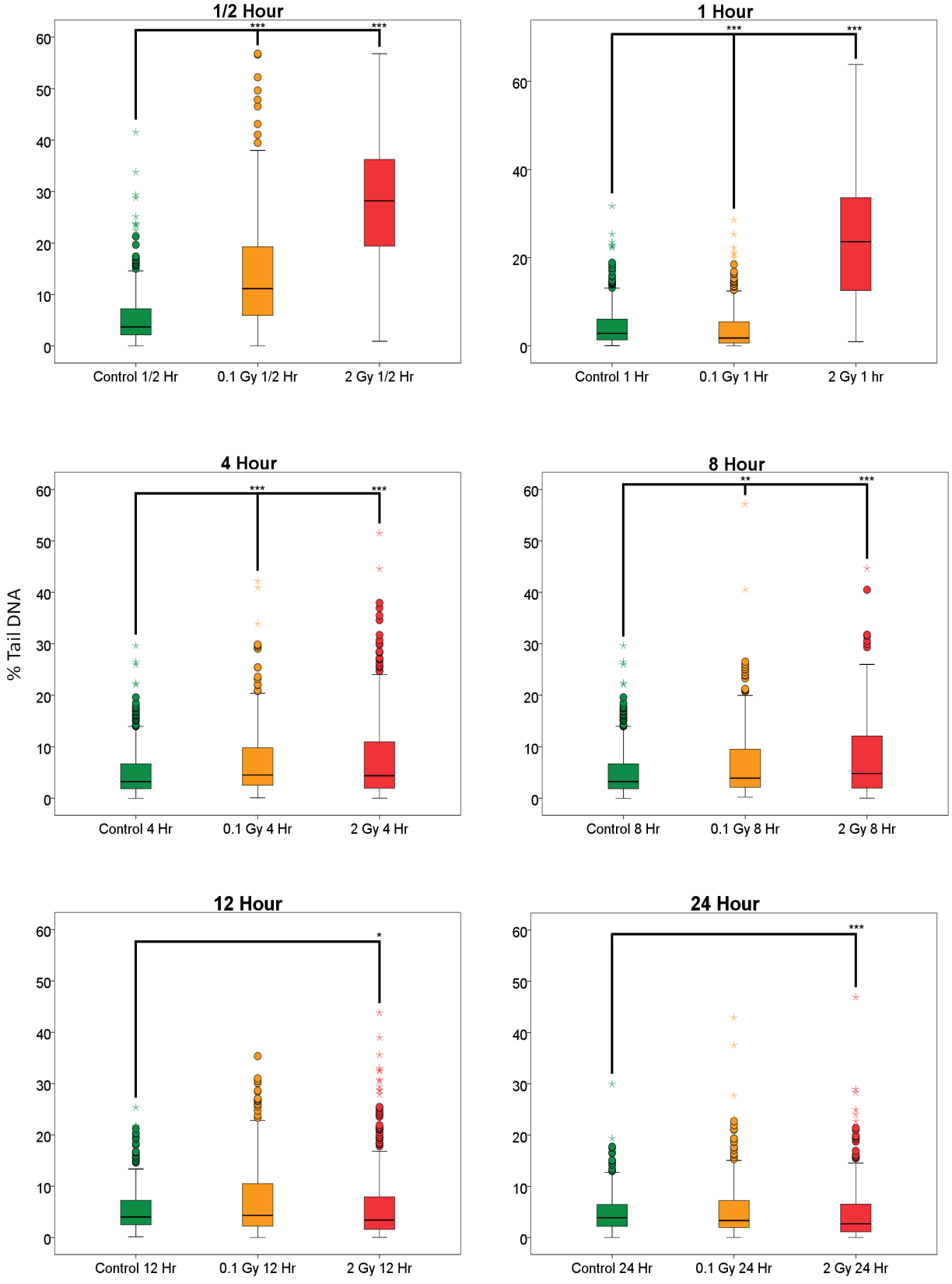
1/2 Hour
1 Hour
4 Hour
8 Hour
12 Hour
24 Hour
% Tail DNA
Control 1/2 Hr
0.1 Gy 1/2 Hr
2 Gy 1/2 Hr
Control 1 Hr
0.1 Gy 1 Hr
2 Gy 1 hr
Control 4 Hr
0.1 Gy 4 Hr
2 Gy 4 Hr
Control 8 Hr
0.1 Gy 8 Hr
2 Gy 8 Hr
Control 12 Hr
0.1 Gy 12 Hr
2 Gy 12 Hr
Control 24 Hr
0.1 Gy 24 Hr
2 Gy 24 Hr

Figure 3.3

Figure 3.3 *(previous page)*: **DNA damage measured by comet assay (% tail DNA) 30 minutes to 24 hours following irradiation.** Cells were irradiated and returned to normal culture conditions as soon as possible following irradiation. Samples were taken at the designated time point. The box-plot shows the distribution of damage, it was evident that early after exposure to 2 Gy there was the greatest range of damage with the majority falling between 25-35% tail DNA at 30 minutes and 15-25% tail DNA at 1 hour. Some cells still exhibited extensive damage 4 and 8 hours with the majority returning to just above control levels at 12 and 24 hours. 0.1 Gy cells had significantly elevated DNA damage at 30 minutes although to a much lesser extent than 2 Gy. Similar patterns were noted between 0.1 Gy and 2 Gy throughout the remaining time period in terms of damage distribution (*=≤0.05, **=≤0.001 ***=≤0.0001)

.

HF19 response to 0.1 Gy bystander signals

There was no induction of a BE, in terms of DNA damage, observed 30 minutes following irradiation (Figure 3.4). However at 1 hour there was a significant increase in damage with more cells classed as outliers *i.e.* some cells exhibited large levels of damage rather than a general increase. Over 4 and 8 hours there was no significant induction of DNA damage although levels were slightly elevated. DNA damage was observed to be significantly elevated 12 hours after receiving the bystander signals. Finally at the 24 hour time point, levels had returned to control values although there were some cells that exhibited damage within the 20 - 30% region of tail DNA.

HF19 response to 2 Gy bystander signals

The response was very similar to that of 0.1 Gy in terms of time and magnitude. Initially at 30 minutes there was no significant induction however there were a number of outliers extending up to 50% tail DNA (Figure 3.5). At 1 hour the bystander signals were seen to have significantly induced DNA damage although the median remained fairly close to control the distribution had shifted upwards. At 4 hours the level of damage remained significantly elevated with similar levels to those observed at 1 hour. By 8 hours the tail DNA was shown to have remained elevated although not significant. Finally at 12 and 24 hours the % tail DNA was observed to be elevated to significant levels (Figure 3.5). The pattern appears to be oscillatory in nature.

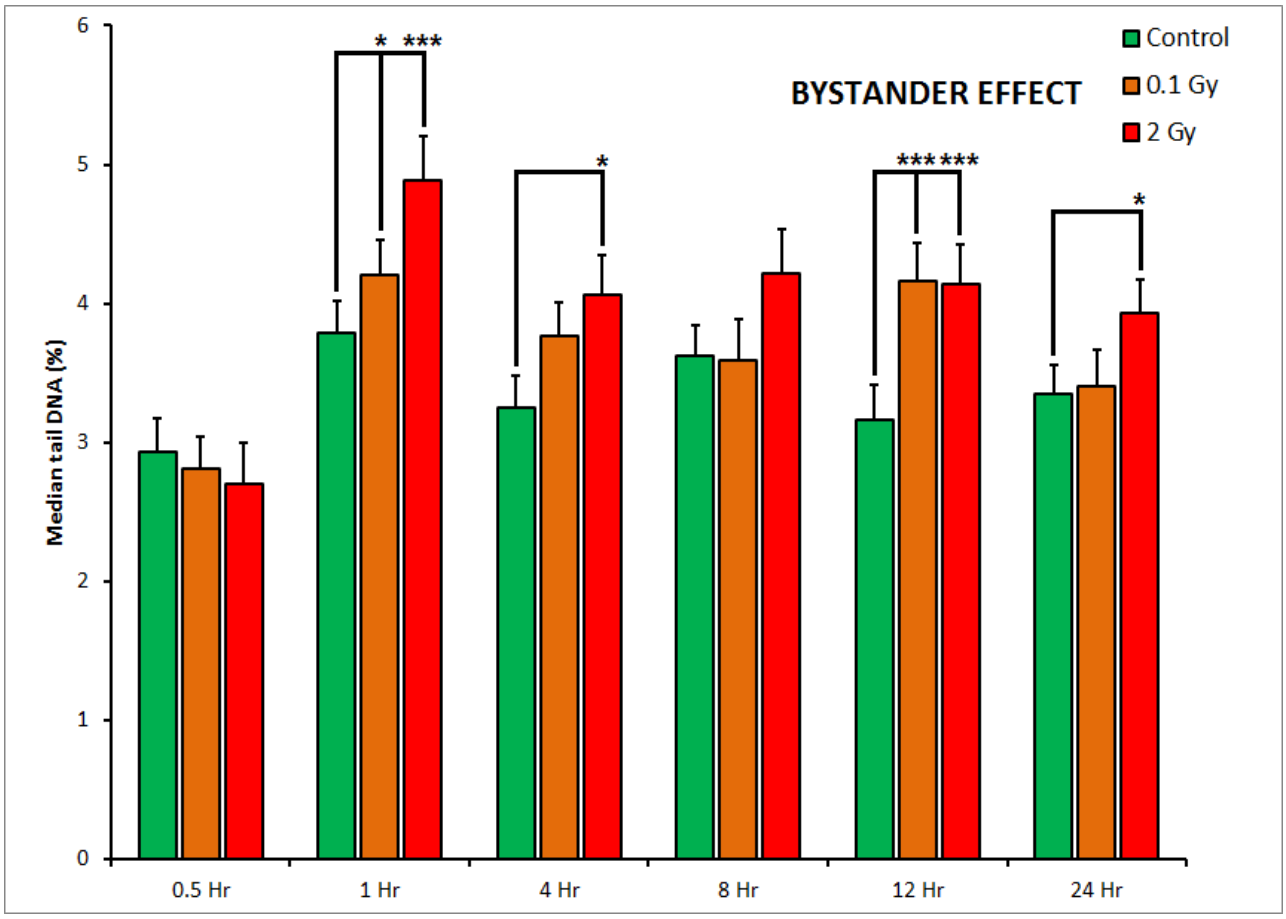

Figure 3.4: **DNA damage measured by comet assay (% tail DNA) 30 minutes to 24 hours following exposure to bystander medium.** Cells were irradiated and returned to normal culture conditions as soon as possible following irradiation. Media was taken 4 hours after exposure, filtered and added to fresh cells to create bystander groups. Samples were taken at the designated time point. The box-plot shows the distribution of damage (*=≤0.05, **=≤0.001 ***=≤0.0001)

.

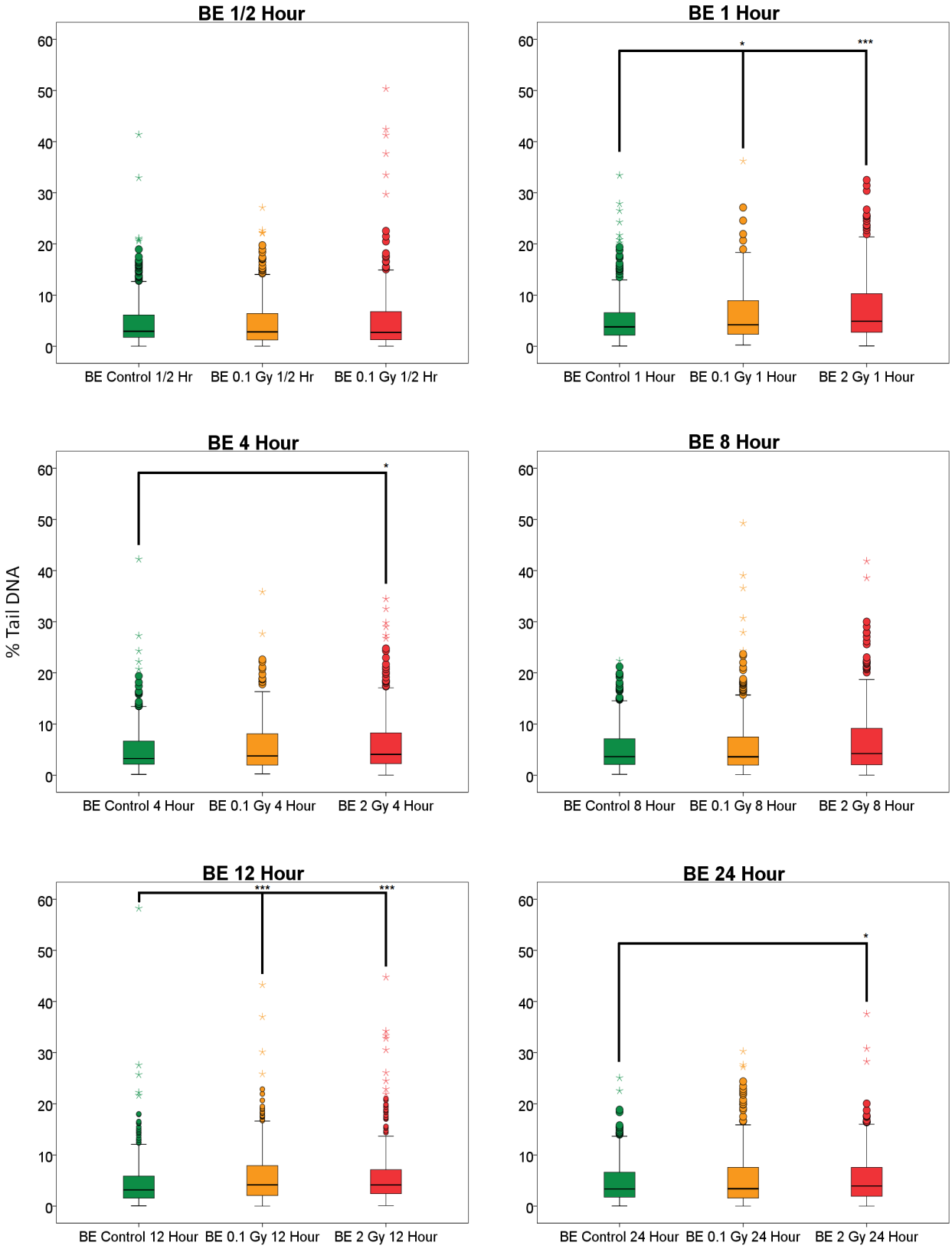
BE 1/2 Hour
BE 1 Hour
BE 4 Hour
BE 8 Hour
BE 12 Hour
BE 24 Hour
% Tail DNA
0
10
20
30
40
50
60
*
***
BE Control 1/2 Hr
BE 0.1 Gy 1/2 Hr
BE 0.1 Gy 1/2 Hr
BE Control 1 Hour
BE 0.1 Gy 1 Hour
BE 2 Gy 1 Hour
BE Control 4 Hour
BE 0.1 Gy 4 Hour
BE 2 Gy 4 Hour
BE Control 8 Hour
BE 0.1 Gy 8 Hour
BE 2 Gy 8 Hour
BE Control 12 Hour
BE 0.1 Gy 12 Hour
BE 2 Gy 12 Hour
BE Control 24 Hour
BE 0.1 Gy 24 Hour
BE 2 Gy 24 Hour

Figure 3.5

Figure 3.5 *(previous page)*: **DNA damage visualised by comet assay (% tail DNA) 30 minutes to 24 hours following exposure to bystander medium.** Cells were irradiated and returned to normal culture conditions as soon as possible following irradiation. Media was taken 4 hours after exposure, filtered and added to fresh cells to create bystander groups. Samples were taken at the designated time point. The box-plot shows the distribution of damage (*=≤0.05, **=≤0.001 ***=≤0.0001)

Induction of GI in HF19 at delayed time points

We also examined DNA damage at delayed time points (Figure 3.6). As well as direct and bystander populations a secondary bystander group was set up from direct groups (0, 0.1 and 2 Gy) at 20 PD, briefly media was taken from these direct groups and filtered as before in a similar fashion to that of normal bystander media prior to being added to control cells.

Increased basal DNA damage in HF19 at 20 population

The data clearly shows an increase in DNA damage at the delayed time point (20 PD) across all groups when compared to control (0 Gy = 4.76% ± 0.13 : 0.1 Gy = 6.86% ± 0.17 : 2 Gy = 7.80% ± 0.36). Cells directly irradiated at both doses demonstrated significant DNA damage ($p \leq 0.001$, $p \leq 0.0001$ respectively). 0.1 Gy and 2 Gy showed very similar levels of tail DNA (Figure 3.6), the 2 Gy group showed some cells with more extensive damage reaching in excess of 70% tail DNA. Interestingly bystander groups almost mimicked exactly those cells directly exposed, both 0.1 Gy (7.63% ± 0.21) and 2 Gy (8.24% ± 0.95) were significantly above control (5.34% ± 0.23) ($p \leq 0.001$), again the population exposed to 2 Gy showed some cells with more extensive damage although these were lower than that of the 2 Gy direct group. The secondary bystander effect groups were shown to have elevated levels of DNA damage which were significant although to a lesser extent than those of the classic bystander and direct groups ($p \leq 0.001$). The distribution in this group was much more even across all groups including the control, although there was an increase in the mean tail DNA (0 Gy = 5.45% ± 0.26 0.1 Gy = 5.85 ± 0.30 2 Gy = 6.00% ± 0.26).

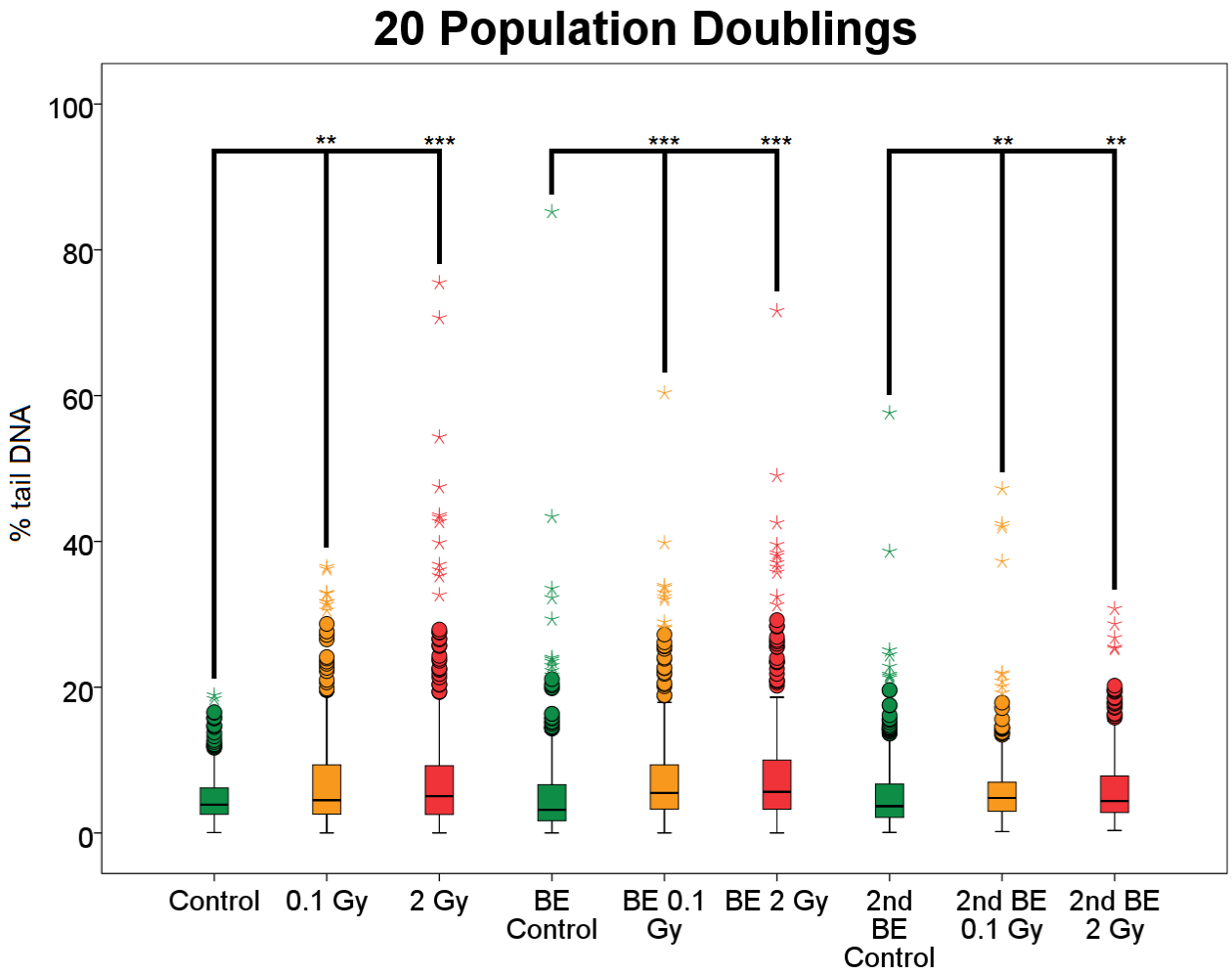

Figure 3.6: **DNA damage measured by comet assay (% tail DNA) 20 population doublings following irradiation (0, 0.1 and 2 Gy) in HF19 direct and bystander populations after.** It is evident that DNA damage was elevated across all treatment groups. The greatest increase was observed in the 2 Gy direct group and 0.1 Gy direct group. Bystander populations also demonstrated significant levels of tail DNA at both doses. The secondary bystander group was observed to have the smallest increase although this was still significant(*=≤0.05, **=≤0.001 ***=≤0.0001)

.

It is evident that DNA damage was elevated across all treatment groups. The greatest increase was observed in the 2 Gy direct group and 0.1 Gy direct group. Bystander populations also demonstrated significant levels of tail DNA at both doses. The secondary bystander group was observed to have the smallest increase although this was still significant. Example comets can be observed in Figure 3.7.

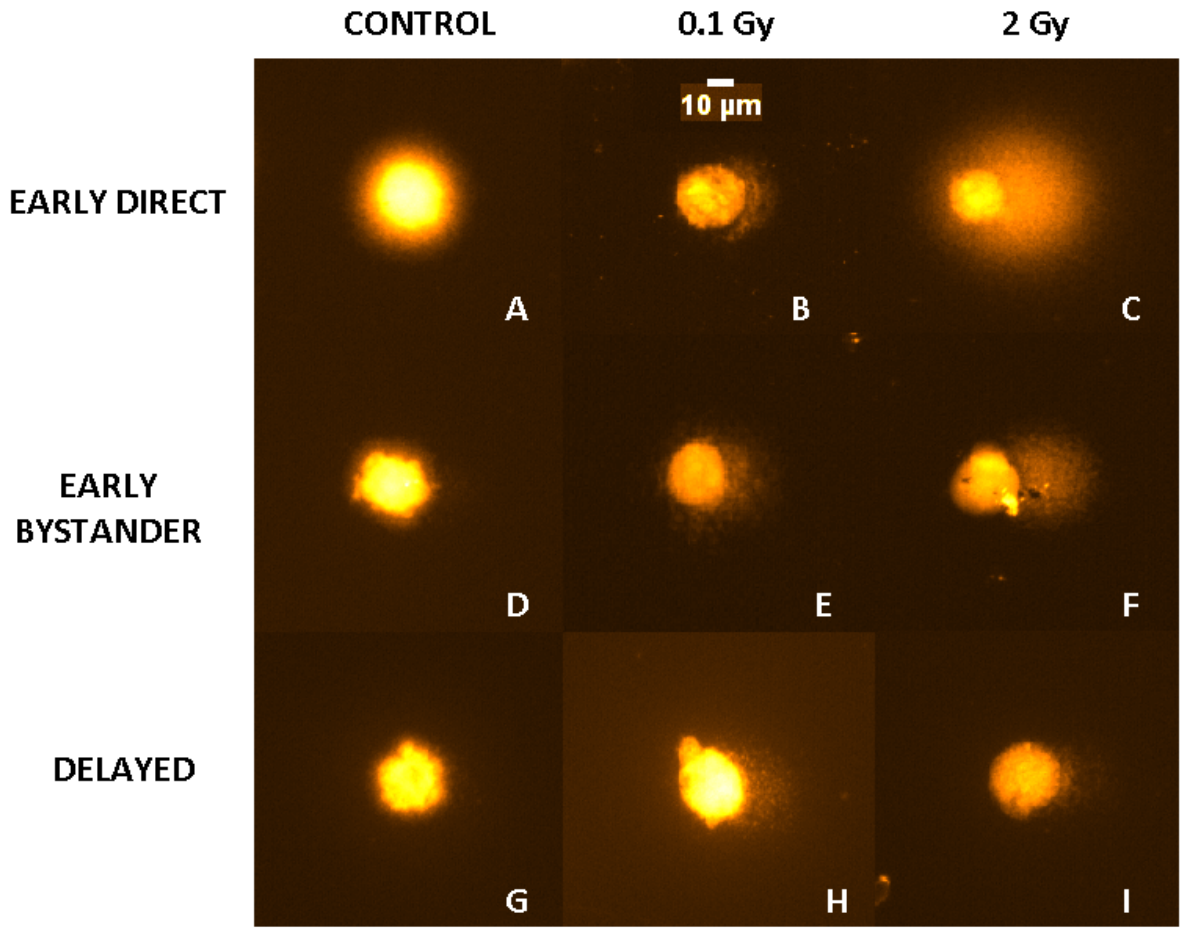

Figure 3.7: **DNA damage was measured by comet assay in HF19 cells following irradiation and exposure to bystander conditions.** HF19 cells were imaged using a fluorescent microscope, typical comets are shown from HF19 cells. Example comets **A:** Control HF19 cell early after irradiation, there is very little evidence of any tail DNA *i.e.* there is a clear boundary around the head. **B:** HF19 cells exposed to 0.1 Gy within 1 hour following radiation show some tail DNA. **C:** HF19 cells exposed to 2 Gy show an extensive tail indicating large levels of DNA damage. **D:** Bystander groups were also analysed, as in direct groups, control cells showed very little damage. **E:** Bystander cells exposed to 0.1 Gy bystander media demonstrated a small increase in DNA damage as did the 2 Gy bystander group (**F**). The cells where sub-cultured and then analysed at 20 population doublings. **G** Control cells did not show any change in levels of damage however 0.1 Gy (**H**), 2 Gy (**I**) showed small increases in DNA damage.

3.3.2 Chromosomal Instability is induced by X-rays at early and delayed time points

Chromosomal aberrations were used to assess the induction of CIN (Figure 3.10). The results for 1 population doubling indicate that radiation even at relatively low doses (0.1 Gy) that are relevant to diagnostic procedures can induce CIN.

CIN induced after exposure to 0.1 and 2 Gy at 1 population doubling

Early chromosomal analysis (PD 1) of cells exposed to 0.1 Gy showed significant induction of chromosomal aberrations with a mean number of aberrations per cell of 0.22 ± 0.066. when compared to the control (0 Gy), see figure 3.8. Those cells exposed to 2 Gy showed double the number of aberrations (0.44 ± 0.10) indicating a relationship to dose as suggested above. The cells exposed to 2 Gy also demonstrated some metaphases with multiple aberrations.

The bystander cells showed no induction of genomic instability in any of the groups with levels of chromosome damage identical to those of the direct control group, although the level of chromosome damage in the 2 Gy group was observed to be slightly elevated (0.08 ± 0.04) above the control (0.06 ± 0.033). This indicated the lack of or inability of any signal to produce chromosomal aberrations at this time point.

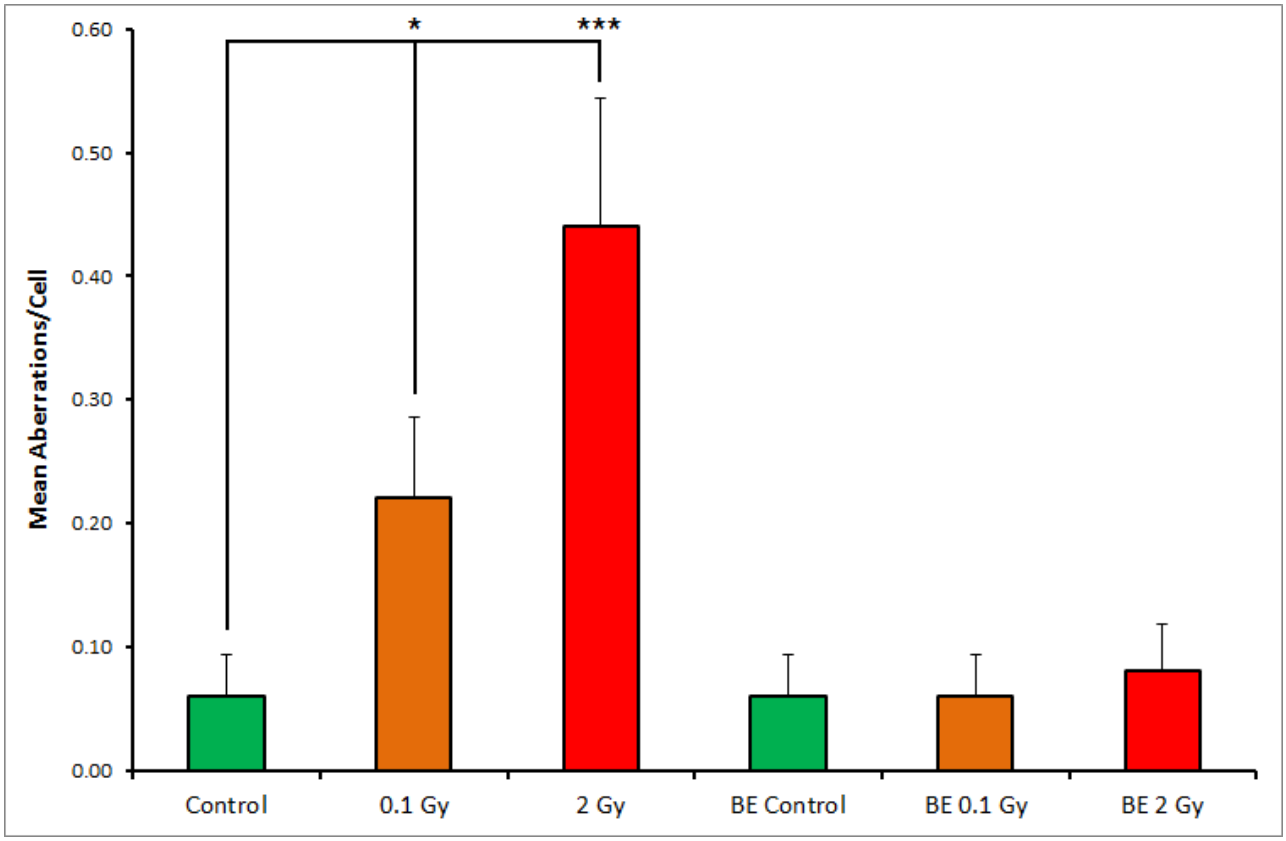

Figure 3.8: **Mean chromosomal aberrations per cell 1 population doubling (PD) following 0.1 and 2 Gy X-ray exposure in direct and bystander groups.** Cells were exposed to either 0.1 or 2 Gy radiation exposure directly or through media transfer. After 1 population doubling cells directly exposed to radiation (0.1 Gy and 2 Gy) both demonstrated significant levels of chromosomal instability. Bystander groups showed no induction of CIN after 1 population doubling(*=≤0.05, **=≤0.001 ***=≤0.0001).

CIN induced after exposure to 0.1 and 2 Gy at 20 population doublings

The chromosome analysis results at 20 population doublings were shown to differ slightly from results obtained at 1 PD, as shown in figure 3.9. Firstly HF19 cells exposed to 0.1 Gy direct irradiation show no significant induction of CIN (0.16 ±0.07) when compared to the 0 Gy control (0.06 ± 0.03). However those exposed to 2 Gy still demonstrated a significant ($p \leq 0.05$) increase in average chromosomal aberrations per cell (0.24 ± 0.06).

A similar effect was observed in bystander groups with the 2 Gy bystander cells showing 0.40 ±0.057 mean aberrations per cell, which was significantly elevated ($p \leq 0.05$) above the 0 Gy bystander group (0.04 ±0.03). However, although the 0.1 Gy bystander group demonstrated an

elevation in the number of mean aberrations per cell (0.14 ±0.0572) this was not significantly different from the control level.

None of the cells exposed to secondary bystander conditions demonstrated significant induction of chromosomal aberrations. Both groups showed an increase in chromosomal aberrations although the increase was negligible. Example aberrations can be observed in Figure 3.10.

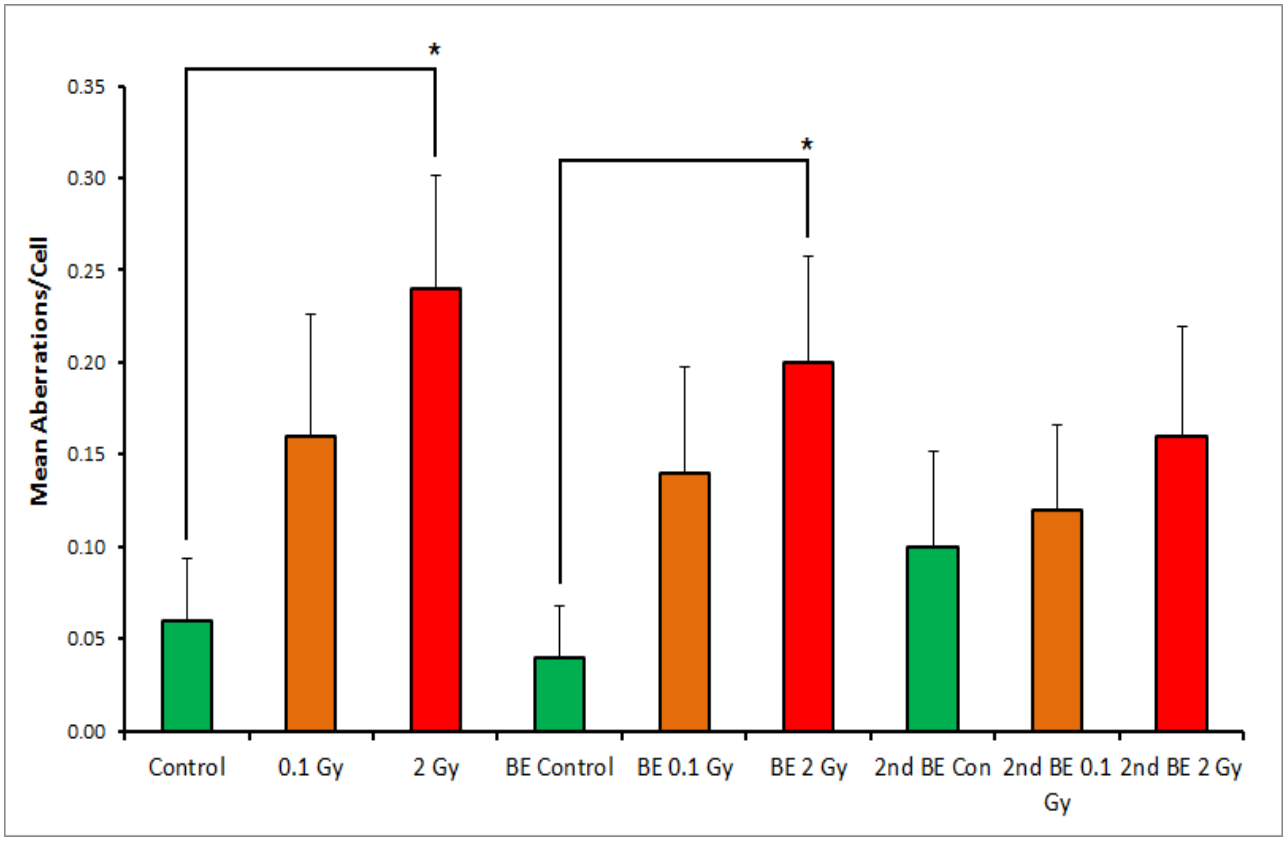

Figure 3.9: **Mean chromosomal aberrations per cell 20 population doublings following 0.1 and 2 Gy X-ray exposure in direct and bystander groups.** Cells were exposed to either 0.1 or 2 Gy radiation exposure directly or through media transfer. After 20 population doubling cells directly exposed to 2 Gy X-rays showed a significant induction of CIN, conversely, cells exposed to 0.1 Gy showed an increase, however this was insignificant. The same effect was observed in bystander groups with 2 Gy demonstrating significant levels of CIN and 0.1 Gy showing an increase but not significantly. The secondary bystander effect demonstrated no significant levels of chromosomal instability in the treated groups (*=≤0.05)

.

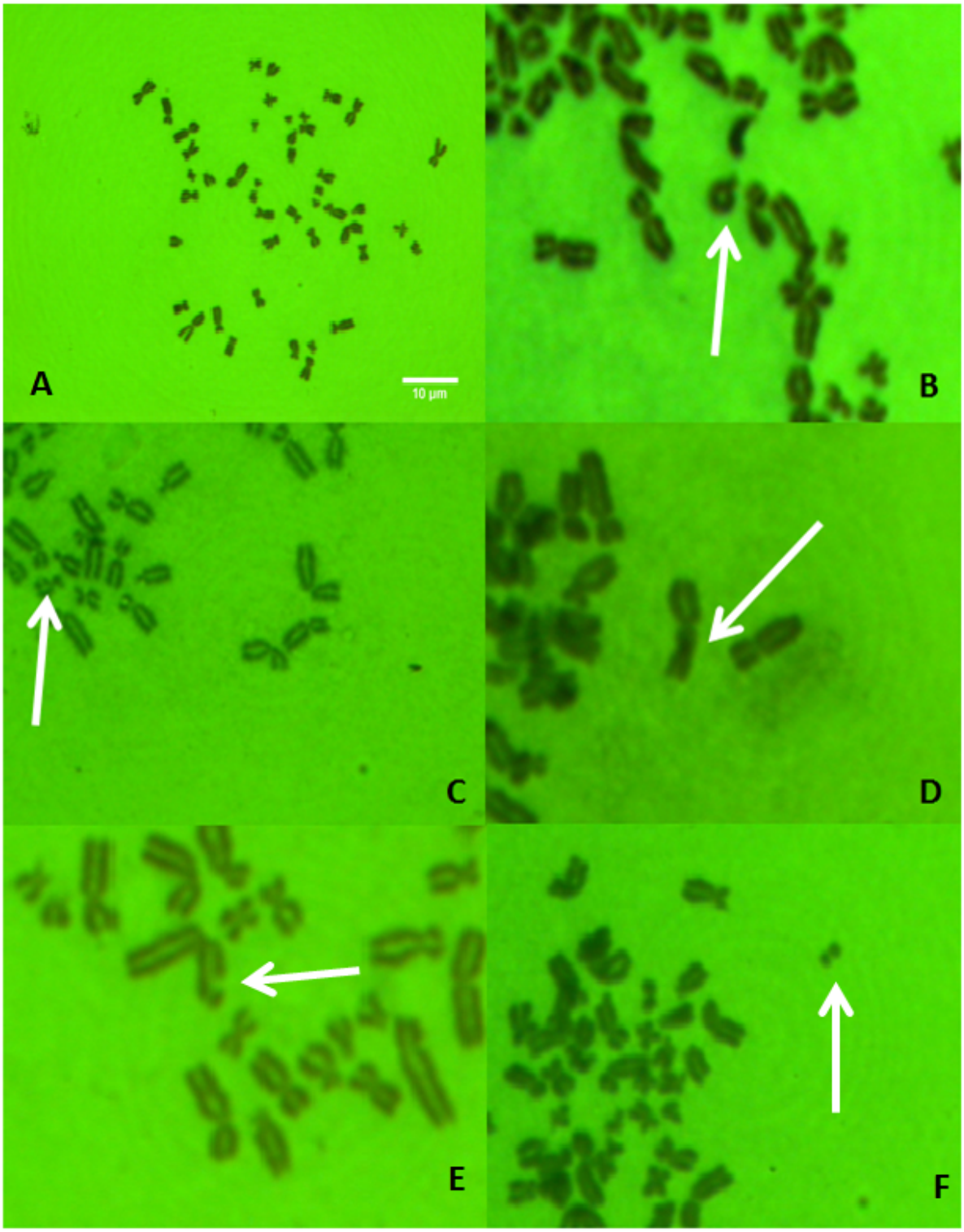

Figure 3.10: **Typical aberrations seen in directly irradiated and bystander HF19 cells** **A:** HF19 metaphase showing no chromosomal 46xx genotype with no chromosomal aberrations. **B:** The appearance of a ring and fragment in a HF19 metaphase. **C:** A chromatid gap in a HF19 metaphase, one of the most common aberrations. **D:** An isochromatid break in HF19 metaphase. **E:** A chromatid break, a more extreme version of a chromatid gap. **F:** An acentric fragment that has migrated away from its the chromosome which it originated.

3.4 Discussion

Genomic instability is a relatively new phenomenon still with many unanswered questions. We do however understand some processes that appear after IR at delayed time points (Watson et al., 2001; Kadhim et al., 1998). It is also documented that it can manifest as chromosomal instability as well as other cellular aberrations (Kadhim et al., 1992; Limoli and Giedzinski, 2003; Han et al., 2010). It is also understood that genetic factors play a large part in GI induction as well as radiation quality and dose (Kadhim et al., 2006; Karotki and Baverstock, 2012). We therefore investigated the susceptibility of the primary human fibroblast, HF19, to the induction of radiation induced GI at 1 and 20 population doublings at doses of 0.1 and 2 Gy.

Our results demonstrated high initial DNA damage seen by the comet assay in both directly irradiated and bystander populations of HF19. From these results we can speculate that HF19 demonstrate a typical DNA damage response from its biphasic nature, where simple damage is removed relatively quickly leaving more complex damage to linger over the 24 hour period (O'Connor et al., 2000; Banth et al., 2004). It is also possible to suggest that some cells are undergoing apoptosis/necrosis from the comet assay distribution (Figure 3.1 1/2 hour and 1 hour) with some cells showing as much tail DNA as 80%. These results also show an increase in DNA damage in bystander groups (Figure 3.4, 3.5). There is no difference after 30 minutes incubation with the bystander signal suggesting it takes some time for the factor to exert its effects, although there are some cells exposed to 2 Gy that show large levels of tail DNA. At 1 hour there is a spike in DNA damage at both doses although only a small increase from 3.79% $\pm$0.23 (0 Gy) to 4.21% $\pm$0.25 (0.1 Gy) and 4.89% $\pm$0.31 (2 Gy). Although this is only small it is possible to see the increased distribution in Figure 3.5 1 hour. Recently Furlong et al. (2013) reported changes in gene expression as early as 1 hour post radiation in doses as low as 0.05 Gy in bystander cells. This result proved that a bystander signal is produced within the first 4 hours following irradiation and that the signal has a detrimental effect on HF19 cells.

At 4 hours, the bystander 2 Gy group still shows a significant level of DNA damage however, this effect is not observed after 0.1 Gy exposure. Nevertheless, looking at the 4 hour time point on Figure 3.5 both distributions in the treated groups look similar. As time progresses to 8 hours

neither dose shows a significant induction but results show that the median tail DNA is still increased in the 2 Gy group (Figure 3.4). At 12 hours both doses show significantly increased tail DNA which is again maintained at 24 hours in the 2 Gy bystander group but not in the 0.1 Gy group. This could suggest that the early BE is oscillating in nature, potentially the cell is shifted from its steady state and while the cell is adjusting it is placed under stress leading to slightly elevated basal levels of DNA damage. There are far fewer cells showing massive DNA damage as seen in the direct group (Figure 3.3) in excess of 30% tail DNA. Lev Bar-Or et al. (2000) reported a mathematical model which suggests that p53 activity is oscillatory in response to γ-rays; they suggested this may avoid the consequences of prolonged p53 activation. This may explain why we observe the slight fluctuations in the level of DNA damage.

The DNA damage data at 20 population doublings indicate that HF19 are susceptible to the induction of GI and BE in the progeny of the irradiated bystander populations (Figure 3.6). In the direct group both doses show significant induction of DNA damage, the effect is only marginally greater in 2 Gy. There are a number of cells that show extensive damage in the 2 Gy group. The bystander groups are both significant as in the direct groups, and similar to the 2 Gy direct group there are a number of cells showing larger levels of tail DNA. Finally the secondary BE effect shows significant increases in tail DNA however the change is much smaller than that observed in the other groups. Although the increases are only slight in each case (1-3%) looking at Figure 3.6 it is possible to see a shift in the distribution of damage. Work presented here, in part, agrees with that of Guryev et al. (2009) who noticed increases in DNA damage in CHO cells up to 21 days following γ-ray exposure; however they then noticed that levels returned to that of control. This highlights the transient and possibly oscillatory nature of these effects. To see if this was the case with HF19 cells more time points would be required.

Although this suggests that HF19 cells are susceptible to GI and BE we also examined HF19 for CIN through cytogentic analysis of chromosomal aberrations. A well known manifestation of GI, CIN is a more reliable method than the comet assay particularly at the delayed time points. Each group was analysed at 1 and 20 population doublings. As expected, 1 population doubling after cells were exposed to X-rays led to an increase in chromosomal aberrations, that appeared to be dependent on dose, this agrees with work published by Mosesso et al. (2010). Figure 3.11 shows the type of aberrations that were encountered, across all groups: the predominant type

of aberration was chromatid in nature *i.e.* chromatid breaks or gaps (Figure 3.10).

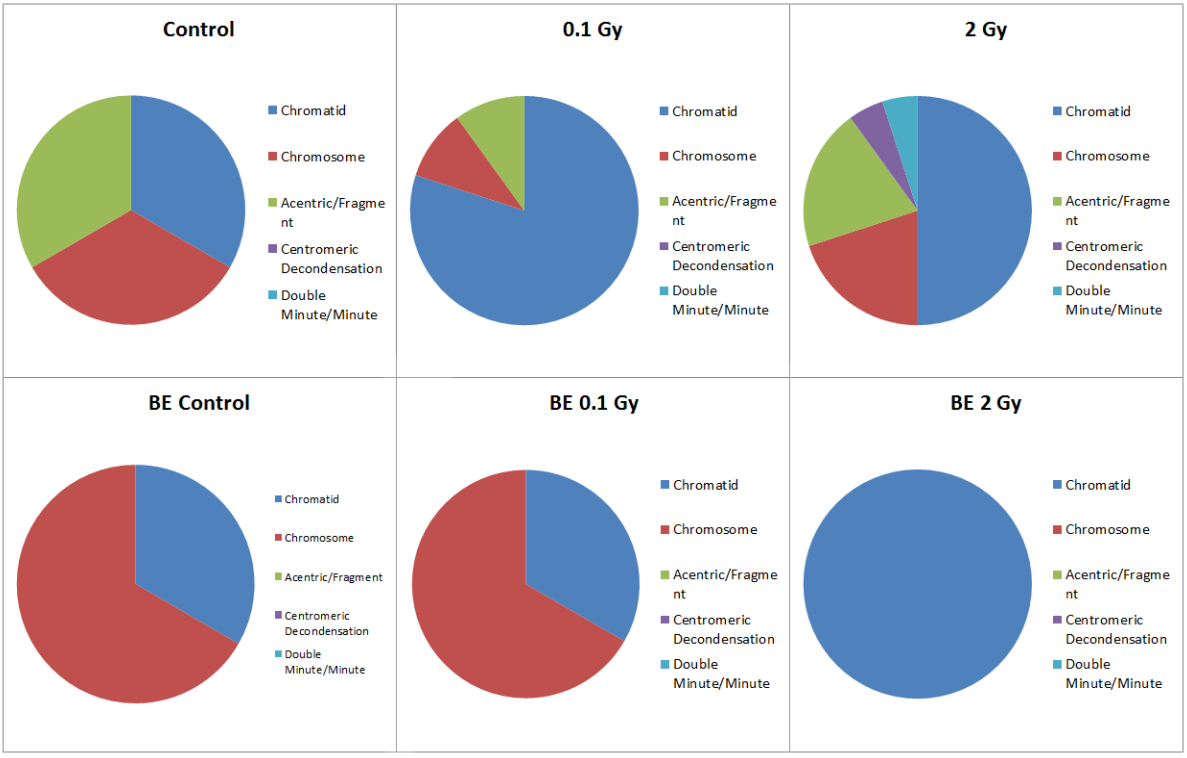

Figure 3.11: **A % breakdown of the type of aberrations observed after radiation at 1 population doubling.** Across all groups the main type of aberration was on the chromatid scale either gaps or breaks. There were also some chromosome aberrations. The 2 Gy direct group showed the greatest range in types of aberration. (Observation numbers: Control = 3: 0.1 Gy = 10: 2 Gy = 20: BE Control = 3: BE 0.1 Gy = 3: BE 2 Gy = 4.)

After 20 population doublings there was a significant induction of CIN in the 2 Gy direct irradiated group, however the cells exposed to 0.1 Gy showed an increase but this was not significant above the control levels. This might be a consequence of the fluctuations associated with these effects (discussed earlier). Alternatively 0.1 Gy maybe ineffective at inducing GI at these delayed time points; again further time points would be required to ascertain this. The predominant type of aberration (Figure 3.12) was chromatid gaps and breaks (Figure 3.10 shows examples) across all groups, similar to 1 PD.

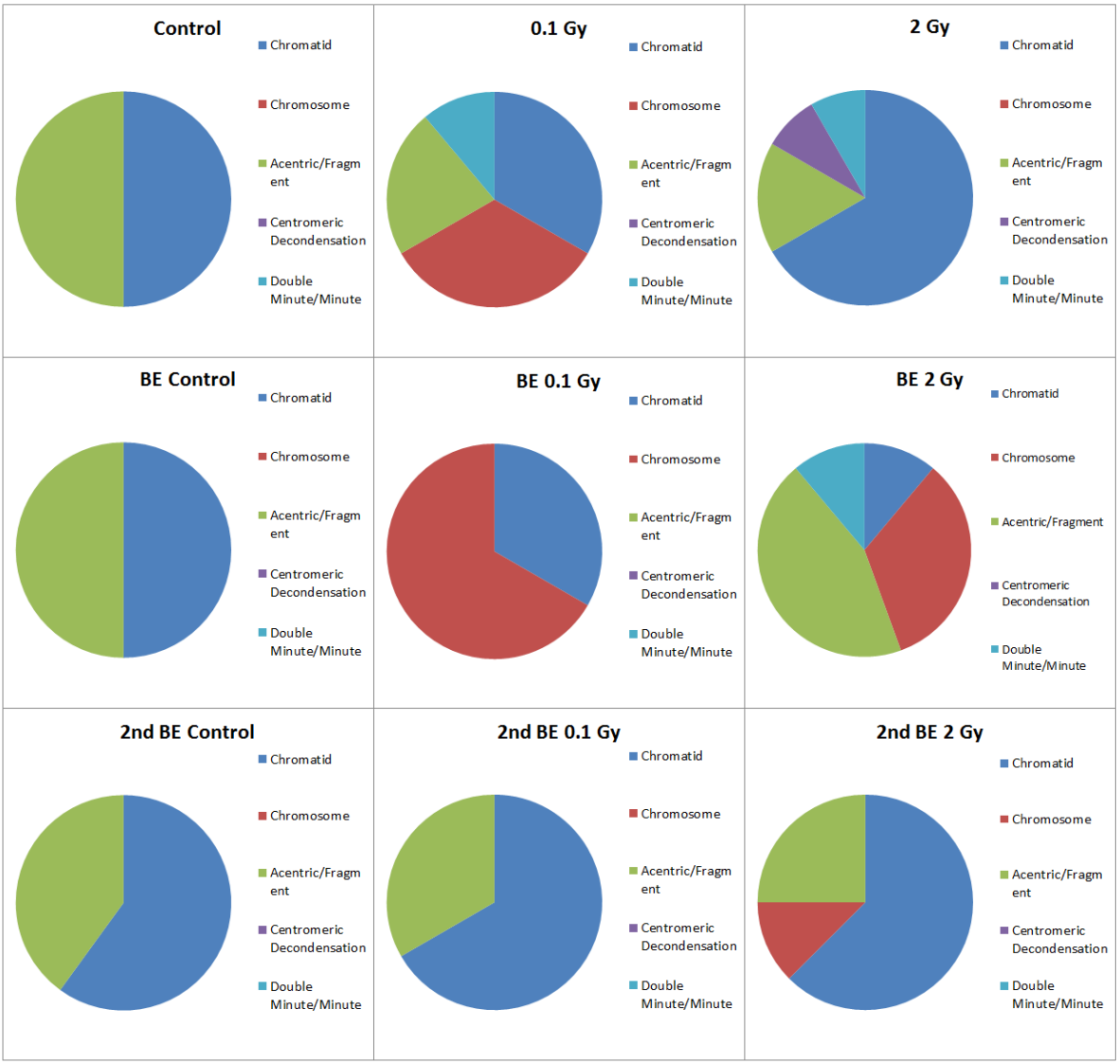

Figure 3.12: **A % breakdown of the types of aberrations observed at 20 population doublings.** The types of aberrations observation were similar to those observed at 1 population doublings, *i.e.* mainly chromatid in nature. (Observation numbers: Control = 2: 0.1 Gy = 9: 2 Gy = 12: BE Control = 2: BE 0.1 Gy = 3: BE 2 Gy = 9: 2nd BE Control = 5: 2nd BE 0.1 Gy = 6: 2nd BE 2 Gy = 8.)

The core biological process of GI induction is not fully understood (Liu et al., 2012). The actual process has been suggested to involve defects in telomeres for example the loss of, or DNA double strand breaks near telomeres that could potentially result in chromosomal rearrangements (Muraki et al., 2012). Mukherjee et al. (2012) suggest that chromosomal instability arises from an inflammatory signal as treatment with anti-inflammatory drugs significantly reduced the levels of CIN. More recently the role of epigentics has been suggested as a potential underlying

molecular mechanism (Merrifield and Kovalchuk, 2013; Kovalchuk and Baulch, 2008). However Aypar et al. (2011) demonstrated that with both low and high LET epigenetic alterations can be induced without accompanying CIN. Very little work has been conducted on lysosomal involvement, therefore having proved that HF19 were susceptible to the induction of GI, a potential role for lysosomes was investigated.

3.5 Conclusions

1. X-rays at diagnostic (0.1 Gy) and therapeutic doses (2 Gy) are able to induce DNA damage early after irradiation (0 - 24 hours), It persists in cells exposed to 2 Gy until 24 hours.

2. HF19 secretes a bystander signal within the first 4 hours following irradiation after both 0.1 and 2 Gy. This signal when placed onto fresh HF19 cells induces DNA damage after 1 hour, the damage then oscillates up and down over the next 24 hours.

3. DNA damage is increased at 20 population doublings in all direct and bystander treated groups. This indicates that HF19 are susceptible to induction of GI and BE.

4. Chromosomal aberrations are significantly elevated early after irradiation (1 PD) in direct irradiated groups. There is no appearance of chromosomal aberrations in bystander groups 1 population doubling after irradiation.

5. At 20 population doublings cells that were exposed to 2 Gy irradiation showed significant levels of chromosomal aberrations. 0.1 Gy also however showed an increase although this was not significant.

6. The delayed classical bystander group showed the same pattern as the direct groups with both doses showing an increase in chromosomal aberrations, although only 2 Gy showed significant levels. The secondary bystander effect showed no significant induction of chromosomal aberrations.

7. The main type of aberration was chromatid in nature, cells exposed to 2 Gy showed the most chromosomal type aberrations.

8. Our results show HF19 are sensitive to X-rays at 0.1 and 2 Gy, they also show that HF19 can be used to investigate potential mechanisms of GI and BE.

Chapter 4

Lysosomal instability is induced in irradiated and bystander cells following irradiation

4.1 Introduction

Lysosomes are sub-cellular organelles (described in detail section 1.4) whose primary function is to degrade various sub-cellular components such as expired organelles or damaged proteins (Oczypok et al., 2013; Chen and Karantza-Wadsworth, 2009; Luzio et al., 2007). Within the acidic lumen there are a number of acid hydrolases that degrade each type of component (Bright et al., 2005; Luzio et al., 2007; Kaminskyy and Zhivotovsky, 2012). These enzymes are held securely within the lysosome by a lipid membrane, however they are susceptible to attack from chemical species such as ROS (Younes et al., 1983), which may compromise the membrane and cause possible leakage of contents into the surrounding cytoplasm (Werneburg et al., 2004; Johansson et al., 2010).

ROS have long been implicated in tissue injury (Ryter et al., 2007). As well as physical damage to intracellular components they can also induce activation of receptors, caspases and Bcl-2 family proteins. There are a number of different types of ROS induced from radiation exposure.

One of the primary species is the hydroxyl radical formed from the radiolysis of water, it has a diffusion distance of about 4-6 nm within the cell (Roots and Okada, 1975).

It is possible the hydroxyl radical and others produced such as the peroxyl radical as well as non-radicals such as hydrogen peroxide may damage the lysosomal membrane as it is well known radicals can interact with lipids (Farmer and Mueller, 2013). It is also probable that Fenton chemistry within the lysosome maybe responsible for its rupture (Kurz et al., 2004; Persson, 2005) and, this may be a potential damaging effect seen following radiation. If ROS interact with lipids they usually initiate a chain reaction that will propagate through the membrane until a terminating event *i.e.* formation of a stable covalent bond with another radical. As the reaction propagates through the membrane it alters the lipid configuration. The deformed lipids thus compromises the functionality of the membrane.

Studies have shown that cytokines and even p53 are able to interact with the lysosomal membrane to induce alterations in its permeability, albeit through an adaptor protein called Lysosome-associated apoptosis-inducing protein containing the pleckstrin homology and FYVE domains (LAPF) (Johansson et al., 2010). It is known that p53 is a key protein for cell response to DNA damage and ionization radiation (Rashi-Elkeles et al., 2011; Hickman et al., 1994; Iliakis et al., 2003), and therefore it is also possible to speculate that this might be involved in lysosomal membrane permeabilization.

Werneburg et al. (2004) have implicated cytokines as upstream triggers for lysosomal membrane permeabilization, which subsequently lead to cathepsin activation and apoptosis. Desai et al. (2013) reported increased levels of various cytokines including TNF-α in a number of cell lines following γ-ray exposure. It is thus possible to speculate that these two processes, lysosomal membrane permeabilization and increased TNF-α production may be linked.

In this chapter we examined the effect of 0.1 and 2 Gy X-irradiation on lysosomal stability amongst other parameters through AO uptake and relocation methods. We also examined levels of ROS in direct and bystander populations, to see if these levels could be correlated with lysosomal disturbance.

4.2 Materials & Methods

4.2.1 Experimental design

In order to examine the effects of IR on HF19 lysosomes we used acridine orange (AO) uptake and relocation methods (Figure 4.1). Cells were seeded between 20 and 24 hours prior to irradiation onto 13mm coverslips within 6 well plates, 2 cover slips were used per well to provide duplicate samples covering time points at 30 minutes 1, 4, 8, 12 and 24 hours. Each well was seeded at a cell density of 2×10^5. Two techniques were used to assess lysosomal membrane permeability. AO relocation was used for early time points (30 minutes and 1 hour) and AO uptake was used for later time points (4 hours - 20 PD)(described in Section 2.2.6).

For early time points (30 minutes and 1 hour): cells were preloaded with AO 15 minutes prior to irradiation (Figure 4.1). After 15 minutes incubation with AO this was removed and replaced with media the cells were then irradiated and returned to standard culture conditions at the earliest opportunity. Each Mattek dish was then imaged at the appropriate time point. *For later time points (4 hours to 20 PD)* cells were loaded with AO 15 minutes before the time point of examination *i.e.* for 4 hours cells would have been loaded 3 hours and 45 minutes following irradiation. For bystander groups, irradiated cells had their media removed and filtered 4 hours after exposure. This was added to the recipient bystander cells, the time of addition was regarded as the treatment time.

A secondary bystander group was also created (described in Section 2.2.3 & Figure 2.2). Direct groups (0, 0.1 and 2 Gy) were sub-cultured; at 20 population doublings their media was removed and filtered. The media was then added to additionally cultured separate control flasks.

Early time points for bystander cells (30 minute and 1 hour) were treated the same as direct irradiated groups. The cells were preloaded with AO, after 15 minutes this was removed and the cells were washed. The bystander media was then added and the cells were analysed at the appropriate time point (Figure 4.1). Later time points (4 hours to 20 PD) were also analysed in bystander cells in the same fashion as direct irradiated cells. For time points that required cell culturing (1 & 20 PD), cells were seeded at a total cell density 1.5×10^6 in T75 flasks the day

prior to irradiation. Following irradiation cells were returned to culture conditions, bystander groups were processed as described in section 2.2.3. After 24 hour exposure to bystander media this was removed and fresh media was added. Twenty four hours prior to analysis cells were seeded onto 13 mm coverslips in 35 mm dishes. Fifty cells were scored from each experiment, the experiment was repeated three times on different days.

All data was statistically analysed using a 2 tailed equal variance t-test.

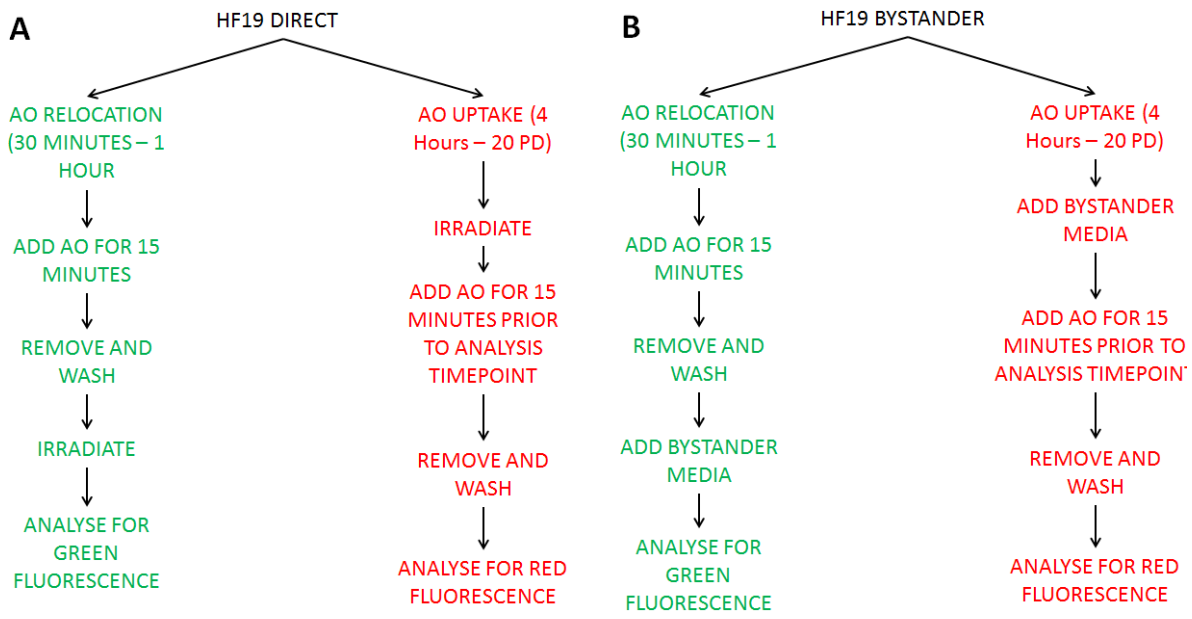

Figure 4.1: **Experimental procedure for assessing lysosomal membrane permeability in HF19 using acridine orange uptake and relocation methods.** For early time points (30 minutes & 1 hour) cells were preloaded with AO before direct irradiation (A) and addition of bystander media (B) and analysed for green fluorescence. For later time points AO uptake methods were employed. HF19 cells were directly exposed to radiation (A) or exposed to bystander media (B). They were returned to standard culture conditions 15 minutes prior to analysis AO was added. After 15 minutes this was removed, the cells were washed and analysed for red fluorescence.

4.2.2 Cell culture

As described in section 2.2.1, HF19 cells were removed from liquid nitrogen and grown for at least 3 passages in standard culture conditions.

4.2.3 Lysosomal Relocation

This technique is designed to detect early changes (30 minutes & 1 hour) in lysosomal permeability (described in detail in section 2.2.6). Briefly cells were loaded with AO for 15 minutes prior to radiation exposure. The AO was removed and the cells were washed with PBS and then returned to fresh media. At the desired time point the coverslips were removed and washed in PBS, they were then mounted on a microscope slide and imaged for green fluorescence (Figure 4.5). Fluorescence was measured using the computer programme Volocity, briefly cell outlines were selected as regions of interest using a standard bright field image. The image was then cropped and the fluorescence from the green channel was measured. For early (0 - 24 hours) direct irradiated groups; 50 cells were scored from 3 separate experiments. Cells exposed to bystander conditions, 25 cells were scored from 2 separate parallel experiments. AO was used at concentrations to minimize nuclear fluorescence however complete exclusion was impossible. In cases where lysosomes did rupture excess AO was occasionally found in the nucleus.

4.2.4 Lysosomal Uptake

This technique is designed to detect alterations in lysosomal permeability (described in detail in section 2.2.6) that occur a little later following radiation insult. Briefly, cells were stained with AO 15 minutes prior to imaging. After 15 minutes the cover-slips were removed and washed with PBS prior to being mounted on a microscope slide and imaged for red fluorescence (Figure 4.3). In order to look at lysosomal uptake cellular red fluorescence was measured in the same was as cellular green fluorescence. For direct and bystander cells 25 cells were scored from 2 separate parallel experiments. Lysosomal number was measured using Volocity, the following filters were imposed: Fluorescence intensity (1-255 AU) - ¿0.5 μm but ¡5 μm - separate touching objects. A spreadsheet of individual lysosome parameters was returned from which number was assessed.

4.2.5 Lysosomal Distribution

It is possible that upon a certain signal or stimulus, lysosomes are reorganized within the cell and possibly fuse with the plasma membrane of the cell and secrete their contents into the extracellular space. These actions may have potential implications for bystander signalling. If such a process is occurring it is likely that a redistribution of lysosomes would be apparent. Using the same images acquired for lysosomal membrane permeabilization, we measured lysosomal distribution. As described earlier in section 2.2.6, we used Image J to measure the intracellular location of lysosomes to ascertain whether there was a distribution shift following radiation exposure. Briefly, images obtained on the Zeiss LSM Confocal microscope were processed using Image J and then, a binary mask was created from each of the cells outline. A series of concentric regions of interest (ROI) were made and the fluorescence was measured in each one to estimate lysosomal dispersion. The cell was divided into quarters and halves and the fluorescence was examined. Both were examined and showed similar patterns, here we show fluorescence per inner half of the cell as this is representative of the trend of dispersion. Data was used from lysosomal uptake and relocation methods, 10 cells were scored from each parallel experiment.

4.2.6 ROS Measurement

ROS was measured using the fluorescent dye H2DCFDA: briefly cells were loaded with the dye for 30 minutes in black 96 well plates, they were returned to culture conditions for a further 30 minutes. Cells were then measured for fluorescence on a fluorescent plate reader using appropriate filter settings. Each group (dose and time point) was allocated 2 columns (16 wells) this was done in duplicate *i.e.* 2 columns on 2 plates.

4.3 Results

Initially we utilised the AO relocation method (Section 2.2.6, Figure 2.3), to assess whether the membrane had been compromised, i.e. green fluorescence levels were shown to have increased corresponding to translocation of AO to the cytoplasm.

Lysosomal response to 0.1 Gy in HF19 direct irradiated cells (30 minutes & 1 hour)

In the first 30 minutes following exposure with 0.1 Gy X-irradiation, there was a significant increase (4-fold) in green fluorescence ($p \leq 0.01$) compared to that observed from the 0 Gy (control) group, thus indicating lysosomal rupture (Figure 4.2). It is unclear from this data whether this was as a result of complete rupture of individual lysosomes or due to a general increase in permeability across a number of lysosomes, although the magnitude of the increase would suggest it was due to complete rupture. At the 1 hour time point, fluorescent levels were shown to have fallen to below that of the control although not statistically significant ($p \leq 0.05$). This observation could potentially be explained by an increase in cell membrane permeability and corresponding AO leakage from the cell to the extracellular space (Figure 4.2).

Lysosomal response to 2 Gy in HF19 direct irradiated cells (30 minutes & 1 hour)

Cells exposed to 2 Gy showed an even greater increase of green fluorescence than those exposed to 0.1 Gy irradiation (Figure 4.2). Levels were almost 7 fold greater in the former than those observed for the control cells ($p \leq 0.01$). These results, when combined with those of the 0.1 Gy data, suggest a dose dependent effect. At the 1 hour time point, levels of fluorescence were still significantly elevated ($p \leq 0.05$), compared to control cells, indicating that lysosomal membrane permeabilization was ongoing (Figure 4.2).

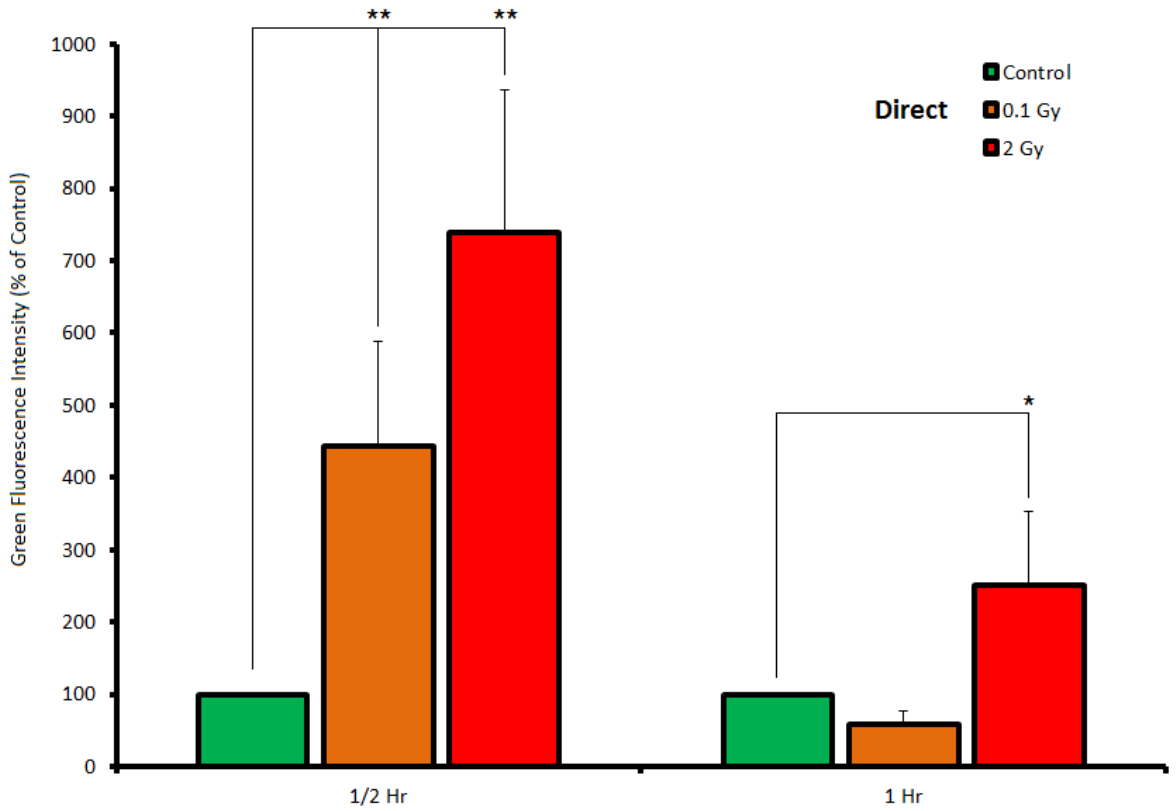

Figure 4.2: **Early alterations in lysosome membrane permeability in HF19 cells were measured using the AO relocation method at 30 minutes and 1 hour following 0.1 and 2 Gy X-ray exposure.** Lysosomes were shown to have a significant level of membrane permeabilization at the 30 minute time point following 0.1 Gy irradiation although the effect had diminished at 1 hour, with levels lower than those of the control group, although this was not statistically significant. Following 2 Gy irradiation, a significant (7-fold) increase in permeability was observed after 30 minutes compared to the control and this permeabilization was still evident after 1 hour. .

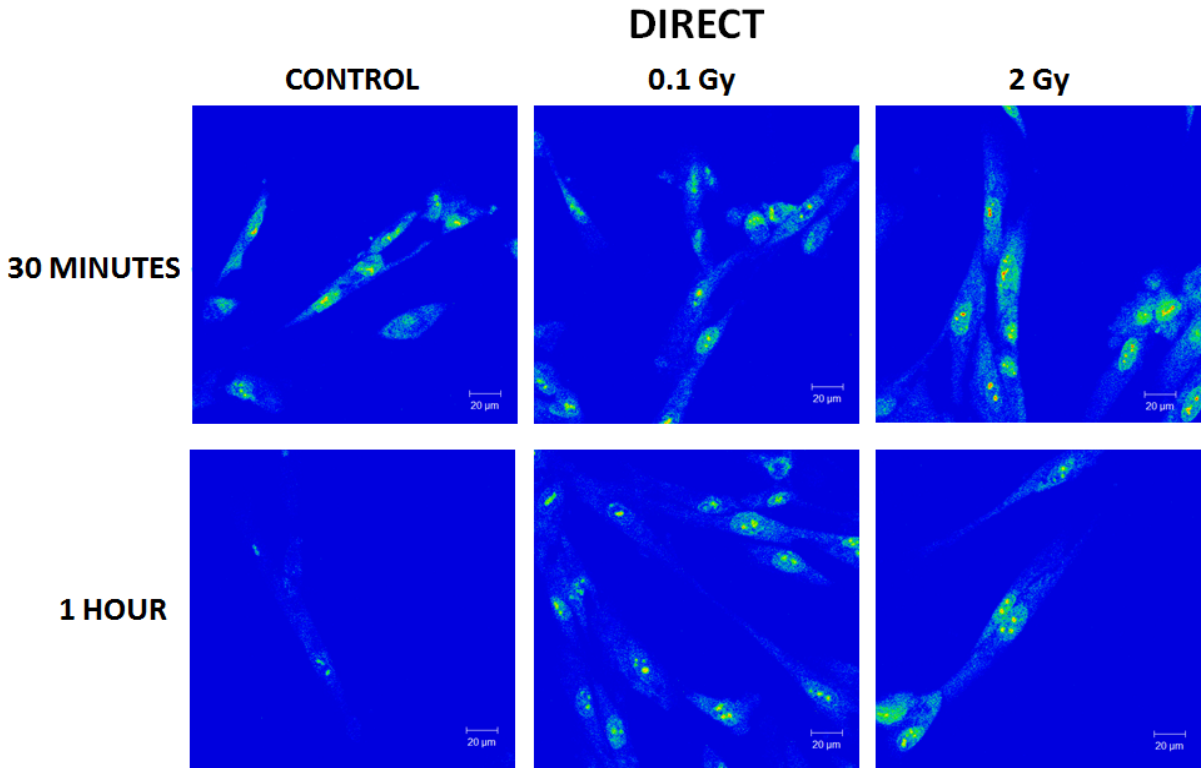

Figure 4.3: **HF19 cells were analysed using the AO relocation method to analyse lysosomal membrane permeabilization.** Cells are displayed with a rainbow overlay to highlight differences in intensity rather than the raw image. It is clear after 30 minutes that radiation induced permeability HF19 lysosomes following 0.1 Gy and 2 Gy. After 1 hour, 2 Gy irradiated HF19 cells still showed an increase in green fluorescence. HF19 cells exposed to 0.1 Gy showed very little change in levels of green fluorescence indicating the permeabilization is likely to have ceased.

Lysosomal response to 0.1 Gy irradiated bystander media in HF19 (30 minutes & 1 hour)

The AO relocation method was also used to measure lysosomal membrane permeabilization in bystander groups (Figure 4.4). Mean levels of green fluorescence were observed to be significantly reduced ($p \leq 0.05$) at 30 minutes following exposure to 0.1 Gy X-rays (65.07% $\pm$ 2.56) compared to those of the control cells. However, at the 1 hour time point, levels had increased to similar values (80.49 % $\pm$ 12.28) to those observed in the control cells.

Lysosomal response to 2 Gy in HF19 bystander effect irradiated cells (30 minutes & 1 hour)

The level of green fluorescence observed in the 2 Gy bystander media group (Figure 4.2) at the 30 minute time point was similar to that of the 0.1 Gy group (65.02 % $\pm$ 11.74) and much reduced from the value observed in the control cells however, this was not significant. At the 1 hour time point, fluorescence levels had increased (109.73 % $\pm$ 12.51) to those of the control cells although the difference was insignificant.

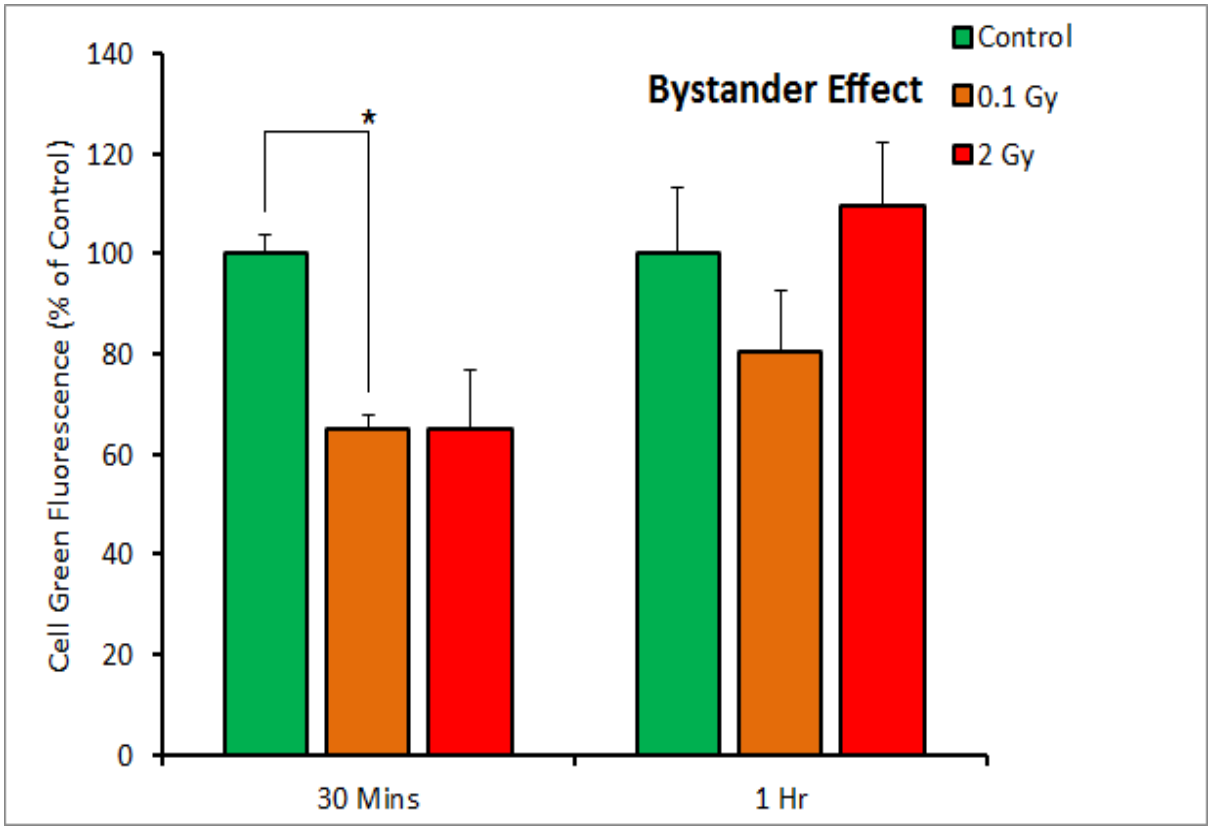

Figure 4.4: **Bystander cells were also measured using AO relocation method and examined for green fluorescence.** Bystander treated cells showed a reduction in green fluorescence 30 minutes following incubation with media, there is no real relation to dose. The exact cause and mechanism of this is unknown, one theory is the cell membrane has become more permeable and allowed the transfer of green AO from the cytoplasm and into the extracellular space. After 1 hour levels appeared to have returned to control values, in particular 2 Gy bystander cells.

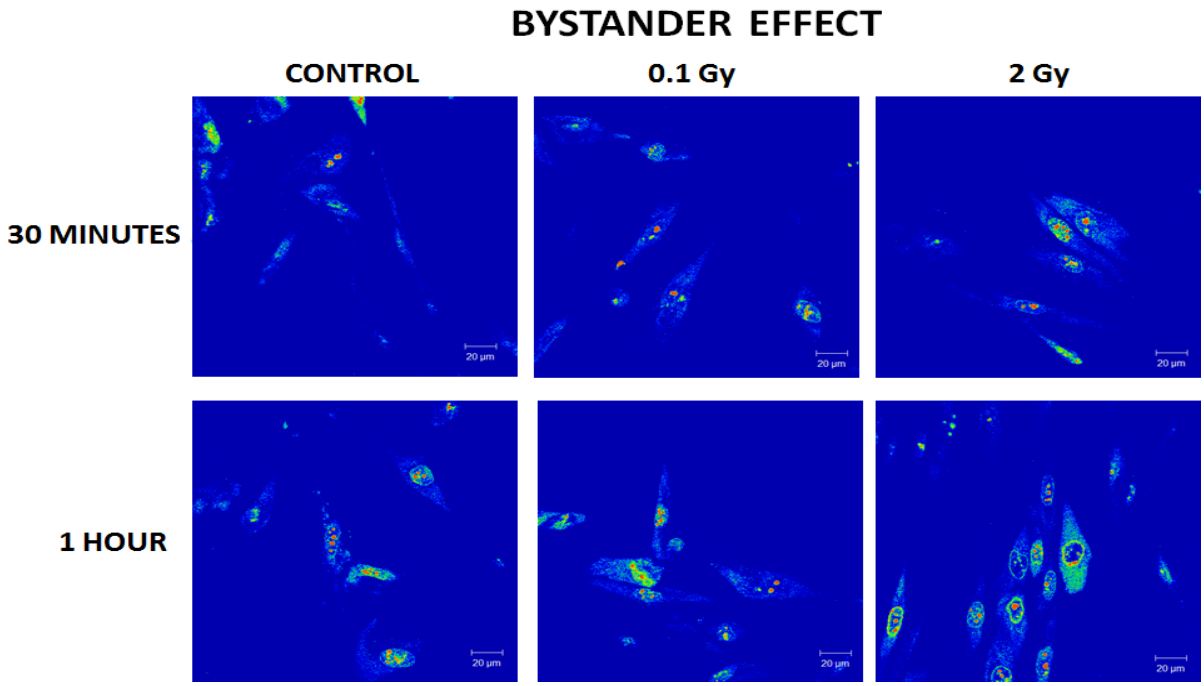

Figure 4.5: **Typical images from lysosomal membrane permeability.** From the raw images it is hard to note obvious changes however analysis using Volocity indicated a number of changes as discussed earlier in this chapter.

The AO uptake method was also utilized in our studies (Figure 4.6). For this technique cellular red fluorescence was analysed; a reduction in fluorescence indicated a reduction in AO uptake by the lysosomes and conversely an increase indicated either an increase in lysosome number or an increase in lysosome size.

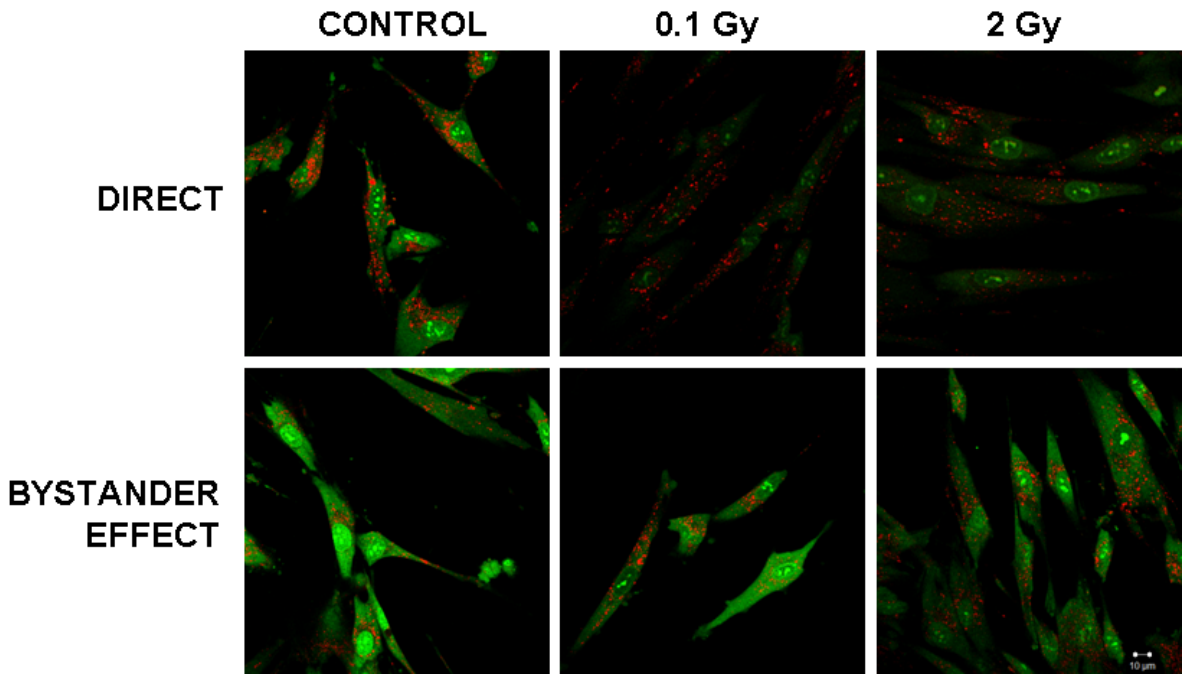

Figure 4.6: **AO uptake methods were used to measure lysosomal membrane permeability at delayed time points.** Cells were examined for cellular fluorescence and lysosomal number. From the raw images it is hard to note obvious changes however analysis using Volocity indicated a number of changes as discussed earlier in this chapter.

4.3.1 Lysosomal response to 0.1 Gy in HF19 directly irradiated cells (4 to 24 hours)

At the 4 hour time point, the lysosomal number per unit area data obtained for the 0.1 Gy exposed cells remained fairly in line with the control value (Figure 4.7). A large decrease was observed at the 8 hour time point (80% of the control) although this was statistically insignificant ($p > 0.05$). Similarly, values remained slightly lower than those observed in the control group at the 12 hour time point, again these were insignificant. Finally at the 24 hour time point, a reduction in lysosomal number was observed, values obtained were 64% of the control for this group.

We also examined cellular red fluorescence to look at the overall integrity of the lysosome (Figure 4.8). The level of fluorescence failed to show any significant deviation from the control value in the 4, 8 and 12 hour time points, although a significant reduction ($p \leq 0.05$) was observed at 24 hours. This result combined with the large, although not significant reduction in lysosomal number (Figure 4.7), demonstrates that lysosomal damage is capable of being induced up to 24 hours following X-irradiation.

4.3.2 Lysosomal response to 2 Gy in HF19 directly irradiated cells (4 to 24 hours)

The lysosomal numbers observed in cells directly exposed to 2 Gy was shown to be elevated at 4, 8 and 12 hour time points compared to control cells (Figure 4.7), although in most cases only slightly (between 5 and 25%), and all failed to show significance at the 5% level. However at the 24 hour time point, there was a significant reduction in lysosomal number ($p \leq 0.05$).

Cellular red fluorescence following 2 Gy exposure appeared to follow the pattern observed in the 0.1 Gy irradiated cells with little deviation from the control at 4, 8 and 12 hour time points (Figure 4.8). However at 24 hours a large reduction in cell fluorescence (70% $\pm$ 11.9) was observed. This data therefore correlates with the reduction in lysosome number (Figure 4.7), supporting the notion of radiation-induced lysosomal membrane permeabilization at least 24 hours following X-irradiation exposure.

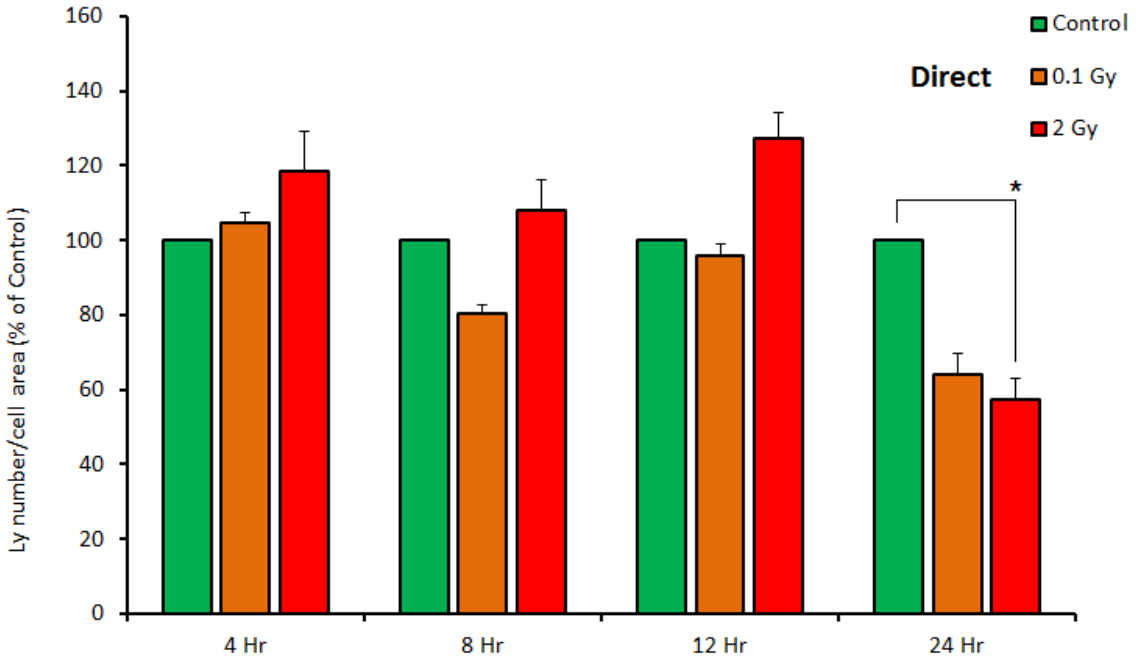

Figure 4.7: **Lysosomal number in directly irradiated HF19 cells at 4 to 24 hour time points following radiation as a percentage of control cells.** In cells exposed to 0.1 Gy irradiation, the lysosomal number remained fairly constant throughout the time points. In this group, numbers were slightly reduced at 8 hours following exposure and again at 24 hours compared to control cells, however they were insignificant reductions. Cells exposed to 2 Gy showed elevated lysosomal numbers at 4 hour through to 12 hour time points, although these were insignificant. However, at the 24 hour time point there was a significant reduction in lysosomal number compared to the control group.

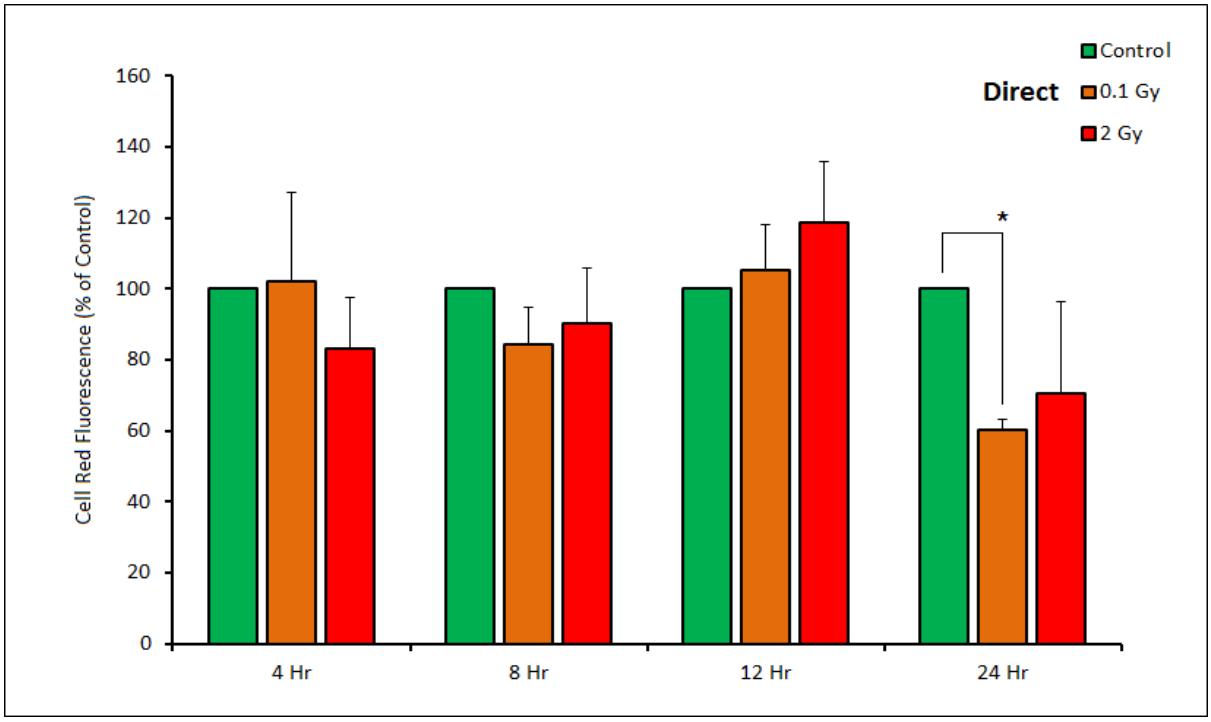

Figure 4.8: **Cellular fluorescence in directly irradiated HF19 cells at 4 to 24 hour time points following X-ray irradiation.** In cells exposed to 0.1 Gy irradiation, cell fluorescence remained in line with that observed in the control group at 4, 8 and 12 hour time points, however, at the 24 hour time point, fluorescence was significantly reduced. Following 2 Gy exposure, cells demonstrated a reduced fluorescence at the 4 and 8 hour time points although levels had gradually increased by the 12 hour time point but a large reduction was again observed at 24 hours, following a similar trend to that of the 0.1 Gy treated cells.

4.3.3 Lysosomal response to 0.1 Gy in HF19 bystander cells (4 to 24 hours)

Bystander cells were analysed utilizing the AO uptake method. Cells were analysed 4, 8, 12 and 24 hours following addition of the bystander media (Figure 4.9). In contrast to the data obtained from the directly irradiated group, large fluctuations in lysosomal number following 0.1 Gy exposure were demonstrated throughout the time series. At 4 hours lysosomal numbers had significantly reduced to 67.43% $\pm$ 6.97 ($p \leq 0.05$). However in contrast, after 8 hours exposure to bystander media, lysosome numbers were shown to have increased to 128.87% $\pm$ 7.02. This oscillating pattern was further demonstrated at the 8 and 24 hour time points, with the biggest effect observed at 24 hours with cells showing 133.16 % in lysosomal number compared to the control. Interestingly this observation was contrary to the results obtained from the directly irradiated group and is suggestive of different mechanisms in play.

A similar response was observed when the cells were analysed for cell fluorescence (Figure 4.10). At 8 hours, cells exposed to 0.1 Gy media showed significant increase ($p < 0.05$) which can be correlated with an increase in the number of lysosomes (Figure 4.9). After 12 hours levels of red fluorescence were reduced to 84.66% ± 0.80. Finally after 24 hours cellular red fluorescence had returned to control levels.

4.3.4 Lysosomal response to 2 Gy in HF19 bystander cells (4 to 24 hours)

Firstly looking at lysosomal number, cells exposed to 2 Gy bystander media showed little change across 4, 8 and 12 hours, *i.e.* levels remained slightly below the control values at these time points (Figure 4.9). However at 24 hours, similar to the 0.1 Gy group, there was a large increase in lysosomal number, this suggests that the bystander effect can induce a form of sub-cellular toxicity that requires elevated lysosomal number to deal with the stress.

Data obtained for cellular fluorescence indicates a similar story to that of lysosomal number with levels remaining in line with control (Figure 4.10). There was a slight dip at 12 hours (81.61% ± 9.87) similar to values observed in the 0.1 Gy group although this was not significant. At 24 hours, levels had increased to 108.32% ± 1.97 ($p \leq 0.05$). These results therefore support the data obtained for lysosomal number and further add weight to the idea that cells had experienced sub-cellular toxicity, and lysosomal pathways had been utilized as a coping mechanism.

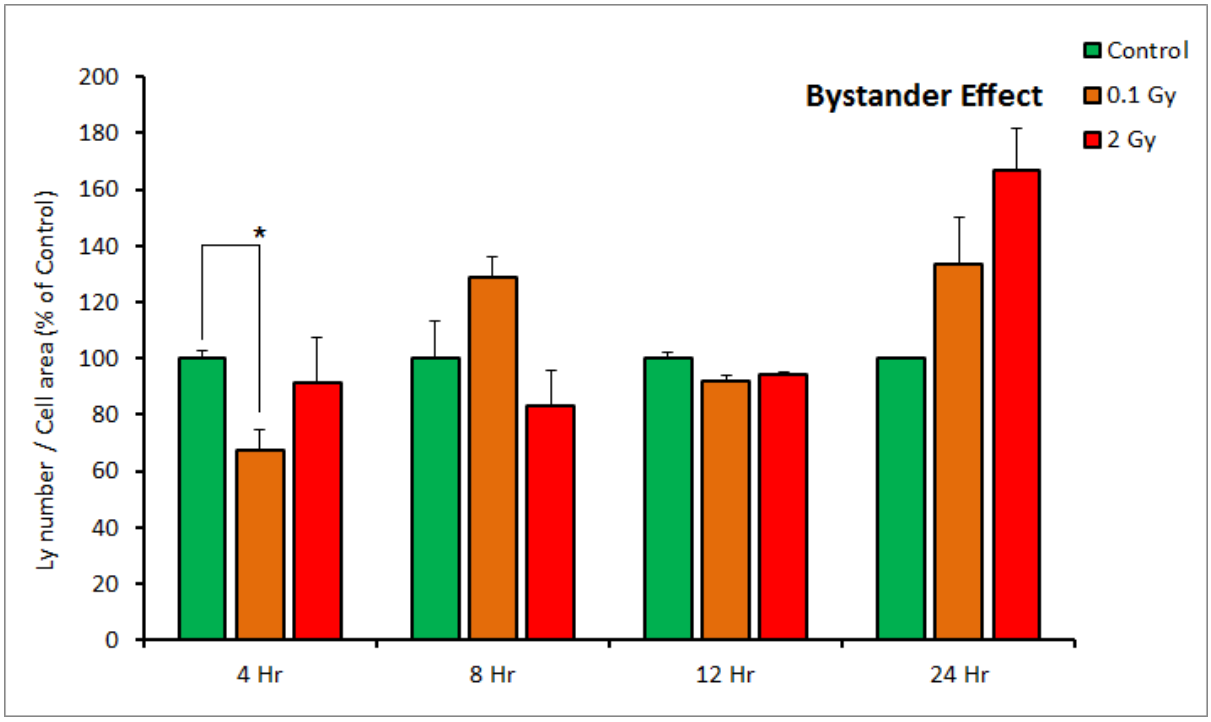

Figure 4.9: **Lysosomal number in HF19 bystander exposed cells from 4 to 24 hours following X-irradiation.** Numbers were shown to fluctuate above and below those of the control cells following both irradiation exposures, although data for the 24 hour time point demonstrated the largest increase for each dose.

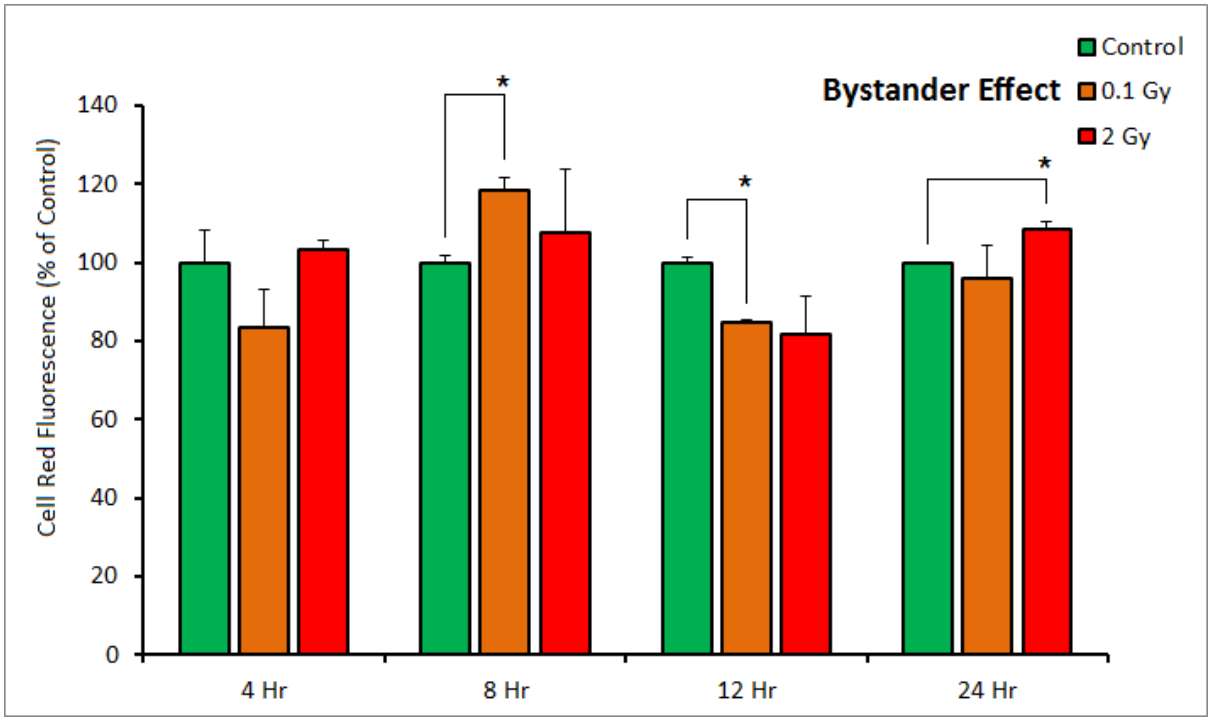

Figure 4.10: **Cellular fluorescence in bystander cells showed similar patterns to those observed for lysosomal number.** The levels were shown to fluctuate above and below the control following both doses for all time points.

4.3.5 HF19 lysosomal response following 1 population doubling in the directly irradiated and bystander cells

HF19 cells were further analysed at 1 population doubling (1 PD) for lysosomal instability using the AO uptake method (*i.e.* red fluorescence from lysosomes). Lysosome numbers were observed to have increased in the directly irradiated groups in a dose dependant manner, *i.e.* fluorescence from the 0.1 Gy exposed cells had increased to 115% ± 6.05 and 2 Gy exposed cells levels had increased to 125% ± 10.37 (Figure 4.11). Although these elevations were not statistically significant the result perhaps suggest that numbers of lysosome increase to deal with various damaged cellular components. Numbers of lysosomes in bystander groups were also slightly elevated to 112.98± 5.05 in 0.1 Gy and 113.38% ± 10.38 in 2 Gy, exposed cells. Again, although values were not significant, it is interesting to note the similarity in fluorescence values between the 2 groups and support results of Zhou et al. (2008) who found that bystander effects are either induced or not and additionally fail to show a dose response.

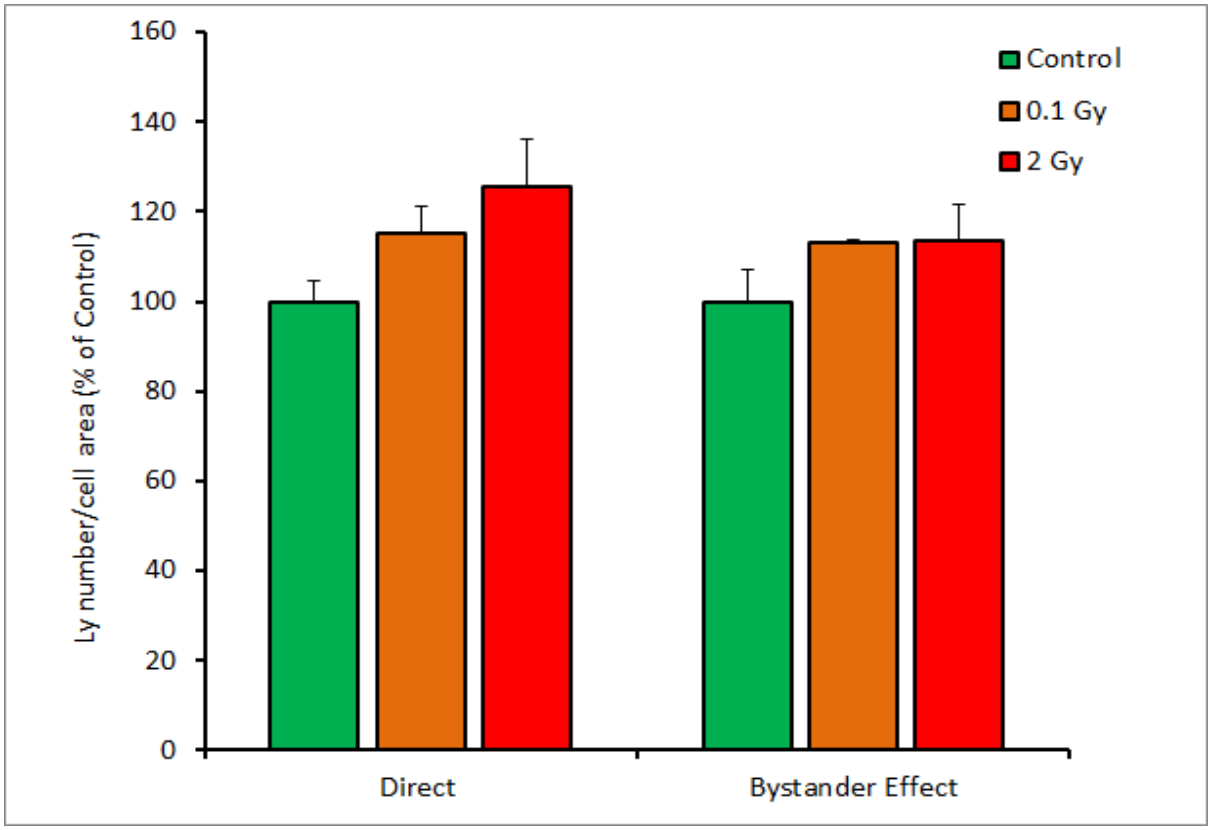

Figure 4.11: **Lysosomal number in directly irradiated and bystander cells 1 population doubling following irradiation exposure.** In directly irradiated cells, lysosomal number had increased in what appears to be a dose dependant manner. Those cells exposed to bystander conditions showed elevations in both treated groups which were at a similar level.

We then moved on to look at cellular red fluorescence at 1 PD in the directly irradiated and bystander cells (Figure 4.12). In the directly irradiated groups there was very little change in fluorescence, 102.50 % ± 12.61 and 96.78 % ± 4.54 for 0.1 Gy and 2 Gy respectively. When we compare the results from both lysosomal number and fluorescence, one might expect that fluorescence would increase with increased numbers of lysosomes, however this effect was not observed. From the data it was also possible to investigate lysosomal size and it appears that there was a small reduction of approximately 0.08 μm per lysosome (data not shown), this may be one possible explanation. Alternatively, the lysosomes may be more permeable resulting in a reduction in the amount of AO sequestered into the lysosome or the amount of AO they are able to retain.

The bystander cells however, demonstrated increased cell fluorescence (Figure 4.12) that match the results observed for lysosomal number (Figure 4.11) although they appear to be of greater

magnitude. Similarly, analysis of lysosome size (data not shown) demonstrated a very small increase of approximately 0.01 μm and 0.02 μm for 0.1 Gy and 2 Gy exposed cells, respectively. Although fluorescence values had increased for both doses, only 2 Gy exposed cells showed a significant increase ($p \leq 0.05$). Thus in contrast to the directly irradiated groups, the bystander groups demonstrated a dose dependent relationship; 124.33 % $\pm$ 0.14 and 139.38 % $\pm$0.63 for 0.1 Gy and 2 Gy respectively, (Figure 4.12).

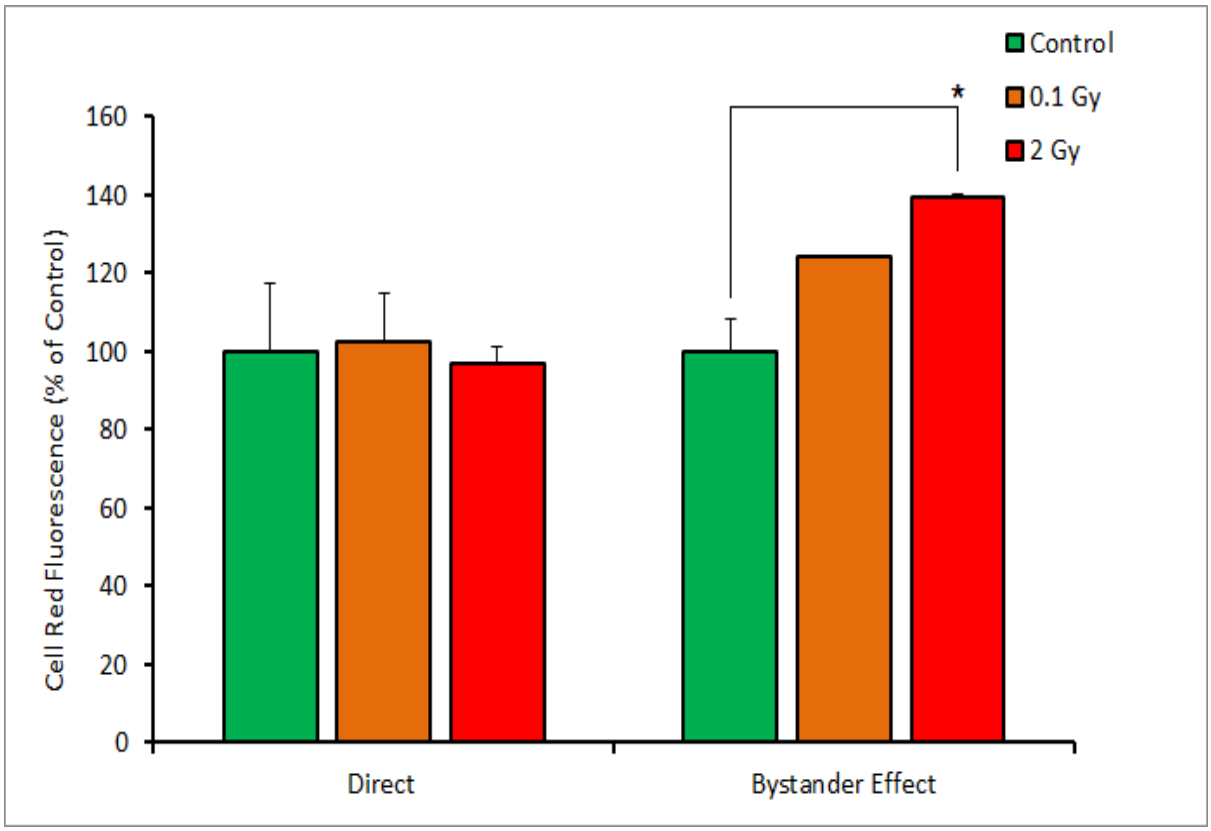

Figure 4.12: **Cellular fluorescence in direct and bystander cells 1 PD following radiation exposure.** Directly irradiated cells showed no change in cell fluorescence at either dose. However bystander cells demonstrated large increases in fluorescence with the largest effect observed following 2 Gy exposure.

The HF19 cells were further cultured until 20 population doublings (20 PD) at which point they were analysed for AO uptake and to establish a possible temporal link between lysosomal membrane permeabilization and GI.

4.3.6 HF19 lysosomal response following 20 population doublings in the directly irradiated and bystander cells

Finally we examined lysosomal number and fluorescence at a time point which we had earlier documented the onset of GI (Section 3.3.2). Again we used the AO uptake technique looking at red fluorescence within the lysosome. We noted in the directly irradiated groups (Figure 4.13) a small increase in number that appeared to have some kind of dose dependence, *i.e.* 0.1 Gy was increased to 104.09% ± 3.59, and 2 Gy was increased to 110.21% ± 5.52%. These increases are small and translate to approximately an increase of only 10 - 15 lysosomes per cell. The bystander cells conversely showed a reduction in lysosomal number for both irradiation exposures, although cells treated with 0.1 Gy bystander media cells demonstrated the only significant decrease (64.18% ± 8.07% as opposed to 72.67% ± 9.1% observed in the 2 Gy bystander media treated group) compared to the control. Finally, the data for the cells exposed to secondary bystander media showed only a modest deviation from the control values.

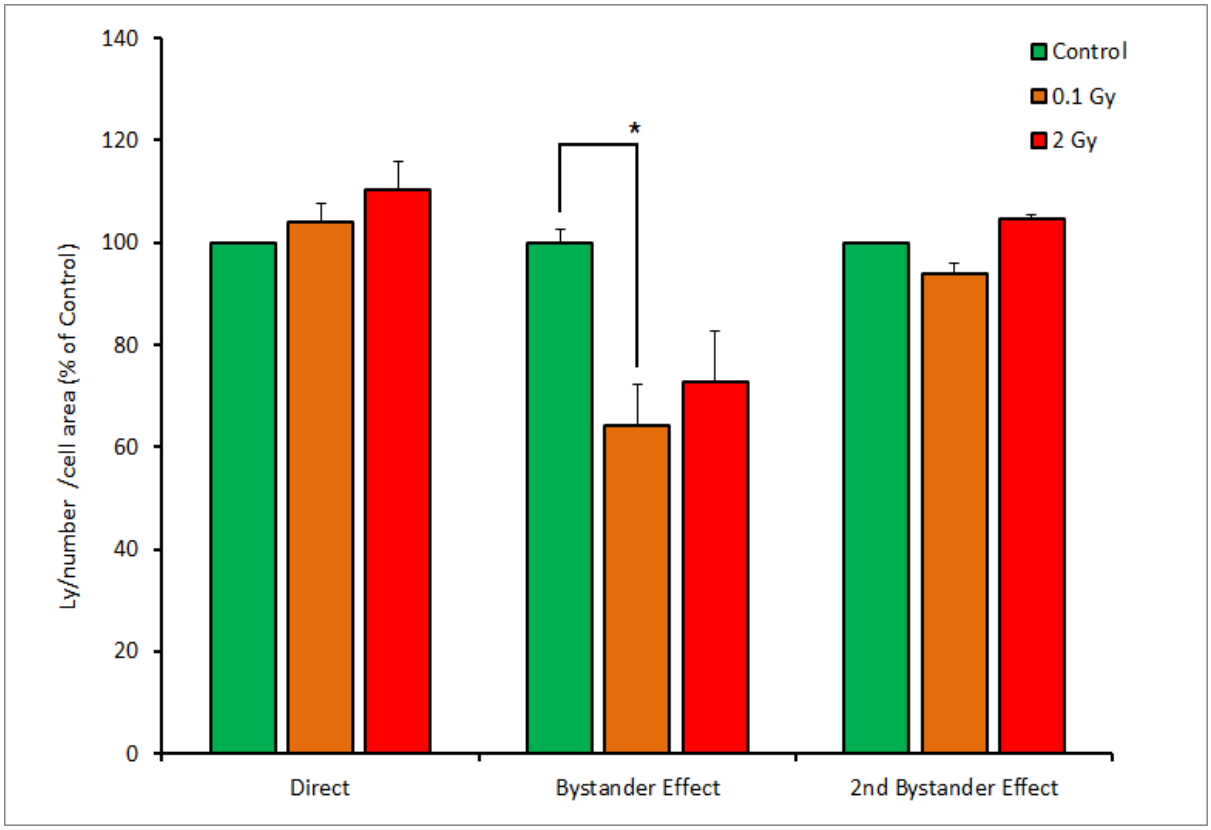

Figure 4.13: **Lysosomal number was assessed in directly irradiated, bystander and secondary bystander groups after 20 PD.** The Direct and secondary bystander effect cells showed small insignificant changes following both 0.1 Gy and 2 Gy exposure, although the effect was largest in the direct group and similar to that observed after 1 PD. In contrast, both 0.1 Gy and 2 Gy irradiated cells in the classical bystander group showed a significant large reduction in lysosomal number.

Directly irradiated cells at 20 population doublings demonstrated a decrease in cell fluorescence for both irradiation exposures (Figure 4.14). This suggests that the lysosomes are less able to retain AO thereby indicating an increase in cell permeability. Values were significant at 2 Gy (76.84 % $\pm$ 4.61, $p \leq 0.05$), although not for 0.1 Gy despite a large reduction (87.31 % $\pm$ 5.61). Similarly, the cells exposed to bystander media demonstrated a reduction in both lysosomal number (Figure 4.13) and in cell fluorescence (Figure 4.14). Whereas the results (lysosome number and fluorescence) for the directly irradiated groups are suggestive of a general increase in permeability, the data for the classical bystander groups suggest that the lysosomes suffered a more complete rupture and thereby lost the subsequent ability to retain any AO. Similarly, the most significant reduction in the bystander cells was observed in the 2 Gy group (80.01 % $\pm$ 1.32, $p \leq 0.05$), although the 0.1 Gy group also showed a large but insignificant reduction

(66.48 % ± 8.46). In contrast, the fluorescence results for the secondary bystander effect group demonstrated no significant differences for both irradiation doses. Following treatment with 0.1 Gy, fluorescence had reduced slightly to 94.88 %, and in the 2 Gy group it had reduced to 75.07 % ± 11.16 of the control values. These results suggest continued propagation of the bystander signal albeit to a lesser extent than that observed in the classical bystander group.

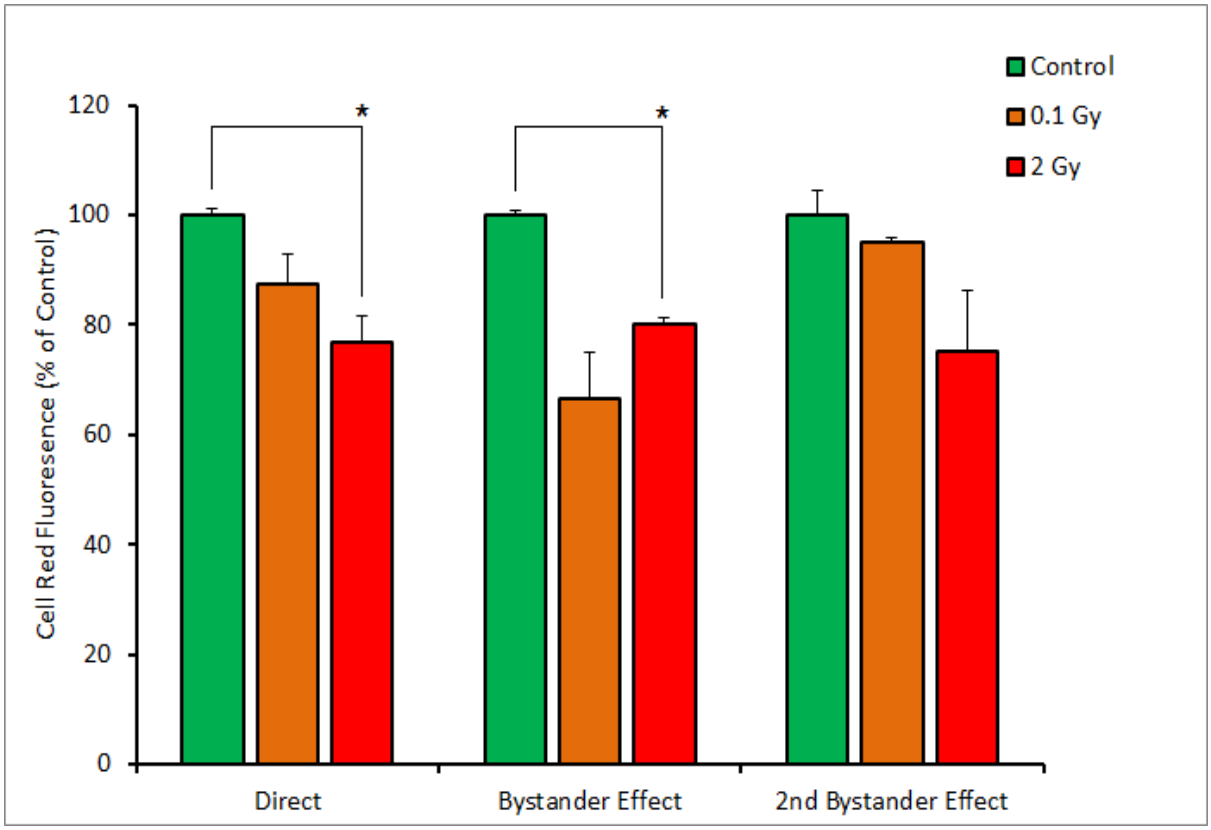

Figure 4.14: **Cellular fluorescence measured in HF19 following radiation at 20 population doublings in direct, bystander and classical bystander groups.** Interestingly the directly irradiated groups showed a reduction in permeability which additionally appeared to increase with dose. The classical bystander groups also showed reductions in fluorescence but failed to show any relation to dose. Finally, the secondary bystander group appeared unaffected following treatment with media exposed to 0.1 Gy irradiation. In contrast, those exposed to 2 Gy demonstrated a small reduction in fluorescence.

4.3.7 Lysosomal Dispersion

We examined lysosomal dispersion to look at the potential migration of lysosomes to the cell membrane following radiation. It has been reported that lysosomes may be involved in cell membrane repair (McNeil, 2002). The main trigger in initiating their exocytosis is alterations

in calcium concentration (Xu et al., 2012). The method we utilized is described in detail in 2.2.6. Briefly, images of AO stained cells were used, and a series of concentric rings were drawn from the cell membrane migrating inwards towards the centre of the cell. A fluorescent measurement was taken from each ring to calculate the lysosomal content in each ring. The data presented here demonstrates the fluorescence within the inner half of the cell at 1 and 20 population doublings.

After 1 PD, there was no significant change in lysosomal dispersion (Figure 4.15), approximately $\frac{2}{3}$ of the cells lysosomes appeared within the inner half of the cell. As previously stated direct irradiation did not appear to alter this although cells exposed to 0.1 Gy showed a small increase to 63.81 % $\pm$ 7.43 compared to control values of 58.68 % $\pm$ 4.22.

Bystander populations also failed to show any variation in the dispersion of lysosomes for either irradiation dose when (Figure 4.15). Similarly, these cells showed approximately $\frac{2}{3}$ of the lysosome population within the inner half of the cell. The condition (*i.e.* direct or bystander) also showed little variation between groups.

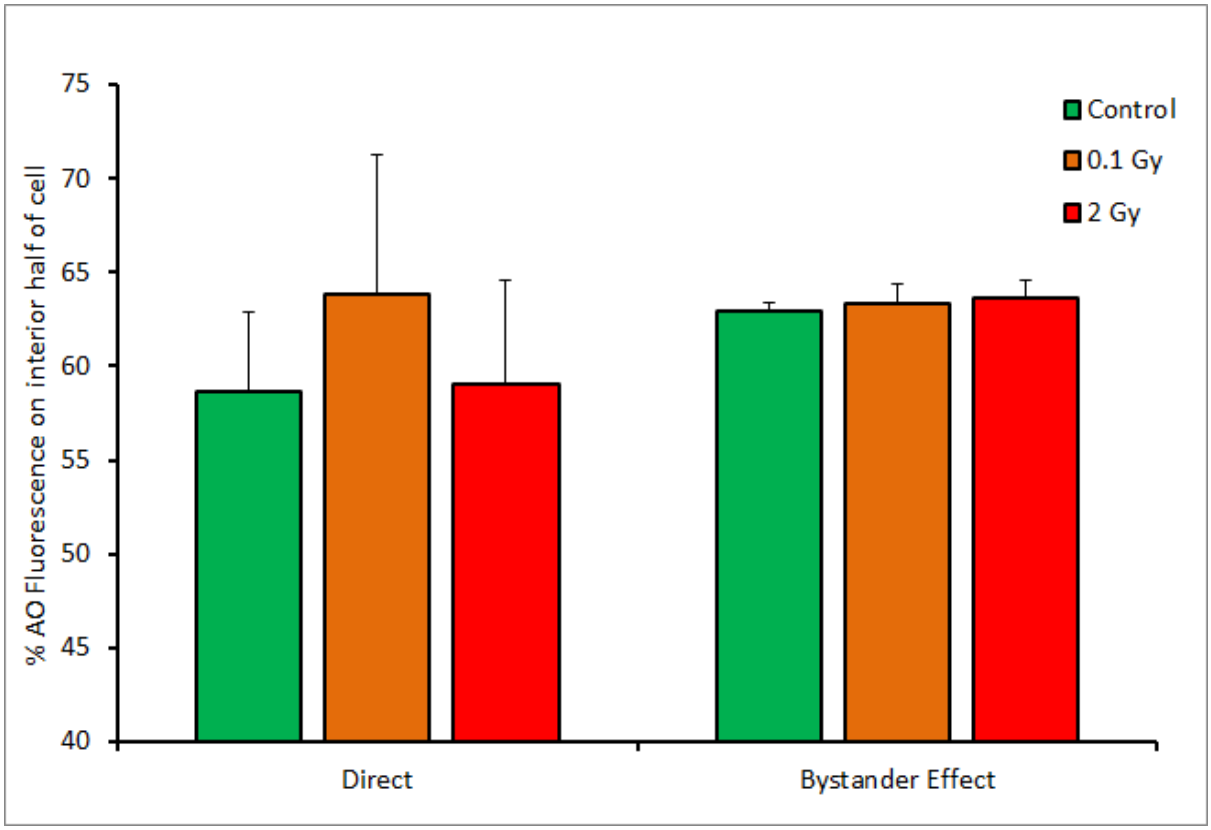

Figure 4.15: **Lysosomal distribution was measured in HF19 cells after 1 PD following direct X-ray exposure or exposure to bystander media.** Neither direct nor bystander groups showed any change in distribution with the average inner cell fluorescence approximately 60 %.

Despite there being little difference between irradiated and control HF19 cells after 1 PD, we still progressed to analyse results from the 20 population doublings cells (Figure 4.16). In the directly irradiated groups the dispersion of lysosomes did not appear to change with prolonged time in cell culture. Both direct 0.1 and 2 Gy irradiated groups (0.1 and 2 , 68.55 % $\pm$ 1.49 64.57 % $\pm$ 1.39 respectively) remained in line with the control (66.92 % $\pm$ 4.56). Both bystander doses showed a reduced fluorescence indicating a slight migration although this was not significant. The secondary bystander group also showed very little change.

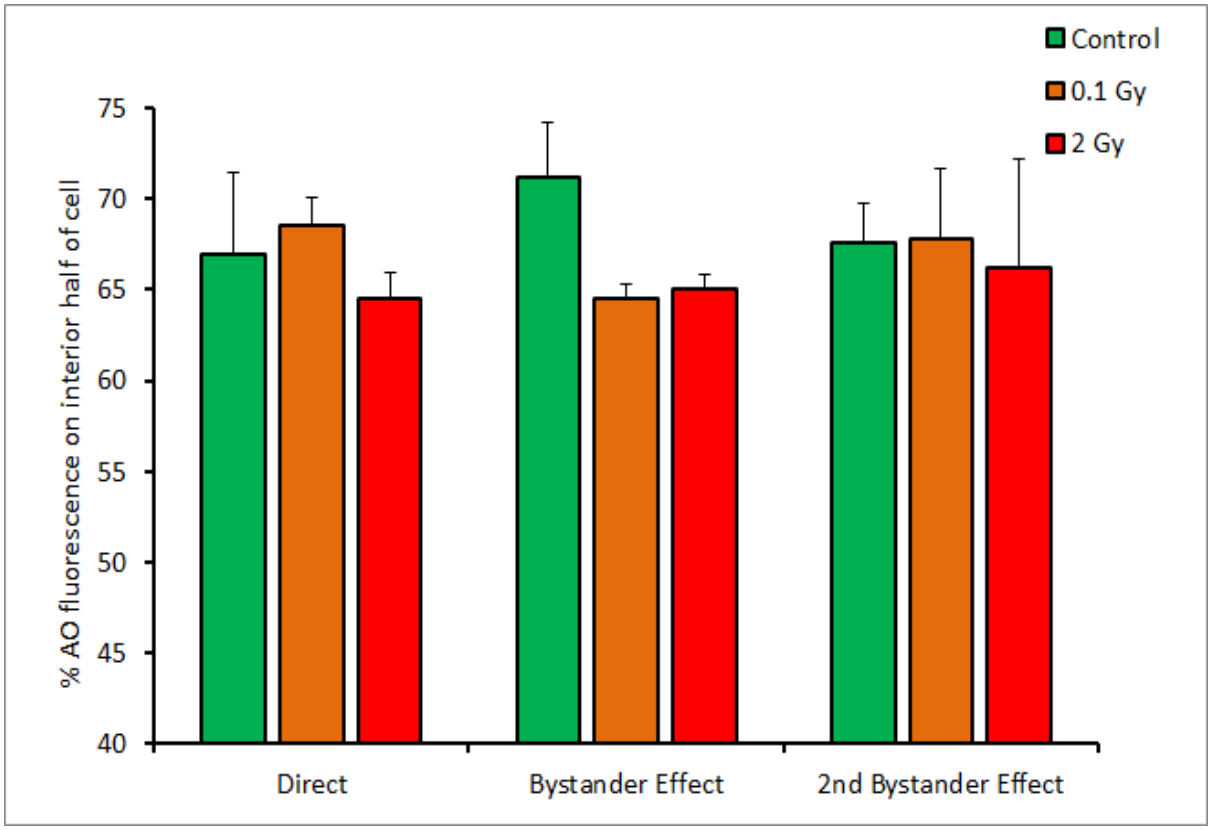

Figure 4.16: **Lysosomal dispersion was measured in direct, bystander and secondary bystander groups following X-ray exposure after 20 PD.** Similar to results obtained for 1 PD there was no real change in the directly exposed and their control samples or in the classic bystander or secondary bystander group. There also appears to be no change in terms of temporal effects.

4.3.8 Levels of ROS in HF19 cells following direct exposure with 0.1 Gy direct X-ray exposure

We analysed HF19 for levels of reactive oxygen species (ROS) using the general ROS marker, H2DCFDA. It is well known IR is able to induce the radiolysis of water producing large numbers of ROS (Hall and Giaccia, 2006), which have the potential to damage various sub-cellular organelles. The majority of investigations states that ROS are present on the scale of milliseconds at most (Lehnert, 2008; Hall and Giaccia, 2006). However we investigated the possibility that the cell is under oxidative stress for a longer period, *i.e.* hours and possibly generations, after exposure.

At the 30 minute time point, cells directly exposed to 0.1 Gy irradiation demonstrated a slight

elevation in the level of ROS (125 % ± 2.10) compared to the control (Figure 4.17). Conversely, levels had reduced to 120% ± 1.17 by the 1 hour time point although they were still significantly elevated ($p \leq 0.05$). Levels were further reduced but remained elevated above the control value through the 4 and 8 hour time points although not significantly. At the 12 hour time point ROS levels were significantly elevated above the control (119.39 % ± 2.77, $p \leq 0.05$), however, by the 24 hour time point, the levels had reduced to nearer the control value (109.93 % ± 3.67).

4.3.9 Levels of ROS in HF19 cells following direct exposure with 2 Gy direct X-rays exposure

The pattern observed following 2 Gy exposure was very similar to that observed following 0.1 Gy, *i.e.* levels remaining elevated at all time points until 24 hours with a small spike observed at 12 hours (122.34 % ± 9.36), see figure 4.17. It is possible to speculate that the increased levels of ROS observed following 0.1 Gy X-ray in contrast to 2 Gy was due to the slightly delayed time at which the cells were analysed. This may have allowed the cell sufficient time to begin production of molecules or enzymes to deal with the large level of ROS. Alternatively, greater levels of ROS may have been produced following 2 Gy exposure, thereby creating greater extinction reactions ultimately resulting in removal of ROS from the system by two oxidative species reacting with each other.

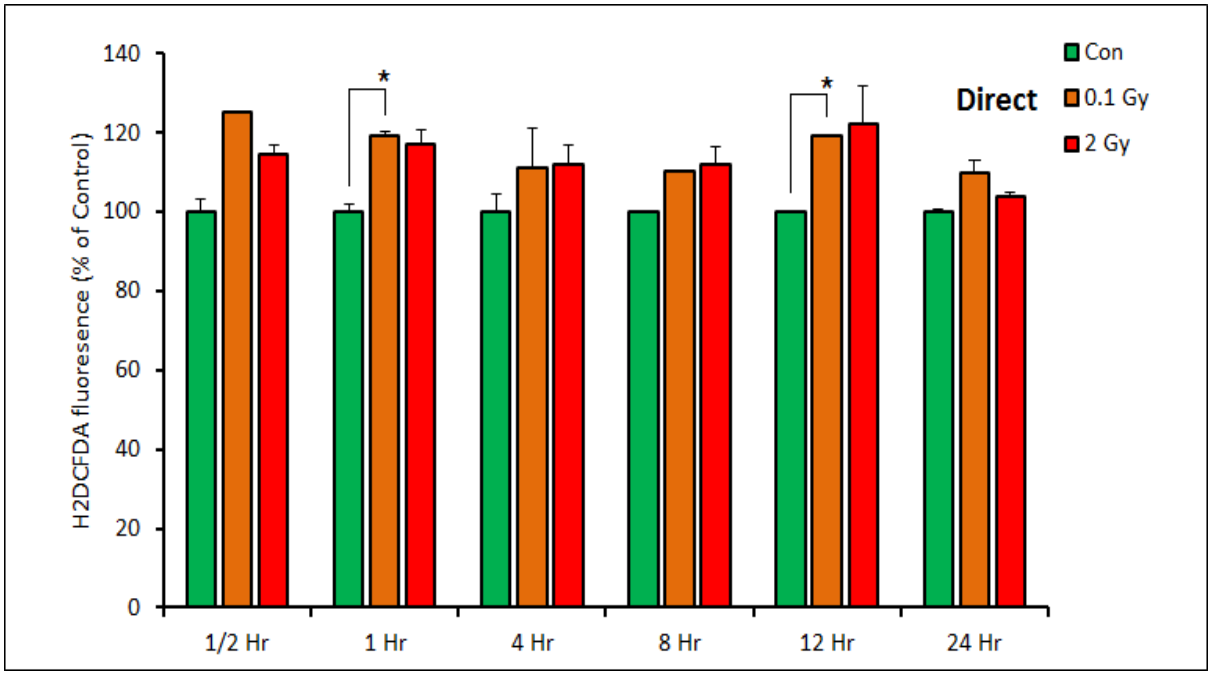

Figure 4.17: **Oxidative stress was measured in HF19 cells following direct exposure to 0.1and 2 Gy X-rays.** It was noted that following 0.1 and 2 Gy exposures, cells maintained similar levels of oxidative stress during the 30 minute to 12 hour time points. However, by the 24 hour time point levels had returned to control level.

4.3.10 Levels of ROS in HF19 cells following incubation with 0.1 Gy bystander media

HF19 cells exposed to bystander conditions demonstrated a different trend in levels of ROS (Figure 4.18) compared to those cells exposed directly to irradiation (Figure 4.17). Initially after 30 minutes the bystander cells incubated with 0.1Gy media displayed no effect on levels of ROS compared to the control cells. At 1 hour, levels had reduced to 91.22 % $\pm$ 0.06, although this was not significant. Cells continued to demonstrate a reduction in ROS through 4 hours to 84.02 % $\pm$ 3.05 but at a significant level ($p \leq 0.05$). ROS levels then returned to approximate control values and were maintained at this intensity for all remaining time points.

4.3.11 Levels of ROS in HF19 cells following incubation with 2 Gy bystander media

The cells that received media from 2 Gy irradiated cells demonstrated a very similar pattern to the 0.1 Gy group (Figure 4.18). Initially at 30 minutes no real change was observed in the level of fluorescence compared to the control cells. At 1 hour, a reduction in fluorescence was observed indicating a lowering in the level of ROS, similar to that observed in the 0.1 Gy cells (91.22 % ± 0.06), however the effect in the 2 Gy was greater with levels reduced to 80.62 % ± 0.27. At 4 hours, the level was reduced significantly to 80.82 % ± 2.07 ($p \leq 0.05$), however between 8, 12 and 24 hours levels oscillated but always remained 5 - 10% below the control values although these were not significant.

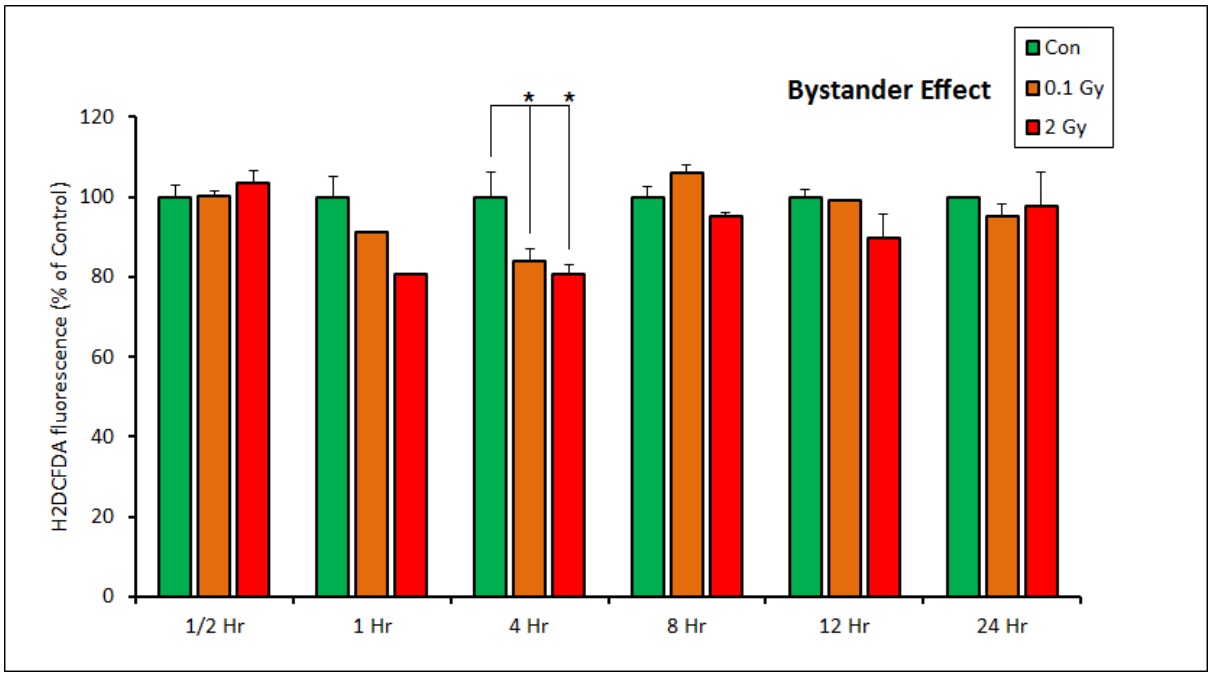

Figure 4.18: **Oxidative stress was measured in HF19 following exposure to 0.1 and 2 Gy X-ray bystander media.** No effect was observed at the initial 30 minute time point, however after 1 hour, oxidative stress appeared to have reduced and this was maintained at 4 hours. From 8 until 24 hours ROS levels had returned to approximately control values.

4.3.12 Levels of ROS in HF19 cells after 1 PD

In the directly irradiated groups there was no change in the level of ROS at 1 population doubling for either 0.1 Gy or 2 Gy,(102.52 % ± 11.66 and 98.91 % ± 10.84 for 0.1 Gy and 2

Gy respectively), see figure 4.19. The bystander group exhibited a slightly greater variation in levels with 0.1 Gy demonstrating an elevated level to 119.92 % ± 0.31. Conversely, cells exposed to 2 Gy exhibited a small reduction to 90.23 % ± 14.63. Although these values were not significant it is possible to speculate that the different doses induce different effects in the irradiated groups.

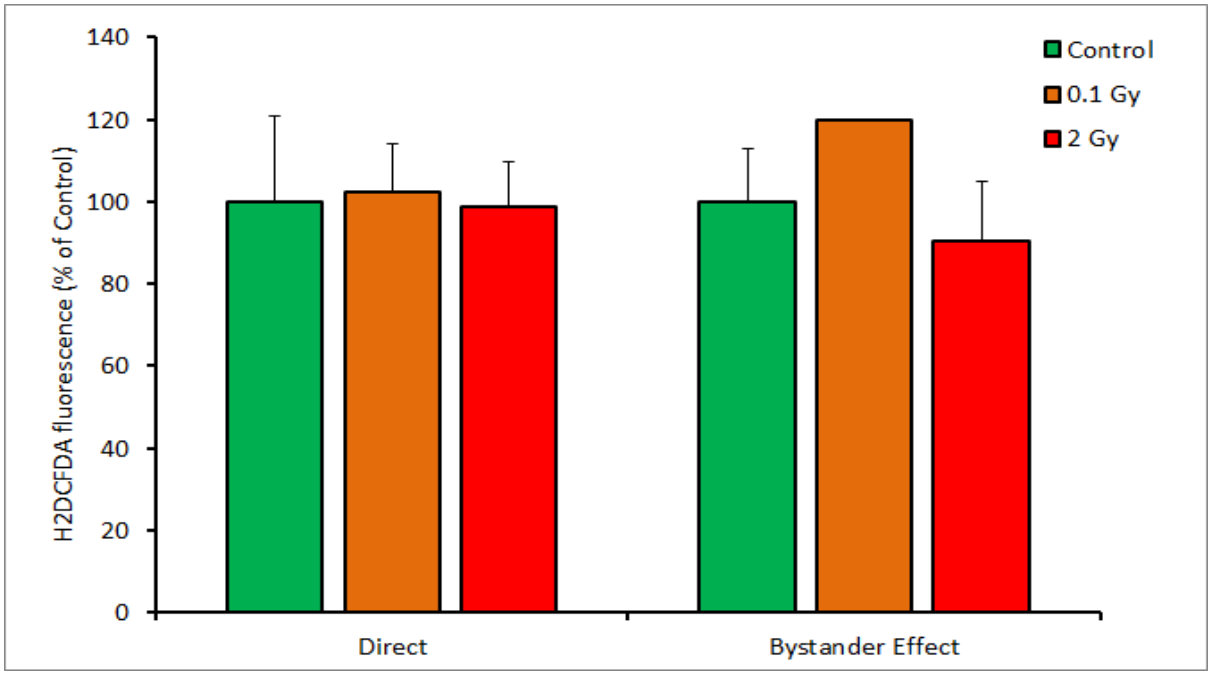

Figure 4.19: **Oxidative stress was measured at 1 PD in HF19 cells in directly irradiated and bystander groups following 0.1 and 2 Gy X-ray exposure.** Directly irradiated cells exhibited no change in oxidative stress for either irradiation dose. Conversely the bystander cells exhibited a slight elevation following incubation with 0.1 Gy media although not significantly.

4.3.13 Levels of ROS in HF19 cells after 20 PD

Finally ROS was examined at the delayed time point of 20 PD. The cells directly exposed to X-ray irradiation by either dose exhibited little difference when compared to the control (Figure 4.20). Interestingly, HF19 exposed to bystander media, showed significant increases in ROS ($p \leq 0.05$) at both doses (118.87 % ± 5.33 and 117.10 %± 2.86 0.1 Gy and 2 Gy respectively). Again it is important to note that 0.1 and 2 Gy demonstrated very similar levels of ROS further supporting the idea that bystander effects may or not be induced and there is little correlation to the magnitude of the effect from the dose received. The secondary bystander effect group,

exhibited no alteration in ROS levels at either dose and therefore behaved in a similar manner to that of the directly irradiated groups.

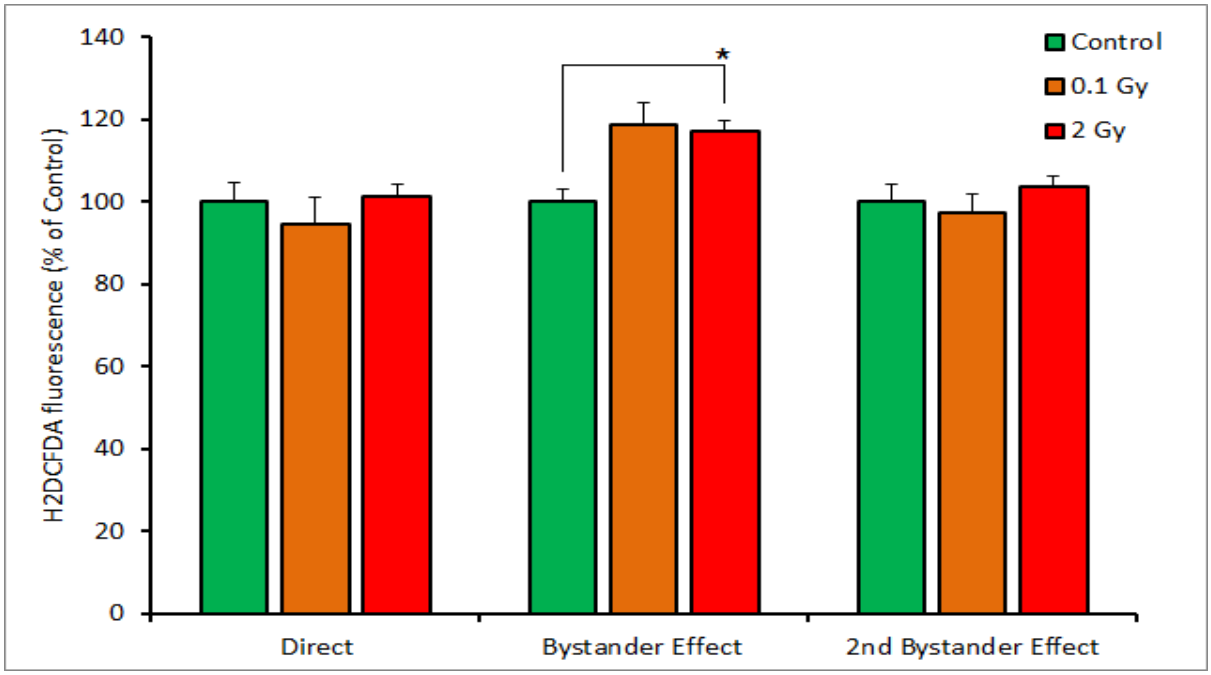

Figure 4.20: **Oxidative stress was also measured at 20 population doublings in direct, bystander and secondary bystander groups.** Similarly, directly irradiated or secondary bystander cells exhibited no change in oxidative stress at either dose. In contrast, the classical bystander group showed an increase in both doses, which were similar in magnitude but only significant following 2 Gy exposure.

4.4 Discussion

Data obtained in the previous chapter (Chapter 3) demonstrated the induction of GI in directly irradiated cells and bystander cells following exposure with 2 Gy X-rays, whilst cells exposed to 0.1 Gy demonstrated an increase in aberrations although not significant. In order to investigate the possibility that lysosomes might be driving this effect, directly irradiated groups as well as a classical bystander group were established and examined within the first 24 hours following irradiation and subsequently at 1 and 20 population doublings. In addition, at 20 population doublings a secondary bystander group was also established. The classical bystander effect was designed to detect early signals and examine the delayed effect. The secondary bystander effect was designed to examine the longevity of the bystander signal and examine potential differences that might occur between these bystander groups.

As described above the aim of this chapter was to investigate the effect of radiation on the sub-cellular organelle, the lysosome. Lysosomes are described in detail in Section 1.4. Briefly lysosomes are the terminal degradation pathway for intra-cellular debris and waste (Settembre et al., 2013). It is emerging that these organelles have a much broader function than just cellular "waste disposal" units, and are involved in secretion, plasma membrane repair, signalling and energy metabolism (Settembre et al., 2013). For example McNeil (2002) proposed that large aberrations to the cell membrane could be patched by intracellular membranes, such as the lysosome, as lysosome specific proteins can be found on the cell surface at sites of disruption. It is certainly possible that this might occur following irradiation. It might also be feasible that generation of products associated with IR such as ROS/RNS could interact with the lysosome causing permabilization. Fenton type chemistry has been cited as a potential cause of lysosomal membrane permeabilization, stemming from the production of ROS (Kurz et al., 2010; Karlsson et al., 2010; Berndt et al., 2010). Various cellular proteins have also been implicated in lysosomal disruption such as TNF-α, as well as calpain 1 (Werneburg et al., 2004; Villalpando Rodriguez and Torriglia, 2013). These mechanisms will be discussed in terms of the results.

The initial findings of the investigations in this chapter suggest that IR is able to induce significant lysosomal membrane permeabilization 30 minutes after exposure to 2 Gy X-ray, the effect was also seen with a dose as low as 0.1 Gy, as detected by the AO relocation method. The

induction of lysosomal membrane permeabilization was also noted 1 hour following exposure although this was specific to the 2 Gy dose. The simplest and most likely interpretation of the findings is that IR, through some chemical means is able to disturb the lysosomal membrane. The primary candidates are reactive oxygen species as it is unlikely that alterations in protein expression would occur on such a fast scale. A number of studies have linked ROS to lysosomal membrane permeabilization although without the use of IR (Johansson et al., 2010; Lin et al., 2010; Karlsson et al., 2010; Kurz et al., 2004, 2010). Some of the previous mentioned studies have linked the process directly to Fenton type chemistry involving the transition metal, iron. Iron is commonly found in the lysosome (Lin et al., 2010), however when Iron encounters H_2O_2 it reacts to form other radicals such as the hydroxyl and superoxide radicals. These radicals then attack the membrane of the lysosome initiating a chain reaction with the lipid membrane inducing permeabilization (Huai et al., 2013). It is possible this might be driving the early lysosomal membrane permeabilization following IR. When we examined cells exposed to bystander media the opposite effect was seen *i.e.* a reduction in green fluorescence was observed. This could potentially be a results of increased lysosomal number. It might also be reasonable to assume that the bystander media is able to alter the cell membrane permeability allowing AO orange to leak out into the extracellular space effectively removing it from the system; this agrees with work published by Lyng et al. (2011). It is also possible to note that the magnitude of the effect is very similar between 0.1 Gy and 2 Gy; this lack of reliance on dose has been well documented, most recently by McMahon et al. (2013).

The AO uptake method was employed to analyse the effect of IR. Initially in direct groups it was noted a large fluctuations above and below the control. However at 24 hours there was a reduction in lysosomal number in both irradiated groups (Figure 4.7). When this was combined with data for cell fluorescence (Figure 4.8), there was a clear reduction in lysosome number per cell. From our data it is unclear what had caused this reduction. Due to the delayed nature, in terms of ROS life span, we speculate that this could be a result of protein interaction. A number of proteins have been reported to induce lysosomal membrane permeabilization. Werneburg et al. (2004); Huai et al. (2013) have demonstrated the involvement of TNF-α in the induction of lysosomal membrane permeabilization, and more recently Huai et al. (2013) documented the same effect. Huai et al. (2013) proposed that TNF-α induces lysosomal membrane permeabi-

lization indirectly by first initiating mitochondrial outer membrane permeabilization (MOMP). This initiates apoptosis and the resulting increase in free radicals causes permeabilization of the lysosomal membrane, amplifying the apoptotic cascade. However, data recently obtained within the lab indicated that mitochondria appear undisturbed in HF19 cells at least at 1 PD following irradiation, and therefore are unlikely to be involved in the lysosomal permeabilization process. TNF-α signalling has been documented following IR (Veeraraghavan et al., 2011) but it is possible to speculate that other cytokines, such as TGF-β, could have similar roles.

Bystander cells over the same period (4 - 24 hours) demonstrated large oscillations in response from above and below the control values (Figure 4.10, 4.9). Saroya et al. (2009) showed similar oscillations in zebra fish with calcium flux, Lev Bar-Or et al. (2000) also proposed oscillations due to p53-mdm2 feedback loop; potentially this could be influential in the observed results.

Other researchers have implicated the calpain protein a non-lysosomal cysteine protease. The protein's action on the lysosomal membrane is thought to be induced by creating hypoxic conditions (Tsukada et al., 2001; Yamashima et al., 1996). This leads to the translocation of lysosomal enzymes to various cellular locations, including the lysosomal enzyme DNase IIα appearing in the nucleus early and up to 5 days following insult. However it is not understood how calpain induced its effect, although Villalpando Rodriguez and Torriglia (2013) recently demonstrated that cleavage of the lysosomal membrane associated protein 2 (LAMP2) was critical in the process.

Perhaps the most likely candidate is p53. It is well known to be involved in radiation response (Hickman et al., 1994; Cianfarani et al., 1998; Rashi-Elkeles et al., 2011). However it has also been shown to play an role in lysosome membrane permeabilization (Li et al., 2007), albeit in the presence of a another protein LAPF (lysosome-associated and apoptosis-inducing protein containing PH and FYVE domains). The authors also note this occurs as a preceding event to TNF-α induced apoptosis.

Although the data obtained for these early time points in our study yield information on the actual response of a lysosome to radiation it fails to address the question if they are potentially involved in GI or BE at delayed time points. We therefore analysed the progeny of the irradiated cells. First looking at the direct irradiated cells the number of lysosomes was shown to have

increased (Figure 4.11). It also appears to be dose dependant although more doses would be required to prove this. This fact suggests a possible clearing period where the cell has a number of damaged components that require degradation. A likely pathway that might explain an increase in lysosomal number is autophagy (described in relation to cell death in Section 1.2.3). This process is usually activated in times of starvation (Hamasaki et al., 2013) and has strong formation links with the endoplasmic reticulum (ER) (Hamasaki et al., 2013). Autophagy has been considered to promote cell survival and therefore potentially facilitate GI possibly progressing to tumour development (Qiang et al., 2013).

Bystander groups at 1 population doubling show an increase in number. There is no difference between 0.1 and 2 Gy suggesting a lack of any dose response. The increase is smaller than that observed after 2 Gy (Figure 4.11). This might be an indicator that those cells exposed to irradiated bystander media are experiencing sub-cellular toxicity and that requires the removal of damaged components.

Finally, lysosomes examined at 20 population doublings demonstrated some interesting characteristics (Figure 4.13). Directly irradiated cells showed an almost identical pattern to that seen at 1 PD with an increased number of lysosomes, although further investigations would be required to establish the origin of this increase in number. One possibility is again autophagy; increased levels of autophagy may confer a pro-survival state to the cell by removing cellular stressors such as damaged organelles. This maintenance of cell fitness by autophagy, while causing the cell to persist is actually making the cell better able to survive (White and DiPaola, 2009). This therefore presents as a double edged sword with its pro-survival aspects while the cell potentially harbours mutations amongst other aberrations. Conversely autophagy prevents such aberrations by removing various stress signals (White and DiPaola, 2009). The benefits and detriments are most likely to be unique to each individual cell. The delayed appearance of this increase (Figure 4.13) matches that of 1 PD (Figure 4.11), it would be interesting to see if this process fell in between these time points and re-emerged with the appearance of chromosomal instability (CIN), potentially promoting cell survival while the cell carries various chromosome aberrations. Furthermore, when cell fluorescence was examined a potential dose dependant reduction was noted, HF19 exposed to 2 Gy direct irradiation showed a significant reduction in fluorescence (Figure 4.14), even though the number had increased (Figure 4.13).

This indicates that although the cell maybe trying to maintain its basal level of lysosomes and more, the membrane may have lost its integrity and become partially permeable.

A potential explanation for this could relate to alterations in a steady state of the cell. A "normal" cell *i.e.* a control cell, will maintain a steady state of various proteins such as cell cycle checkpoint proteins, DDR proteins and others. Obviously these adjust according to situation the cell finds itself. For example in a low nutrient environment, the cell would most likely adjust the level of cell cycle check point proteins to prevent the cell dividing, however this all remains within a range of homeostatic fluctuations. At this delayed time point irradiated cells may have undergone genetic and epigentic changes that alter levels of proteins such as TNF-α, or a reduction in expression of key membrane proteins such as LAMP 1 & 2. A more conventional explanation might propose that the lysosomal membrane carries a form of fragility in its lipid membrane that transferred from its point of biogenesis. One might also be able to attribute the fragility to a change in composition of the membrane, this has been noted in other diseases (Goldberg and Riordan, 1986). Irrespective of the cause, an increase in permeability has potential implications for lysosomal enzyme relocation.

We also examined the bystander groups for aberrations in lysosomal characteristics (Section 2.2.3). The secondary bystander group showed very little change in lysosomal number, however the classical bystander group showed large reductions (approximately 25 - 30 %) at both doses, although only significant at 0.1 Gy (Figure 4.13). Interestingly we noted increases in ROS (discussed later) at 20 population doublings, this was exclusive to the classical bystander groups. This could potentially explain why we see a reduction in lysosomal number in the classical bystander group. It is unclear where the ROS emanate from, though potentially from within the lysosome and a result of Fenton chemistry (discussed earlier in this section). Alternatively they may arise from aberrant mitochondria; bystander signals have been shown to induce large changes in mitochondrial function (Lyng et al., 2000; Rajendran et al., 2011; Zhou et al., 2008; Dayal et al., 2009). The fact that a reduction in number is observed suggests that lysosomes are undergoing complete rupture with no structural integrity conserved. When compared to direct groups which demonstrated a reduction in fluorescence rather than number, this indicates some structural integrity but a more permeable state. The results obtained for cellular red fluorescence in the classical bystander group also showed a reduction that correlates with the

reduced number of lysosomes. Interestingly the secondary bystander group showed a reduced level of red fluorescence although not significant and not as severe as the other groups.

We also measured lysosomal fluorescence using the dye 5-(and-6)-chloromethyl-2',7'-dichlorodihydrofluorescein diacetate (CM-H2DCFDA). The cells were analysed for increases in fluorescence indicating oxidative stress. Due to the short lived nature of reactive oxygen species it was expected the majority would appear and be removed within the first few minutes following irradiation (Hall and Giaccia, 2006; Redpath and Gutierrez, 2001). However our results show that either some of these species have a longer half life or more likely are being produced at a higher rate than in the control group. It appears that oxidative stress is elevated following IR in both 0.1 and 2 Gy groups. This is maintained from 30 minutes all the way through to 12 hours. By 24 hours levels have started to return to control although still remain slightly increased. Intriguingly its possible to see a small increase in both doses at 12 hours, although this does not correlate with any pattern seen in lysosomal disturbances. The most likely cause of the elevation is likely to involve an imbalance between cellular antioxidant mechanisms and ROS production. The initial radiation insult is likely to remove a large number of antioxidants, this in combination with a likely increased production of ROS from damaged mitochondria will overwhelm the cells steady state. Redpath and Gutierrez (2001) combined work with Polyak et al. (1997) to suggest that a cause for delayed ROS production may be attributable to p53 and its potent transcriptional activity, in this instance up-regulating redox related genes which were responsible for ROS induction and mitochondrial failure.

Conversely, bystander cells showed the opposite effect. There was no real change after 30 minutes but 1 hour and 4 hours following medium transfer levels of oxidative stress had been reduced. This not only informs on the temporal effects of receiving bystander signals but also yields information on the cargo. Data obtained from Chapter 3 Figures 3.5 & 3.4 demonstrated that the bystander signal was detrimental in that it was able to increase levels of DNA damage, however our results show a potential beneficial effect by reducing oxidative stress (Figure 4.18), this double edged bystander effect has been documented previously and is reviewed by Mitchel (2004).

At 20 population doublings direct irradiated groups showed no abnormalities in the level of

fluorescence, indicating oxidative stress was at the same level as the control sample. This was also the case for the secondary bystander group. Conversely, the bystander group had elevated levels of oxidative stress: both 0.1 and 2 Gy showed very similar levels though only 2 Gy showed a significant increase. This indicates that signalling might play more of a role for delayed cellular damage than the memory of the direct insult. One hypothesis is that although the damage is greater in the direct group, the cell activates its entire defence from DNA damage repair to anti-oxidant production whereas the bystander groups receive a less severe insult and therefore do not activate so many defence mechanisms. Moreover this would explain why the same effect is not seen in the direct group because they have received the same secreted signals. It may also be possible the aforementioned alterations in transcription with regards to redox enzymes could cause this effect (Redpath and Gutierrez, 2001; Polyak et al., 1997). It is also important to mention that although no alterations were seen in the direct irradiated and secondary bystander group, these groups may display different temporal characteristics.

Finally in this chapter we investigated the possibility that reduced lysosomal fluorescence could be accounted for by lysosomal exocytosis. To this end we looked at lysosomal dispersion within the cell with the aim to detect no change or a greater level of fluorescence towards the edge of the cell. This would provide an indication that lysosomes move towards the cell membrane. This was conducted at 1 and 20 population doublings in order to correlate with lysosomal changes at time points relevant to GI and BE.

Very little difference was actually observed between control and treated groups at either time point of 1 or 20 population doublings. No group significantly changed from the control. The 0.1 Gy classical bystander group at 20 PD showed a slightly reduced level of fluorescence within the interior half of the cell however the control sample was slightly elevated when compared to others at this point. As a side note and for future investigation, approximately $\frac{2}{3}$ of lysosomes appeared within the inner half of the cell proximal to the nucleus. Should lysosomal enzymes be able to translocate we speculate the majority will be close to the nucleus.

In summary the data presented in this chapter has first shown that lysosomal membrane permeability can be induced by direct exposure to X-rays even at a relatively low dose of 0.1 Gy X-rays, and the effect is increased with dose. It has also been demonstrated that a secreted

bystander signal can influence lysosomal parameters such as number. The magnitude of the effect in bystander cells appears to be dose independent. The effects from 4 to 24 hours vary and are a likely consequence of a very dynamic situation occurring within the cell. Perhaps most importantly lysosomes appear to still be affected 20 population doublings after the insult in the direct and bystander group. No link between these alterations and ROS could be established suggesting another mechanism is driving the process. Yet bystander cells showed increased levels of oxidative stress at 20 population doublings the same time that a reduced number of lysosomes were observed, it is possible to speculate that the former might be driving the latter.

With reference to the project aim, it has been documented that lysosomal membrane permeabilization is increased following radiation in direct and bystander cells early after exposure. This response/phenotype continued until at delayed time points that correlate with the induction of GI in HF19 cells. Therefore it is possible that lysosomes are able to leak their contents into the cytoplasm, with their final destination possibly being the nucleus or cell membrane, or other structures such as the endoplasmic reticulum.

4.5 Conclusions

1. Direct exposure to X-rays at 0.1 and 2 Gy can cause significant lysosomal rupture

2. Over the first 24 hours there are large oscillations in lysosomal response.

3. Lysosomal membrane permeability was induced at delayed time points; the effect appeared greater in bystander cells; this was correlated with an increase in ROS.

4. Direct irradiated cells showed prolonged oxidative stress from 30 minutes until 12 hours, and some slight elevation at 24 hours. However the progeny of those cells failed to show the appearance of oxidative stress at 20 PD.

5. There does not appear to be a redistribution of lysosomes within the cell at 1 or 20 population doublings.

6. It is possible to conclude that X-rays disturbs the lysosomal membrane directly and indirecty. This has potential to allow leakage of lysosomal contents into the cytoplasm.

Chapter 5

Lysosomal breakdown has the potential to release enzymes into the cytoplasm where translocation to various sub-cellular locations is possible

5.1 Introduction

Following the observation of radiation induced lysosomal membrane permeability in HF19 cells we next looked at the potential downstream effects this might have on the cell, with regards to lysosomal content. Previously we have shown that radiation is able to induce lysosomal damage (Chapter 4). The damage caused to the lysosome is focused around its membrane and as such its integrity is reduced. Potentially, reactive oxygen species produced within the cytoplasm and within the lysosome, are able to interact with the lipid membrane acting as the causative agent of the increased permeability. There is also likely to be other processes involved, as permeability was increased in cells that showed no increase in oxidative stress. Possible mediators of radiation

induced lysosomal break down are the increased production of cellular cytokines, which have been previously implicated (Werneburg et al., 2004; Huai et al., 2013), along with the repair protein p53 (Li et al., 2007) (discussed in Section 4.4).

The reduced integrity of the lysosomal membrane results in either complete membrane rupture and ensuing release of the entire contents held within or a leaky state with partial release of the content. The contents are primarily composed of the enzymes used to degrade and recycle waste that has been targeted for removal. The cocktail of enzymes is enough to breakdown every component of the cell. However the lysosome provides a niche environment for these enzymes to work providing an optimum pH and cofactors. Interestingly, Yasuda et al. (1992) had shown that certain enzymes that work optimally at pH 5 are still functional at pH 7, therefore suggesting some lysosomal enzymes are able to work outside of their normal environment and importantly in the cell cytoplasm, or other location. They also demonstrated that lysosomal DNase was still functional at pH 6.5; however other researchers have shown lysosomal DNase to be active in the nucleus of mammalian cells (Tsukada et al., 2001; Villalpando Rodriguez and Torriglia, 2013; Nakagami et al., 2003)

Enzymes of particular interest include DNase IIα and acid sphingomyelinase (A-SMase), both are enzymes held within the lysosomal lumen and both have the capability to induce large changes within the cell. DNaseIIα is an enzyme which breaks down DNA (Alberts et al., 2008). Its estimated size is 42 kDa and is therefore thought too large to passively diffuse across the nuclear membrane (D'Angelo et al., 2009). However it is possible that radiation exposure has the ability to alter the nuclear membrane potentially making it more permeable allowing the translocation of DNase IIα into the nucleus, where it has access to a substrate, nuclear DNA.

The translocation of DNaseIIα to the nucleus has the potential to cause large scale damage in a direct fashion *i.e.* the enzyme activity is the damaging event, whereas effects induced by other enzymes such as acid sphingomyelinase are upstream of the damaging event, and more likely to be involved in signalling. A-SMase catalyzes the breakdown of sphingomyelin to ceramide, which is important in a number of pathways including apoptosis. The action of A-SMase maybe within the cell cytoplasm or at the cell surface. It is possible that lysosomes fuse with the cell surface promoting signalling rich regions of the cell membrane. The contents

may also be released into the extracellular space and, it is possible the release of such enzymes could relocate to distant sites and thus potentially have important roles in the BE.

In this study we initially examined nuclear permeability; we postulated that if the nuclear permeability had increased then this had the potential to let a whole range of material into the nucleus allowing access to the nuclear DNA.

5.2 Materials & Methods

In order to examine the effects of IR on lysosomal enzyme redistribution in HF19 cells immunohistochemical and live cell imaging techniques were employed. Cells were sub-cultured for at least 3 passages before experimentation. Approximately, 20 - 24 hours prior to irradiation cells were seeded onto 13mm or 9 mm coverslips within a 6 well plate for analysis at 1 and 20 population doublings. Each well was seeded at a density of 2×10^5. Bystander conditions were established as previously described (Section 2.2.3), briefly irradiated cells were returned to standard culture conditions for 4 hours following radiation. After 4 hours the media was removed and filtered and finally added to un-irradiated cells for 24 hours. Cells were propagated for 20 population doublings and then analysed again. At this time point a secondary bystander group was established as previously described (Section 2.2.3).

5.2.1 Cell culture

HF19 cells were removed from liquid nitrogen and placed in standard culture conditions as described in section 2.2.1.

5.2.2 Cell Irradiation

Cells were exposed to 0.1 Gy and 2 Gy X-ray irradiation and returned to standard culture conditions. Bystander groups and 0 Gy (control) were established in parallel. Cells were analysed for alterations in lysosomal enzyme location and nuclear permeability.

5.2.3 Nuclear Membrane Permeability

The method for nuclear membrane permeability was described in detail in section 2.2.9. Briefly: HF19 were permeabilized with digitonin in permeabilization buffer, they were then washed with permeabilization buffer minus digitonin three times; equilibrated initially in transfer buffer and then in transfer buffer containing FITC and finally imaged on a Zeiss confocal microscope.

Fluorescence was measured by selecting the nuclear area in a bright field image, this region of interest was analysed for fluorescence. Results were generated from 10 nuclei per group.

5.2.4 Immunohistochemistry: DNase IIα

The staining procedure was described in detail in Section 2.2.8. Briefly cells were fixed with ice cold methanol. The methanol was removed and any residual was washed away with PBS. The cells were blocked for 1 hour at room temperature with a combination of BSA and goat serum. They were then stained overnight with a 1:1500 dilution of DNaseIIα antibody in blocking solution at 4°C. The following morning the primary antibody was removed and the cells were washed; they were then stained with the fluorescent secondary antibody prior to being mounted and imaged. The nucleus was selected as a region of interest using a threshold of DAPI fluorescence, this region was analysed for DNase IIα fluorescence using Volocity. Nuclei from 20 cells were scored from 3 parallel repeats.

5.3 Results

Having documented lysosomal alterations in the directly irradiated cells then the potential downstream effects of this effect was investigated by examining lysosomal enzyme relocation in particular DNaseIIα. We also examined nuclear permeability to see if alterations could facilitate a redistribution of lysosomal enzymes.

5.3.1 Nuclear Permeability

Nuclear permeability was measured by influx of fluorescent dextran; which has a molecular weight of 40 kDa and is thus too large to passively diffuse across the membrane (Figure 5.3). Therefore we postulated that an increase in nuclear fluorescence would suggest an increase in nuclear membrane permeability.

Initially after 1 PD, the nuclear membrane permeability in the directly irradiated groups remained unchanged in either direction (Figure 5.1). However the cells exposed to either 0.1 and 2 Gy bystander media both demonstrated reductions in nuclear fluorescence indicating that they had become less permeable. Fluorescence was reduced to 11.95 A.U.$\pm$ 1.01 and 12.93 A.U.$\pm$ 1.24 in 0.1 and 2 Gy exposed groups respectively. Comparing across all the direct and bystander groups, the bystander control group also demonstrated a small reduction in fluorescence compared to the direct group although this was not statistically significant.

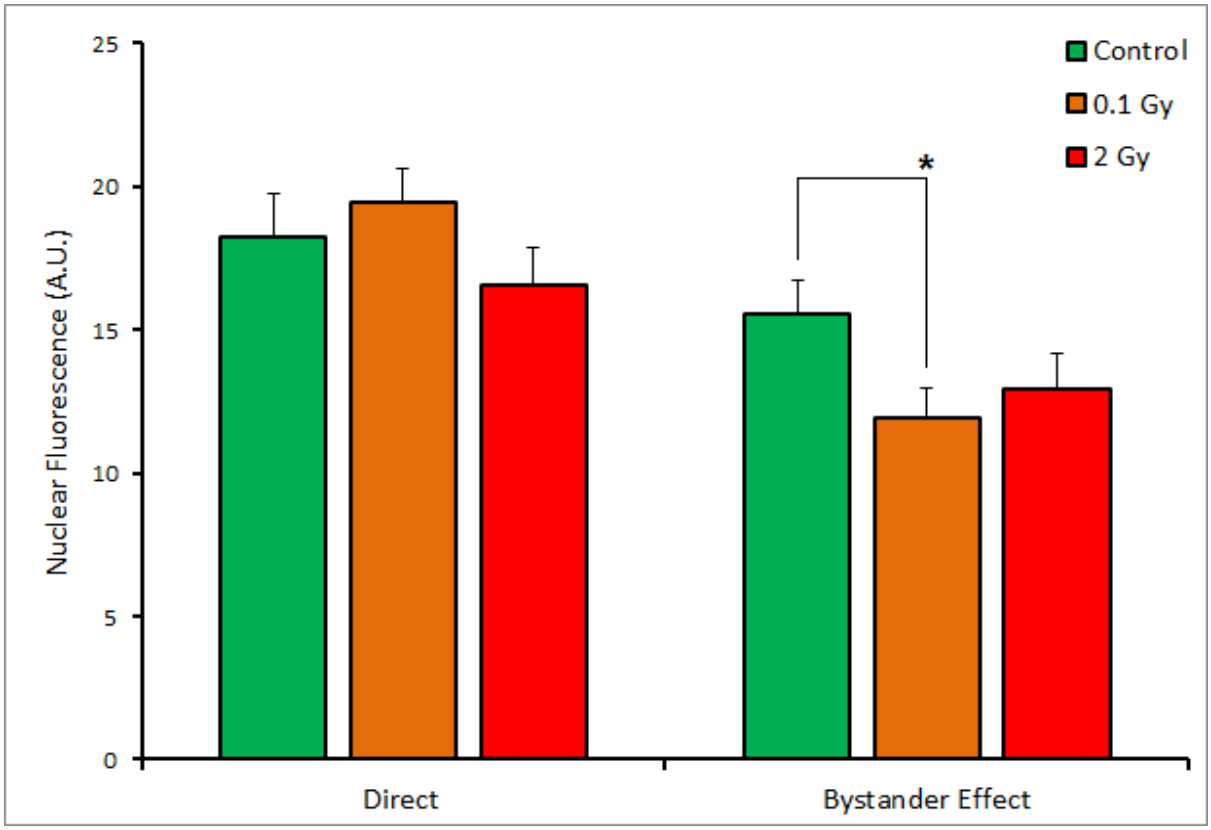

Figure 5.1: **HF19 cells were loaded with fluorescently labelled dextran with a molecular weight of 40 kDa, too large to passively diffuse across the nuclear membrane.** Cells were examined 1 population doubling (1PD) after direct and bystander exposure. The directly irradiated groups showed no significant change in nuclear fluorescence/permeability; however both bystander groups showed a reduction which was similar in magnitude, although only significant in the 0.1 Gy treated group, 2 Gy also showed a reduction although this was not significant. Interestingly the bystander control group also showed a small reduction in fluorescence again this was not significant.

Cells were further analysed at 20 population doublings later (Figure 5.2), to investigate possible differences between control and treated samples and also to examine temporal effects within control groups *i.e.* natural deterioration of the cell through age.

The directly irradiated groups both showed a similar significant reduction in cell fluorescence compared to the control *i.e.* 10.44 A.U.$\pm$ 1.12 (p $=\leq$ 0.05) in 0.1 Gy irradiated cells and 11.40 A.U.$\pm$ 0.85 (p $=\leq$ 0.05) in 2 Gy irradiated cells. These values were similar to those observed in the bystander groups at 1 PD. The control group showed no real change in the level of fluorescence to that observed at 1 PD.

The classical bystander groups (0.1 and 2 Gy) also showed a reduction, which were very similar

to those observed in the corresponding directly irradiated groups although the reductions were not significant (Figure 5.2). However in the secondary bystander group opposing effects *i.e.* increased fluorescence was observed at both doses although only significant at 2 Gy. Compared to the other control samples (Direct and Bystander groups) the level in the secondary bystander group was greatly reduced by approximately 10 A.U. The elevation seen in the secondary bystander treated cells was in line with the direct and classical bystander groups.

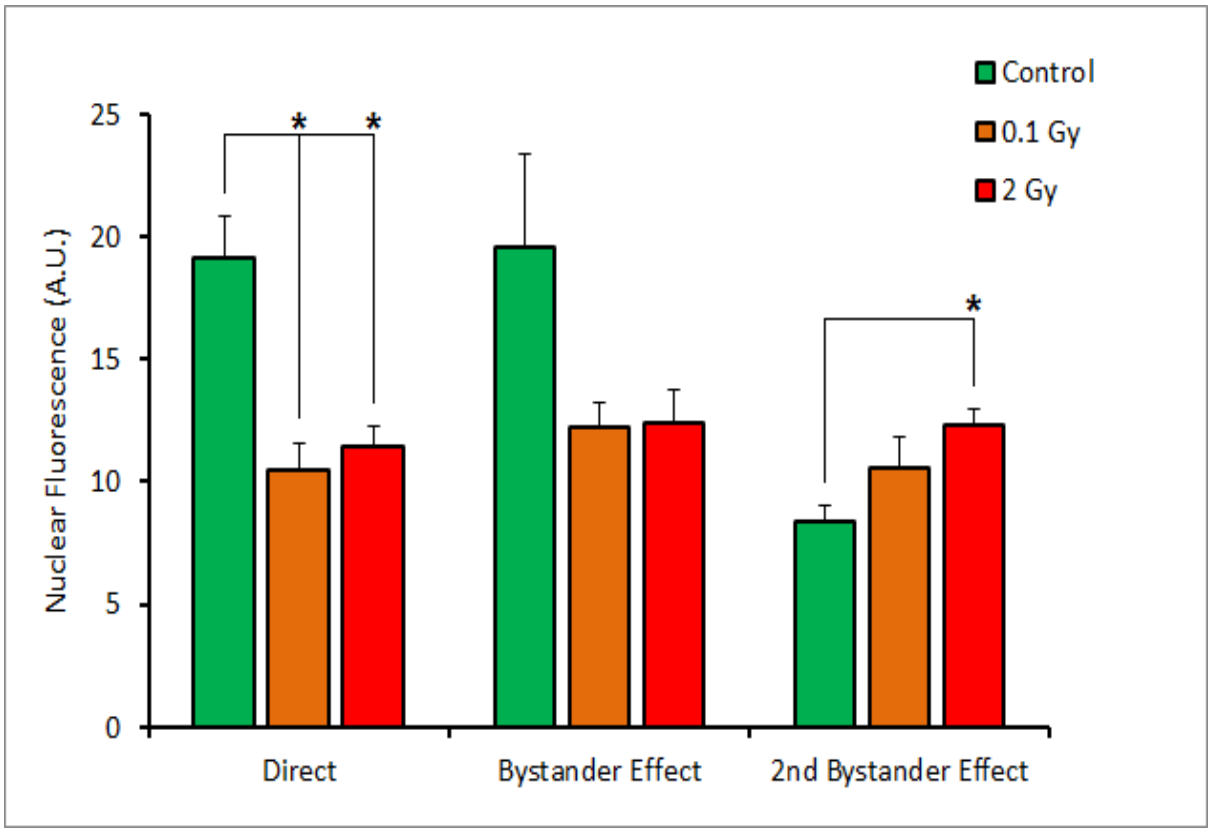

Figure 5.2: **HF19 cells were loaded with fluorescently labelled dextran with a molecular weight of 40 kDa, too large to passively diffuse across the nuclear membrane.** Cells were examined 20 population doubling following direct and bystander exposure. The directly irradiated groups showed significant reductions in permeability almost half that of the control. The classical bystander group showed reductions similar to the direct irradiated group. The secondary bystander group demonstrated the opposite effect, although the secondary bystander control group was reduced compared to the other controls.

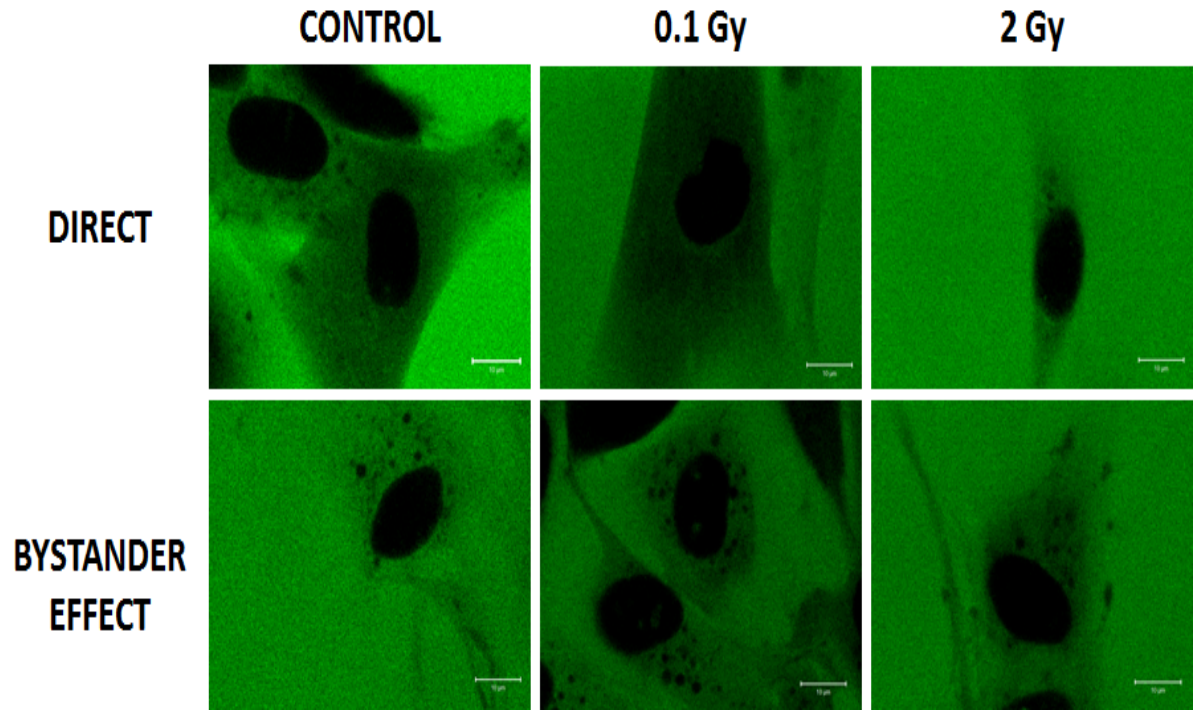

Figure 5.3: **Nuclear permeability was examined using a dextran exclusion assay in semi-permeabilized cells.** In direct irradiated cells there was no change in nuclear permeability however bystander groups did show a reduction indicating that the nucleus is less permeable than in control cells. At 20 population doublings there was a reduction in permeability in direct and bystander groups.

5.3.2 Translocation of DNase IIα to the nucleus

We first examined the level of fluorescence in the nucleus as an indicator of lysosomal enzyme translocation (Figure 5.6). Initially at 1 PD, qualitative observations revealed a number of punctate structures within the cell likely to be DNaseIIα held within the lysosomes. We further analysed the level of fluorescence within the cell nucleus marked by DAPI staining (Figure 5.4). In the directly irradiated cells at 1 population doubling both groups showed no significant change in levels of nuclear fluorescence. Cells exposed to 0.1 Gy had a fluorescence level of 2.86 A.U. $\pm$ 0.23 and cells exposed to 2 Gy 2.43 A.U. $\pm$ 1.01 compared to the control at 4.33 A.U.$\pm$ 0.67.

Cells exposed to bystander conditions also showed no significant difference when compared to their control. Media from cells exposed to 0.1 Gy demonstrated a small increase to 3.82 A.U. $\pm$ 0.57 compared to 2.89 A.U. $\pm$ 0.73 for the control. In comparison, HF19 cells exposed to 2 Gy bystander media showed a small reduction in nuclear fluorescence (2.35 A.U.$\pm$ 0.11).

It is worth noting that A.U. extends to 255, therefore whilst these changes may look large the actual difference between samples is relatively small.

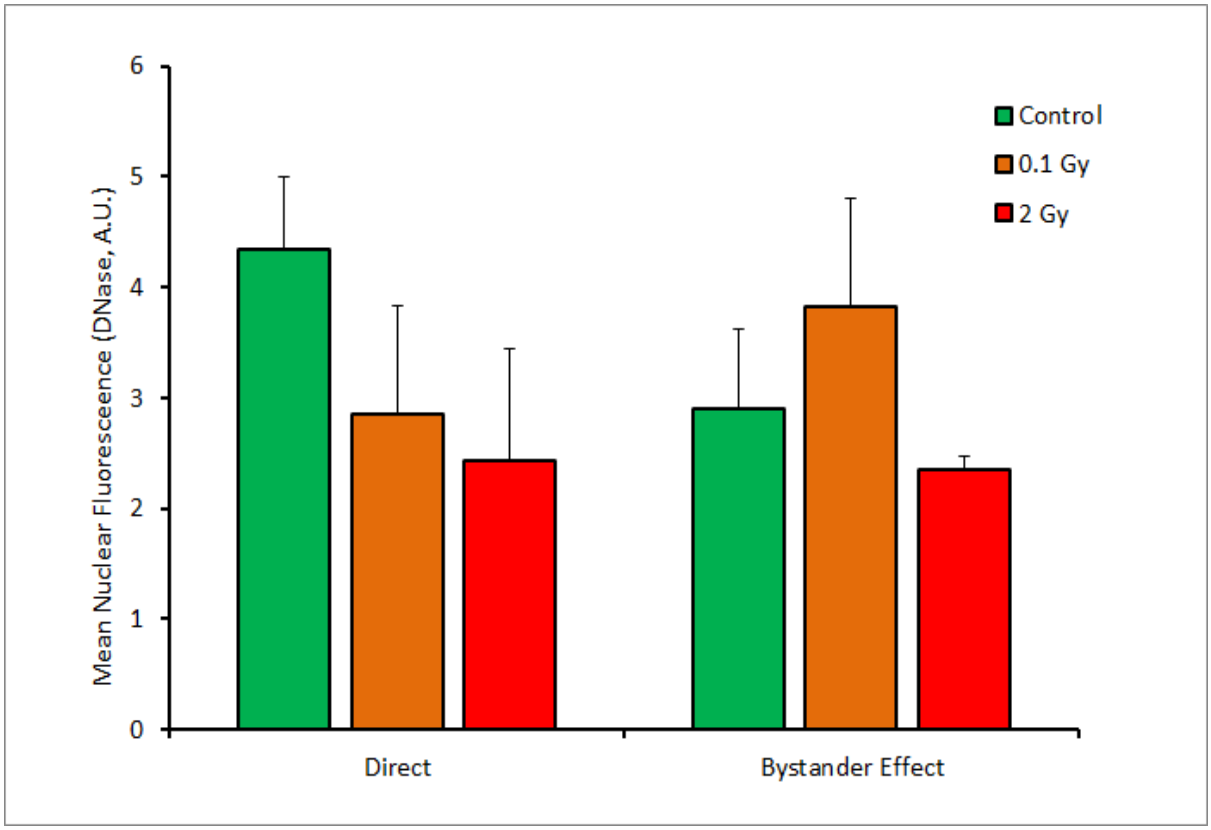

Figure 5.4: **HF19 cells were fluorescently labelled for DNase IIα 1 PD following radiation exposure.** A region of interest was selected based on a threshold of DAPI fluorescence and then analysed for presence of DNase IIα within this region. Directly irradiated groups demonstrated small decreases in nuclear fluorescence, whilst bystander groups showed an increase after 0.1 Gy and a reduction after 2 Gy. All of these changes were quite subtle and showed no statistical significance.

We subsequently analysed the HF19 cells at 20 PD, (Figure 5.5) a time point that we had previously noted chromosomal and lysosomal aberrations (Chapters 3 & 4). However, we were unable to demonstrate any significant alteration in nuclear fluorescence in any of the groups. The directly irradiated cells had slightly reduced and slightly elevated fluorescence compared to their control (3.39 A.U. $\pm$ 0.38) with levels at 2.68 A.U. $\pm$ 0.64 and 3.70 A.U. $\pm$ 0.18 for 0.1 and 2 Gy respectively.

Cells that received bystander signals demonstrated elevated levels of nuclear fluorescence compared to the bystander control. This effect increased with dose, i.e. cells that received media from 0.1 Gy irradiated cells had increased nuclear fluorescence to 4.70 A.U.$\pm$ 1.07, but this was further raised in the 2 Gy exposed group (6.21 A.U.$\pm$ 1.28). Additionally, the pattern observed

in the secondary bystander group appeared to mimic that observed in the directly irradiated groups in respect to dose and magnitude of the difference.

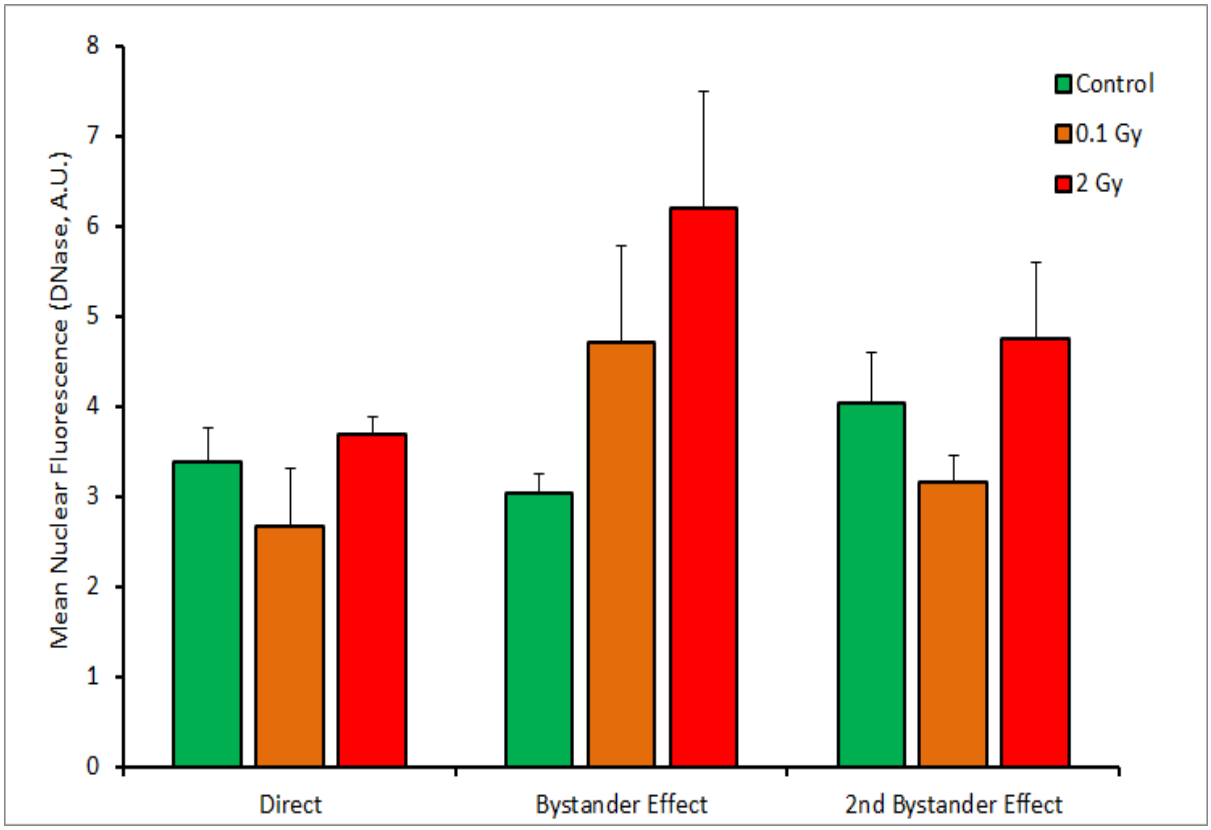

Figure 5.5: **HF19 cells were fluorescently labelled for DNaseIIα 20 PD following radiation exposure.** As observed at 1 PD, no significant differences were demonstrated between treated and control groups. However the classical bystander groups showed the largest increases in nuclear fluorescence after exposure with 2 Gy and 0.1 Gy respectively. The secondary bystander group appeared to mimic results of the directly irradiated groups.

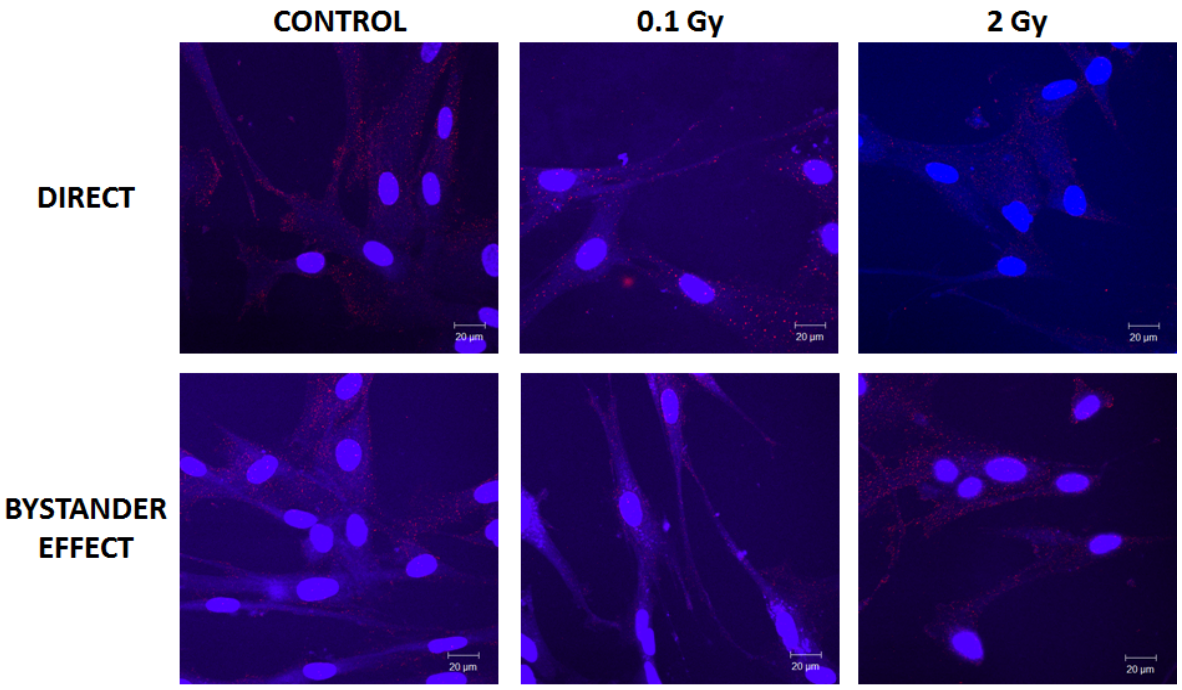

Figure 5.6: **The sub-cellular location of DNaseIIα was examined in HF19 cells.** The nuclear DNase IIα signal was measured in nuclei stained with DAPI. No significant presence of DNaseIIα was noted in the nucleus in any group or time point.

5.4 Discussion

In order to investigate a potential role for lysosomes in radiation-induced genomic instability and bystander effects it was first necessary to identify doses and time points at which GI was induced and if radiation was able to induce changes in lysosomes. Our data first showed induction of GI and BE in HF19 cells following X-rays and additionally, that X-rays were capable of altering lysosomes at delayed time points (Chapters 3 & 4 respectively).

Firstly examining nuclear permeability at 1 population doubling, we noted no change in permeability in the directly irradiated cells. However in bystander groups, we observed a reduction in nuclear fluorescence indicating that the nuclear membrane had become less permeable *i.e.* more restrictive in allowing molecules to traverse from the cytoplasm to the nucleus. The reduction in nuclear fluorescence observed in the bystander group but not in the directly irradiated cells after 1 PD was an unexpected result. We first hypothesized that the radiation had caused some physical damage to the membrane reducing its permeability. However, we further reasoned that it was more likely that the cells with damaged nuclear membranes had actually undergone cell death and had thus been removed from the system.

The nuclear membrane or (envelope as it is sometimes known) shares a structure similar to that on the plasma membrane: a lipid bilayer that separates the genetic material from the cytoplasm allowing control over what has access to the DNA. In between the two membrane layers is a space called the perinuclear cisterna. Within the membrane are a number of proteins that form nuclear pores and it is through these pores that a normal cell is able to communicate with the cytoplasm. It appears that radiation can reduce the membrane permeability suggesting communication maybe reduced. This has potential implications for access of various signalling molecules and other proteins such as those involved in DNA repair. The reduction in permeability can be possibly attributed to a reduction in number of nuclear pores potentially orchestrated through an epigenetic mechanism. A reduction in the number of pores would result in fewer entry/exit routes for the dextran. In terms of native biological effects a reduction in the number of pores could be detrimental to transcription and translation, potentially also including cell division.

Nuclear membrane permeability research has mainly been associated with cell division, little

has been conducted in terms of damaging agents particularly ionizing radiation. The general research themes addressed by other research groups revolves around nuclear membrane breakdown for cell division and are therefore focused on increases in permeability. Hormones that belong to the glucocorticoid family have been shown to increase the membrane permeability of the nuclear membrane (Shahin et al., 2005). However, more recently research has investigated the potential for calcium to induce an increase in permeability (Strasser et al., 2012). It was found that calcium spikes were both necessary and sufficient to increase membrane permeability. Lyng et al. (2011) demonstrated rapid calcium fluxes after addition of bystander media. We suggest that if this rapid influx had occurred in bystander HF19 cells then either the nuclear membrane was resistant to calcium alterations or they were insufficient to induce such a change. It is said the more active in transcription the cell is the greater the number of pore complexes (Alberts et al., 2008). Irradiation may reduce transcription in HF19 cells and therefore this maybe another cause of reduced permeability.

At 20 population doublings, both the directly irradiated cells and the classical bystander groups demonstrated a reduction in fluorescence similar in magnitude to that observed after 1 PD in the bystander group. It is thus evident that the cell maintains some kind of memory of the irradiation to show such a change at this delayed time point. This may potentially be attributable to the aforementioned mechanisms such as epigenetic down-regulation in the number of pores present. Alternatively the membrane composition may create a more restrictive barrier.

Alterations in nuclear membrane permeability are not limited to cellular damaging agents and can arise from mutations. A common family of these diseases are called laminopathys and result from defects in nuclear lamin proteins. One such condition results from a truncation in lamin A where it was found the loss of function led to chromosomal aberrations and DNA damage *i.e.* GI (Liu et al., 2005). The authors postulate that this is a result of hampered DNA damage response and repair, associated with an increase in nuclear permeability. However HF19 cells showed a reduction in permeability, this has also been demonstrated to play a role in cellular damage with profound implications for tissues and organs. Zhang et al. (2008) studied the nuclear pore complex and noted mutation in a particular protein, NUP155, that resulted in reduced membrane permeability. The downstream effect of which was to reduce nuclear export of HSP70 mRNA as well as reducing nuclear import of the HSP70 protein; no change was seen

for HSP27. It was suggested that the effective down regulation of HSP70 was due to decreased nuclear permeability which had the potential to prevent the transcription of proteins important in atrial function. Mice with the mutation in NUP155 showed increased incidence of atrial fibrillation.

Translating these findings to our results could lead to the suggestion that radiation induced reduced nuclear membrane permeability could alter the expression of transcription factors or other important proteins that are important in maintaining GI, or DNA damage response proteins.

In terms of our hypothesis, a more exclusive nucleus, due to a reduction in membrane permeability makes it unlikely that DNaseIIα is able to translocate to the nucleus. However it raises more questions as to the mechanisms behind such an alteration and its potential implications. Moreover it highlights an additional sub-cellular structure that IR is able to cause delayed alterations in.

Of note the permeability of nuclei did not appear to show any age-dependent deterioration in the control groups, contrary to results published by D'Angelo et al. (2009). This study demonstrated age-dependent deterioration of nuclear pore complexes in isolated rat brain cells from animals aged 3 months and 28 months; the increase was attributable to oxidative damage. We had previously noted that oxidative damage was not present in HF19 cells at 20 population doublings and we hypothesized that the cells were efficient at removing such damaging agents that induce oxidative stress and in doing so protected the nuclear membrane.

We also examined lysosomal enzyme location, in particular DNaseIIα. Having shown that the lysosomal membrane has increased permeability after radiation, particularly at delayed time points (PD20); we wanted to know if this permeability resulted in the translocation of DNaseIIα to the nucleus. A brief examination was carried out into the presence of any nuclear localization signal that might be present within the DNase IIα amino acid sequence. We used nuclear localization signal prediction software (Kosugi et al., 2009; Horton et al., 2007) however there was no sequence homology. However it is very unlikely that DNase IIα is targeted for processing through the nuclear membrane. Therefore if it is causing nuclear DNA damage it has to freely diffuse across the membrane.

Our results suggested DNaseIIα did not translocate to the nucleus of HF19 cells following radiation exposure. The directly irradiated group showed very little change in fluorescence level within the nucleus or it was below detectable levels. In contrast both bystander groups (0.1 & 2 Gy) showed elevated nuclear fluorescence indicating that there was potentially more DNaseIIα within the nuclear membrane although these results were not statistically significant. However any potential translocation to the nucleus was likely to result in a DNA damaging effect. The enzyme, DNaseIIα, has been strongly implicated in apoptosis and DNA clearing (Evans and Aguilera, 2003), and it is thought other enzymes in the lysosome act in concert with DNaseIIα to remove histones and other DNA associated proteins.

The effect of DNaseIIα on DNA is to preferentially degrade it to form 3' phosphate termini (Schafer et al., 2009). However Pisoni (1996) states that DNaseIIα is active at two sites within the enzyme and is therefore able to induce DSBs, a likely lesion contributing to the progression of GI (Nagaria et al., 2013). More sensitive techniques might aid in the discovery of significant levels of DNaseIIα within the nucleus such as western blotting of nuclear fractions.

One avenue we did not explore relating to DNaseIIα was its potential to act on mitochondrial DNA. The mitochondrial DNA (mtDNA) is a 16 kB circular DNA molecule that encodes 13 proteins involved in the electron transport chain (Kim et al., 2006). It is known that mtDNA is susceptible to damage as it has limited repair capacity and is in a fairly relaxed with no histones to protect it. Potential DNase interaction with mtDNA could result in aberrant oxidative phosphorylation possibly increasing ROS production although this was not observed in the HF19 cell line. We have previously discussed that mitochondria might be involved in NTE (Section 1.3.3)

Although our studies have focused on one enzyme in particular, the lysosome contains a number of enzymes that are able to degrade various cell components, whether it be lipids or proteins. Three of the most important bioactive lipids are sphingosine, sphingomyelin and ceramide. These are all inter-changeable with the action of enzymes. One enzyme of particular interest is acid sphinogomyelinase. This enzyme catalyses the production of ceramide from sphingomyelin (Garca-Barros et al., 2013). Ceramide itself is a potent signalling molecule (Henry et al., 2013), especially in apoptosis. However Ceramide can be further converted to sphingosine which has

actually been linked with lysosomal membrane permeabilization (Johansson et al., 2010). There are likely to be many more pathways affected by lysosomal enzymes that could alter cellular homeostasis.

In summary we have shown that X-ray irradiation can reduce membrane permeability in direct irradiated cells and classical bystander cells at 20 population doublings. We didnt investigate the potential causes of this but it could be down to altered number of nuclear membrane pores. Other research has indicated this can alter protein synthesis and potentially up and down regulate proteins. However this is likely to make it harder for DNaseIIα to translocate to the nucleus. Immunohistochemical studies showed that DNaseIIα did not appear to translocate to the nucleus, although our classical bystander groups showed an increase in nuclear fluorescence. However the increased permeability in lysosomes could release other enzymes that are influential in signalling

5.5 Conclusions

1. Ionizing radiation does not appear to alter nuclear permeability 1 population doubling after X-ray exposure. However bystander groups showed a reduction in nuclear permeability.

2. At 20 population doublings the directly irradiated and classical bystander groups both showed reductions in permeability

3. Alterations in membrane permeability have potential implications for cell homeostasis as protein import and mRNA export

4. DNaseIIα does not appear to be present in the nucleus following radiation at early (1PD) or delayed time points (20 PD) or is beyond the detection limits of the method used.

5. Although DNaseIIα does not appear to be present in the nucleus other lysosomal enzymes could relocate to various other cellular destinations such as the plasma membrane

6. Nuclear permeability does not appear to alter with age in HF19 cells.

Chapter 6

General Discussion

6.1 Thesis Summary

Ionizing radiation is a potent environmental and man-made carcinogen (Hall and Giaccia, 2006). This has been well documented over many years and it was thought the mechanisms by which it caused biological effects were well understood, through direct and indirect damage immediately after exposure (Hall and Giaccia, 2006). However the discovery and documentation of non-targeted effects (NTE) (Kadhim et al., 1992; Nagasawa and Little, 1992), has initiated another level of radiation research into various effects such as genomic instability (GI) and bystander effects (BE) (discussed in Section 1.3) for which we don't as yet, fully understand the exact mechanisms (Morgan and Sowa, 2013). Genomic instability can be defined as an increase in rate of genetic alterations generation after the initial ionizing radiation (IR) insult; as of yet the causes of this delayed response have remained elusive. It has been shown that cytokines, ROS, epigentics and inflammation can be involved in the process (Lorimore et al., 2003; Schaue et al., 2012; Aypar et al., 2011; Liu et al., 2012; Kadhim et al., 2013). Some research has implicated the mitochondria having potential involvement (Dayal et al., 2009), indicating sub-lethal and sub-cellular damage at an organelle level can play a role in radiation induced NTE. It is also apparent that genetic factors play a large part (Kadhim et al., 2004). Even factors such as sexual inheritance have been implicated (Koturbash et al., 2008). There are many aspects of cell and molecular biology that contribute to these NTE that remain elusive such as:

cross talk between NTE to propagate or inhibit one another, the phenotypic differences observed between cell lines: are they the result of epipgenetics or genetic background? Perhaps one of our biggest gaps in knowledge are non-DNA aberrations; as mentioned earlier the mitochondria has been researched to some degree compared to other sub-cellular structures such as the nucleus, endoplasmic reticulum and the lysosome.

This study was constructed to investigate potential lysosome involvement in NTE as well as to characterise lysosomal responses to X-ray irradiation. As well as establishing their response early after irradiation (30 minutes - 24 hours) we also wanted to explore the effects that X-rays would induce in lysosomes many generations after the initial insult and if this could be correlated with the induction of GI and BE.

1. Initially we examined the susceptibility of HF19 cells to the induction of GI and BE following X-rays at 0.1 and 2 Gy. These are 2 doses that might be encountered in diagnostic and therapy related health care respectively. Chromosomal aberrations and total DNA damage were both assessed by solid Giemsa staining and the Comet assay i.e. occurrence of tail DNA respectively, as a measure of GI and BE induction.

2. Once the primary human fibroblast HF19 cells had demonstrated GI in the form of chromosomal instability at certain time points, lysosomal alterations were additionally measured at these time points in all groups (directly irradiated and corresponding bystander groups).

3. Lysosomal alterations were noted at delayed time points in all groups but particularly in bystander groups. Therefore cells were subsequently analysed for alterations in enzyme location to assess whether DNase IIα had translocated to the cell nucleus. In conjunction with this we wanted to note any changes in nuclear membrane permeability which might facilitate enzyme translocation and their role in the chromosomal/genomic instability in the irradiated and bystander groups.

6.2 HF19 susceptibility to GI induction following IR

Initially DNA damage was examined following IR exposure. Directly irradiated and bystander groups were analysed for their DNA damage response. We noted an increase in DNA damage after IR exposure that was dose dependent, and that the directly irradiated groups showed a biphasic response. We surmised that simple damage had been repaired within the first hour of radiation exposure but the more complex damage persisted up to 24 hours following exposure, however further analysis would be required to confirm this.

Thirty minutes after incubation with the bystander media there was no change in DNA damage. However, DNA damage was detected after 1 hours incubation with bystander media. This indicated that the bystander signal may require time to enter into the cellular system; alternatively the signal maybe endocytosed quickly but require time to exert its effects. Lyng et al. (2000) noted the induction of a calcium flux within seconds of media addition which might support the theory, requiring an hour for the effect *e.g.* DNA damage, to take place rather than time taken for signal uptake. Subsequent analysis at 20 PD in our studies, revealed an increase in DNA damage which was a first indication that HF19 cells were susceptible to GI induction at these doses. The experiment also included analysis of chromosomal aberrations at 1 and 20 population doublings. As expected there were a large number of chromosome aberrations 1 PD after exposure particularly after 2 Gy in direct groups. Bystander groups also showed elevated chromosomal aberrations at 20 population doublings.

As indicated above, we initially wanted to examine the susceptibility of HF19 cells to the induction of GI following IR. Cells were examined at 20 population doublings following irradiation. We found significant levels of chromosomal aberrations, mainly chromatid in nature, in the 2 Gy irradiated cells. 0.1 Gy cells also increased numbers of aberrations although not significantly. Bystander groups also showed induction of chromosomal aberrations although this was only significant in 2 Gy irradiated cells. Interestingly an early bystander response observed was a reduction in oxidative stress, it may be possible that the signal carries some antioxidant properties. The secondary bystander effect failed to show any significance, indicating the bystander signal was not continually produced.

Chromosome aberrations are known to occur through the manifestation of double strand breaks (DSBs), which ionizing radiation is particularly effective at inducing especially after high LET radiation (Lehnert, 2008; Hall and Giaccia, 2006). A number of variations exist to describe how chromosome aberrations are initiated and at the heart of all of them is the DNA DSB. It is thought that 2 DSBs are required, although one model suggests that one is sufficient (Lehnert, 2008). It is more likely to involve two strand breaks, the broken ends either reform with other broken ends or themselves forming a ring, alternatively the ends may fail to repair and the chromosome undergoes a deletion.

Irrespective of the mechanism, chromosomal aberrations have significant implications for the cell. In terms of genetics, large scale deletions may occur, partially or completely removing a gene. One such studied gene is the *HPRT* locus (Thacker et al., 1990). In primary human fibroblasts it was found that X-rays could cause complete deletion of the *HPRT* locus as well as partial deletions ultimately altering the phenotype (Simpson et al., 1993).

Chromosomal aberrations are also able to affect oncogenes and tumour suppressor genes, therefore these aberrations play a role in tumourogenesis and carcinogenesis. Perhaps the most well known example of this is the translocation between chromosome 9 and 22 to produce the *abl* fusion protein with *bcr* gene creating a potent oncogene.

6.3 X-ray induced lysosomal damage

Lysosomes are the terminal destination for a number of cellular components where a number of enzymes are able to degrade and recycle those components. The potential for these enzymes to interact freely with the cell is restricted by a lipid membrane and a protein trafficking pathway which directs the enzymes from production to the lysosome interior. However, should some agent damage the membrane it is possible active enzymes may leak into the cytoplasm/nucleus.

The susceptibility of lysosomes to induce permeability as a result of X-ray irradiation at early and delayed times in directly irradiated and bystander groups was investigated. the results demonstrated that the first hour following irradiation, there is a large increase in permeability that appeared to increase with dose. The opposite effect was seen in the bystander cells, although only at 1 hour. Over the next 24 hours in directly irradiated cells, we observed large fluctuations, perhaps oscillations in the number and fluorescence of lysosomes. Bystander cells also appeared to fluctuate over the same period. However, directly irradiated and bystander groups showed different responses at 24 hours, with direct groups demonstrating a reduction and bystander groups increased numbers of lysosomes.

More importantly, in terms of radiation induced GI in the irradiated and bystander groups, the cells were examined at 20 population doublings. At this time point any abnormalities seen would be as a result of transmissible GI to the cell progeny. In the case of directly irradiated groups the number of lysosomes remained fairly constant but there was a significant reduction in cell fluorescence demonstrating increased permeability in lysosomes. In the bystander groups there was a reduction in number and cell fluorescence. These results suggest that lysosomes become more, leaky, or possibly undergo complete rupture.

It was thought that ROS and oxidative stress may be responsible for such effects although experiments showed that although there were early increases in ROS (first 24 hours in direct irradiated groups) there was no substantial change at 20 population doublings, indicating this was not likely to be the cause or, the initial increase may have started the cascade of reactions that results in the delayed damage. A number of other possibilities could be attributed as the cause of this effect such as cytokine and protein signalling. Ultimately in terms of a potential

role in GI and BE the fact that lysosomes become more permeable suggests lysosomal enzymes are leaked into the extracellular space.

It was thought that radiation might alter the distribution of lysosomes to deal with various damaged cell components. It might also be possible that lysosomes are involved in the bystander effect by fusing with the cell membrane and secreting their contents into the extracellular space, indeed lysosomes have been involved in a reorganization to repair the plasma membrane in response to pore forming toxins (Xu et al., 2012; Toops and Lakkaraju, 2013). Although structurally lysosomes were altered, lysosomes did not appear to show any spatial reorganization 1 or 20 population doublings following irradiation.

6.4 Nuclear Permeability

The nuclear membrane plays an important role in cell homoeostasis however there is little research on how radiation may affect this important structure. In terms of our hypothesis we wanted to investigate whether this structure was perturbed in a way which would facilitate enzyme translocation into the nucleus.

Cell nuclei were measured for their fluorescence; a greater fluorescence intensity indicted more dextran inside the nucleus and therefore a more permeable nucleus. One population doubling after radiation exposure the directly irradiated groups demonstrated no reduction in fluorescence at either dose. However bystander groups demonstrated reductions in permeability as seen by reduced nuclear fluorescence. The cells were cultured to 20 population doublings where we had observed lysosomal permeability reductions and examined for nuclear permeability. At this delayed time point, cells showed a reduction in fluorescence in the directly irradiated and classical bystander groups suggesting a more exclusive nucleus. A reduction in permeability is known to have implications for protein import and mRNA export, affecting various processes such as transcription and translation, DNA damage response and cell cycle progression. It is possible to speculate that the reduction in nuclear permeability could be a cellular response to damage as a potential mechanism to prevent any further damage. This effect in fact makes it harder for DNaseIIα to translocate to the nucleus. However, in secondary bystander groups nuclear permeability appeared to be increased.

Potential mechanisms for this are likely to revolve around alterations in nuclear pores as these are the main entry route into the nucleus. Possible genetic or epigenetic effects could result in fewer/disrupted nuclear pores. A reduction in nuclear pore number can normally be correlated with a reduction in cell division index, which may occur as a result of GI. Moreover, we noted no age related deterioration in nuclear membrane permeability between 1 and 20 population doublings.

6.5 DNaseIIα

DNase IIα is a lysosomal enzyme with the ability to degrade DNA and cause single or double strand breaks. DSBs are potentially a causative agent for the chromosomal aberrations seen at the delayed time points, even though nuclear permeability appeared to decrease after radiation. Obviously small amounts of DNaseIIα will still be able to induce excess strand breaks; however we failed to see any evidence of significant elevation within the nucleus. Classical bystander groups showed an increase but both directly irradiated and secondary bystander groups remained at the control level.

Immunohistochemical techniques were used to detect the DNaseIIα within the nucleus. This technique has some issues regarding detection limits. While every effort was made to achieve the highest possible sensitivity with minimal background staining the method may not be able to detect levels of DNaseIIα if they are present in small quantities.

6.6 Summary & Conclusions: Role of lysosomes in radiation induced GI & BE

To summarise, we hypothesized that lysosomes maybe involved in the induction of genomic instability and bystander effects following exposure to ionizing radiation. Firstly, we studied HF19 cells for their suitability as a model system to examine lysosomal involvement. The appearance of chromosomal instability was induced and transmitted to the progeny of irradiated and bystander populations. These responses were observed at 1 and 20 population doublings which suggests a mechanistic link between the two processes. Lysosomes showed little change early following irradiation, but appeared altered in the progeny of both direct and bystander exposed cells. The properties of the lysosomal change varied between groups, the classical bystander groups were reduced in lysosomal number, and the lysosomes in the directly irradiated group appeared more permeable rather than a reduced number. We then investigated if nuclear permeability was altered and if this could facilitate the translocation of DNaseIIα. Again early post radiation, there was little change in nuclear permeability. In the progeny, however, nuclear permeability was decreased in the direct and classical bystander groups the consequence of which is to make it harder for DNaseIIα or any other enzyme to enter the nucleus. This has serious implications for protein import and mRNA export although further investigations would be required to prove this. There was no significant increase in the DNaseIIα signal as measured in cell nuclei. Therefore, it is possible to surmise that DNaseIIα is unlikely to contribute to GI or BE; however lysosomes still remain altered and could potentially alter the cellular environment.

In a broader perspective, although the particular enzyme DNaseIIα did not show significant accumulation within the nucleus, radiation was still able to alter the sub-cellular environment including large organelles such as the lysosome and the nuclear membrane. It is feasible that other constituents in the lysosome such as proteases, RNAses and lipases could be playing a role and it is also possible that other sub-cellular organelles could be involved in the process, such as mitochondria and endoplasmic reticulum, all of which add to a changing sub-cellular environment including calcium fluxes.

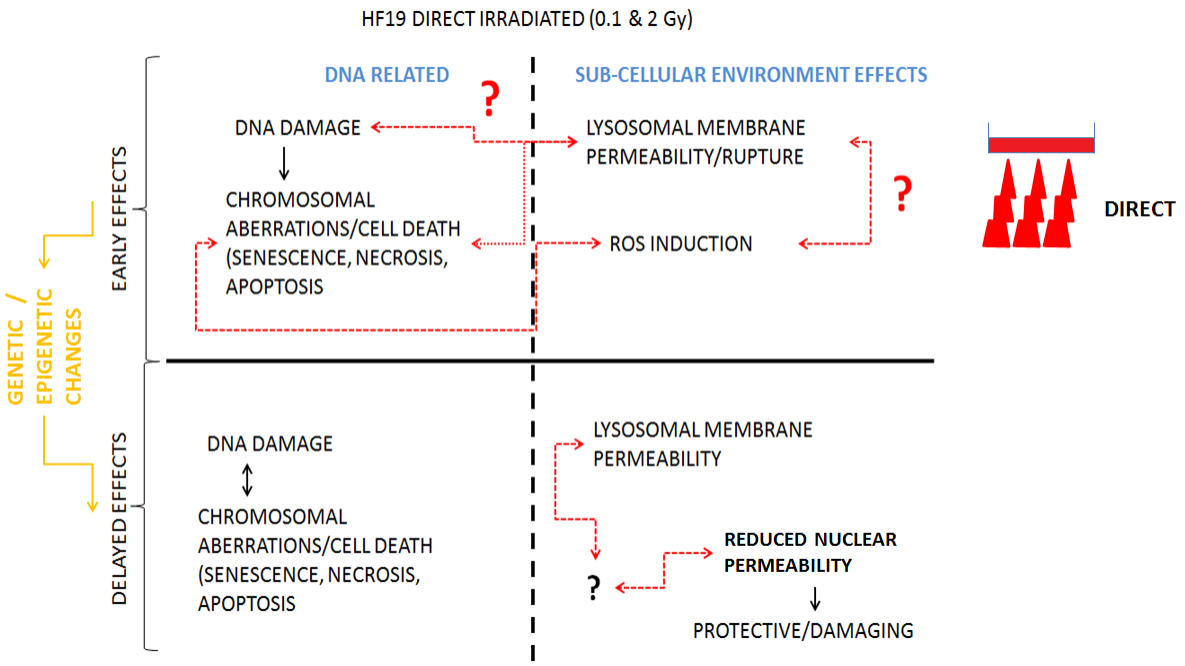

Figure 6.1: **A schematic of possible mechanistic interactions between DNA, lysosomal membrane permeability, ROS and nuclear membrane permeability in the induction of GI post radiation exposure.** Lysosomes in HF19 cells appear more permeable at early and late time points after radiation and this is correlated with an increase in ROS. At corresponding times, alterations in sub-cellular environment, DNA damage and increases in chromosomal aberrations were noted. As time progresses, we suggest that cells undergo genetic and epigenetic changes which may propagate the effects observed in the progeny of the irradiated cell that were seen at 20 PD. Lysosomal membrane permeability was altered at this time point although oxidative stress could not be directly correlated with this response.

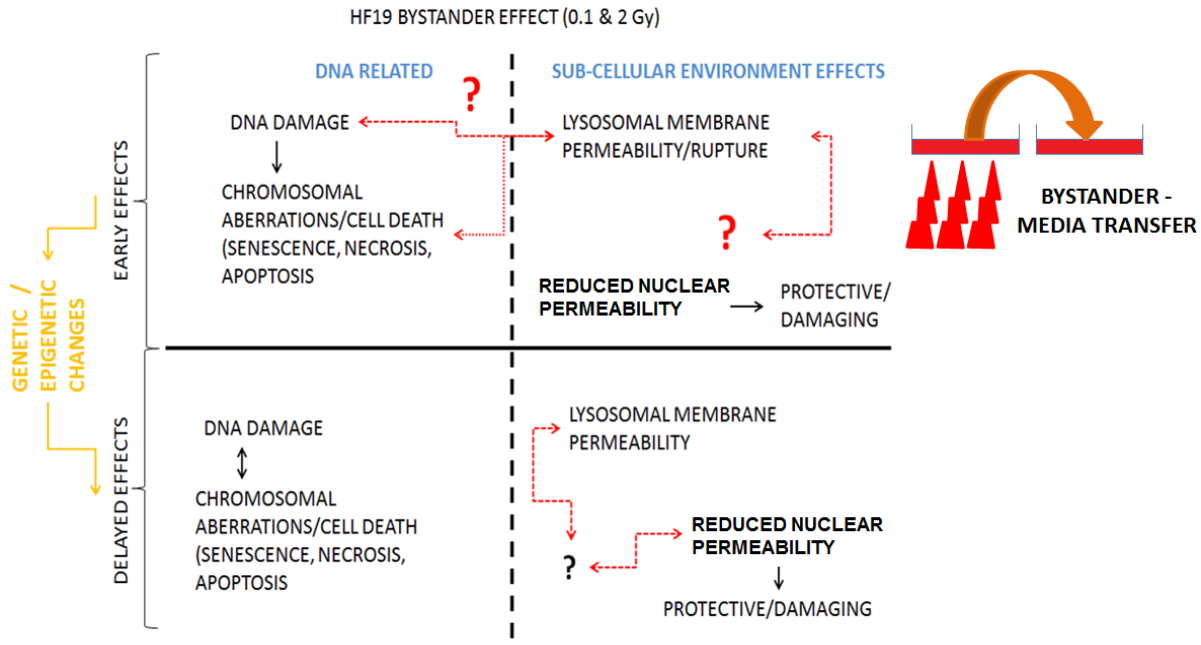

Figure 6.2: **A schematic of possible mechanistic interactions between DNA, lysosomal membrane permeability, ROS and nuclear membrane permeability in bystander exposed cells.** HF19 cell's lysosomes appear more permeable at early and late time points in bystander cells after media transfer although this failed to show any correlation with ROS. At corresponding times, alterations in sub-cellular environment, DNA damage and increaeses in chromosomal aberrations were noted. As time progresses, cells may undergo genetic and epigenetic changes which may propagate the effects seen in the progeny of the bystander population at 20 PD such as lysosomal membrane permeability, however, ROS could not be directly correlated with this response.

6.7 Future Work

A number of questions have arisen from the results generated in this project. Firstly looking narrowly at the specific experiments conducted, it would be interesting to examine what causes the delayed permeability in lysosomes. A number of methods could be employed to investigate this. Firstly the role of oxidative damage could be completely excluded by examining lysosomes for lipid oxidation a number of approaches exist in order to measure this mainly using imaging techniques. Secondly, having excluded oxidative stress as a cause investigations would be made into a potential role for protein interactions that induce lysosomal membrane permeabilization such as TNF-α and p53 amongst others.

Thirdly, enquiries into other lysosomal constituents would yield further information on its potential effects in radiation induced NTE. Enzymes such as acid sphingomyelinase (A-SMase) has the potential to effect potent signalling pathways. Further experiments to examine its sub-cellular location involving immunohistochemical techniques. Other proteins including LAMP 1 could be included to provide conclusive evidence that lysosomes fuse with the plasma membrane and release their contents into the extracellular space or not. Also within the lysosome are various lipases, RNAases and proteases. A number of these could potentially affect the sub-cellular location.

The results also demonstrate that ionizing radiation can reduce nuclear membrane permeability. This raises a number of questions about causes and effects. Research has shown that a reduction in nuclear permeability may have impacts on cellular transcription and translation (as discussed earlier Section 6.4). Firstly examining the nuclear membrane by electron microscopy would reveal ultrastructural abnormalities; some research has even modelled nuclear pore complexes using tomography, this could potentially identify causes of reduced permeability. To examine the potential effects this may have on the cellular fate, nuclear pores can be blocked by wheat germ agglutinin, subsequent phenotypes can then be measured.

In a broader research sense, this work has shown that sub-cellular components, in particular lysosomes and the nucleus, are affected by IR which correlate with GI and BE induction. This therefore poses the question what other sub-cellular components are altered; could the endo-

plasmic reticulum (ER) and Golgi body be involved? This could be visualised using fluorescent tagged proteins important in both structures to identify targets that are altered post irradiation. Previous investigations have already linked oxidative stress in the ER with apoptosis (Wei et al., 2008), thus could this be a mechanism in radiation induced NTE? Indeed some early stage research within Kadhim's group documented changes in the ER examined by electron microscopy and so this is a promising base to further explore the role of organelle damage in non-targeted radiation effects.

Bibliography

IL. Aivaliotis, IS. Pateras, M. Papaioannou, C. Glytsou, K. Kontzoglou, EO. Johnson, and V. Zoumpourlis. How do cytokines trigger genomic instability? *Journal of Biomedicine and Biotechnology*, 2012, 2012. doi: 10.1155/2012/536761.

B. Alberts, A. Johnson, J. Lewis, M. Raff, K. Roberts, and P. Walter. *Molecular biology of the cell: Reference edition*. Garland Science, 2008.

A. C. Allison. The possible role of lysosomes in carcinogenesis. *Proceedings of the Royal Society of Medicine*, 59(9):868–871, 1966.

AC. Allison and GR. Paton. Chromosome damage in human diploid cells following activation of lysosomal enzymes. *Nature*, 207(5002):1170–1173, 1965.

MM. Antoshchina, NI. Riabchenko, VA. Nasonova, EV. Fesenko, and II. Pelevina. [the genome instability in the descendants of the chinese hamster of the cells, irradiated by the low dose and by various intensities of gamma-radiation]. *Radiatsionnaia Biologiia, Radioecologiia / Rossiskaia Akademiia Nauk*, 45(3):291–293, 2005.

F. Antunes, E. Cadenas, and UT. Brunk. Apoptosis induced by exposure to a low steady-state concentration of h(2)o(2) is a consequence of lysosomal rupture. *The Biochemical journal*, 356:549–555, 2001.

N. Autsavapromporn, M. Suzuki, T. Funayama, N. Usami, I. Plante, Y. Yokota, Y. Mutou, H. Ikeda, K. Kobayashi, Y. Kobayashi, Y. Uchihori, TK. Hei, EI. Azzam, and T. Murakami. Gap junction communication and the propagation of bystander effects induced by microbeam

irradiation in human fibroblast cultures: The impact of radiation quality. *Radiation Research*, 29, 2013.

U. Aypar, WF. Morgan, and JE. Baulch. Radiation-induced epigenetic alterations after low and high let irradiations. *Mutation Research*, 707(1-2):24–33, 2011.

E. I. Azzam, S. M. de Toledo, T. Gooding, and J. B. Little. Intercellular communication is involved in the bystander regulation of gene expression in human cells exposed to very low fluences of alpha particles. *Radiation Research*, 150(5):497–504, 1998.

Edouard I. Azzam, Sonia M. De Toledo, Douglas R. Spitz, and John B. Little. Oxidative metabolism modulates signal transduction and micronucleus formation in bystander cells from alpha-particle-irradiated normal human fibroblast cultures. *Cancer Research*, 62(19): 5436–5442, 2002.

EI Azzam, SM de Toledo, and JB Little. Oxidative metabolism, gap junctions and the ionizing radiation-induced bystander effect. *Oncogene*, 22:7050–7057, 2003.

EI Azzam, SM de Toledo, and JB Little. Stress signaling from irradiated to non-iraddiated cells. *Current Cancer Drug Targets*, 4:53–64, 2004.

BM. Babior. Nadph oxidase: an update. *Blood*, 93(5):1464–1476, 1999.

RD. Bagshaw, DJ. Mahuran, and JW. Callahan. A proteomic analysis of lysosomal integral membrane proteins reveals the diverse composition of the organelle. *Molecular & Cellular Proteomics: MCP*, 4(2):133–143, 2005.

Richard D. Bagshaw, John W. Callahan, and Don J. Mahuran. The arf-family protein, arl8b, is involved in the spatial distribution of lysosomes. *Biochemical and Biophysical Research Communications*, 344(4):1186–1191, 2006.

F. Ballarini, D. Alloni, A. Facoetti, A. Mairani, R. Nano, and A. Ottolenghi. Modelling radiation-induced bystander effect and cellular communication. *Radiation Protection Dosimetry*, 122(1-4):244–251, 2006.

JP. Banth, SH. MacPhail, and PL. Olive. Radiation sensitivity, h2ax phosphorylation, and

kinetics of repair of dna strand breaks in irradiated cervical cancer cell lines. *Cancer Research*, 64:7144–49, 2004.

GC. Barnett, RM. Elliott, J. Alsner, CN. Andreassen, O. Abdelhay, NG. Burnet, J. Chang-Claude, CE. Coles, S. Gutirrez-Enrquez, MJ. Fuentes-Raspall, MC. Alonso-Muoz, S. Kerns, A. Raabe, RP. Symonds, P. Seibold, CJ. Talbot, F. Wenz, J. Wilkinson, J. Yarnold, AM. Dunning, BS. Rosenstein, CM. West, and Bentzen SM. Individual patient data meta-analysis shows no association between the snp rs1800469 in tgfb and late radiotherapy toxicity. *Radiotherapy and Oncology : journal of the european soceity for radiology and oncology*, 105(3): 289–95, 2012.

K. Baverstock and OV. Belyakov. Some important questions connected with non-targeted effects. *Mutation Research*, 687(1-2):84–88, 2010.

O. V. Belyakov, S. A. Mitchell, D. Parikh, G. Randers-Pehrson, S. A. Marino, S. A. Amundson, C. R. Geard, and D. J. Brenner. Biological effects in unirradiated human tissue induced by radiation damage up to 1 mm away. *Proceedings of the National Academy of Sciences of the United States of America*, 102(40):14203–14208, 2005.

OV. Belyakov, KM. Prise, KR. Trott, and BD. Michael. Delayed lethality, apoptosis and micronucleus formation in human fibroblasts irradiated with x-rays or alpha-particles. *International Journal of Radiation Biology*, 75(8):985–993, 1999.

C. Berndt, T. Kurz, M. Selenius, AP. Fernandes, MR. Edgren, and UT. Brunk. Chelation of lysosomal iron protects against ionizing radiation. *The Biochemical journal*, 432:295–301, 2010.

DA. Bowler, SR. Moore, DA. Macdonald, SH. Smyth, P. Clapham, and MA. Kadhim. Bystander-mediated genomic instability after high let radiation in primary haemopoietic stem cells. *Mutation Research*, 597(1):50–61, 2006.

NA. Bright, MJ. Gratian, and JP. Luzio. Endocytic delivery to lysosomes mediated by concurrent fusion and kissing events in living cells. *Current Biology*, 15(4):360–365, 2005.

AL. Brooks, SA. Benjamin, FF. Hahn, DG. Brownstein, WC. Griffith, and RO. McClellan.

The induction of liver tumors by 239pu citrate or 239puo2 particles in the chinese hamster. *Radiation Research*, 96(1):135–151, 1983.

PE. Bryant. Effects of ara a and fresh medium on chromosome damage and dna double-strand break repair in x-irradiated stationary cells. *The British Journal of Cancer. Supplement*, 6: 61–65, 1984.

PE. Bryant, AC. Riches, and SYA. Terry. Mechanisms of the formation of radiation-induced chromosomal aberrations. *Mutation Research*, 701(1):23 – 26, 2010.

M. Castedo, J. Perfettini, T. Roumier, K. Andreau, R. Medema, and G. Kroemer. Cell death by mitotic catastrophe: a molecular definition. *Oncogene*, 23:2825 – 2837, 2004a.

M. Castedo, JL. Perfettini, T. Roumier, K. Yakushijin, D. Horne, R. Medema, and G. Kroemer. The cell cycle checkpoint kinase chk2 is a negative regulator of mitotic catastrophe. *Oncogene*, 23(25):4353 – 61, 2004b.

AE. Chang. *Oncology: an evidence-based approach*. Springer, 2006.

KL. Chapman, JW. Kelly, R. Lee, EH. Goodwin, and MA. Kadhim. Tracking genomic instability within irradiated and bystander populations. *The Journal of Pharmacy and Pharmacology*, 60(8):959–968, 2008.

MA. Chaudhry. Base excision repair of ionizing radiation induced dna damage in g1 and g2 cell cycle phases. *Cancer Cell International*, 24:7–15, 2007.

B. Chen, Y. Zhong, W. Peng, Y. Sun, YJ. Hu, Y. Yang, and WJ. Kong. Increased mitochondrial dna damage and decreased base excision repair in the auditory cortex of d-galactose-induced aging rats. *Molecular Biology Reports*, 38:3635 – 3642, 2011.

N. Chen and V. Karantza-Wadsworth. Role and regulation of autophagy in cancer. *Biochimica Et Biophysica Acta*, 1793(9):1516–1523, 2009.

S. Cianfarani, B. Tedeschi, D. Germani, SP. Prete, P. Rossi, P. Vernole, D. Caporossi, and Boscherini B. In vitro effects of growth hormone (gh) and insulin-like growth factor i and

ii (igf-i and -ii) on chromosome fragility and p53 protein expression in human lymphocytes. *European Journal of Clinical Investigation*, 28(1):41 – 7, 1998.

PJ. Coates, SA. Lorimore, BA. Rigat, DP. Lane, and EG. Wright. Induction of endogenous b-galactosidase by ionizing radiation complicates the analysis of p53-lacz transgenic mice. *Oncogene*, 20:7096 – 7, 2001.

MJ. Czaja. Functions of autophagy in hepatic and pancreatic physiology and disease. *Gastroenterology*, 140(7):1895 – 1908, 2011.

MA. D'Angelo, M. Raices, SH. Panowski, and MW. Hetzer. Age-dependent deterioration of nuclear pore complexes causes a loss of nuclear integrity in postmitotic cells. *Cell*, 136(2):284 – 295, 2009.

D. Dayal, SM. Martin, KM. Owens, N. Aykin-Burns, Y. Zhu, A. Boominathan, D. Pain, CL. Limoli, PC. Goswami, FE. Domann, and DR. Spitz. Mitochondrial complex ii dysfunction can contribute significantly to genomic instability after exposure to ionizing radiation. *Radiation Research*, 172(6):737–745, 2009.

BM. De Rey, ME. Itoiz, AC. Frasch, and RL. Cabrini. Ultrastructural localization of acid phosphatase in normal and x-irradiated epidermis. *Journal of Cutaneous Pathology*, 3(1): 25–34, 1976.

ID. Desai, PL. Sawant, and AL. Tappel. Peroxidative and radiation damage to isolated lysosomes. *Biochimica Et Biophysica Acta*, 86:277–285, 1964.

S. Desai, A. Kumar, S. Laskar, and BN. Pandey. Cytokine profile of conditioned medium from human tumor cell lines after acute and fractionated doses of gamma radiation and its effect on survival of bystander tumor cells. *Cytokine*, 61(1):54–62, 2013.

A. Deshpande, EH. Goodwin, SM. Bailey, BL. Marrone, and BE. Lehnert. Alpha-particle-induced sister chromatid exchange in normal human lung fibroblasts: evidence for an extranuclear target. *Radiation Research*, 145(3):260 – 7, 1996.

GL. Dianov and JL. Parsons. Co-ordination of dna single strand break repair. *DNA Repair*, 6 (4):454–60, 2006.

JS. Dickey, BJ. Baird, CE. Redon, MV. Sokolov, OA. Sedelnikova, and WM. Bonner. Intercellular communication of cellular stress monitored by gamma-h2ax induction. *Carcinogenesis*, 30(10):1686–1695, 2009.

B. Dieriks, WH. De Vos, H. Derradji, S. Baatout, and P. Van Oostveldt. Medium-mediated dna repair response after ionizing radiation is correlated with the increase of specific cytokines in human fibroblasts. *Mutation Research*, 687(1-2):40–48, 2010.

S. Elmore. Apoptosis: A review of programmed cell death. *Toxicologic Pathology*, 35(4):495 – 516, 2007.

E. Eskelinen and P. Saftig. Autophagy: a lysosomal degradation pathway with a central role in health and disease. *Biochimica Et Biophysica Acta*, 1793(4):664–673, 2009.

CJ. Evans and RJ. Aguilera. Dnase ii: genes, enzymes and function. *Gene*, 322:1–15, 2003.

EE. Farmer and MJ. Mueller. Ros-mediated lipid peroxidation and res-activated signaling. *Annual review of plant biology*, 64:429–50, 2013.

M. Frankenberg-Schwager, M. Becker, I. Garg, E. Pralle, H. Wolf, and D. Frankenberg. The role of nonhomologous dna end joining, conservative homologous recombination, and single-strand annealing in the cell cycle-dependent repair of dna double-strand breaks induced by h(2)o(2) in mammalian cells. *Radiation Research*, 170(6):784–793, 2008.

H. Furlong, C. Mothersill, FM. Lyng, and O. Howe. Apoptosis is signalled early by low doses of ionising radiation in a radiation-induced bystander effect. *Mutation Research*, 741:35–43, 2013.

M. Garca-Barros, N. Coant, JP. Truman, AJ. Snider, and YA. Hannun. Sphingolipids in colon cancer. *Biochimica Et Biophysica Acta*, 13, 2013.

DM. Goldberg and JR. Riordan. Role of mmembrane in disease. *Clinical Physiology and Biochemistry*, 4(5):305 – 36, 1986.

AA. Goodarzi and PA. Jeggo. The repair and signalling responses to dna double strand breaks. *Advances in Genetics*, 82:1–45, 2013.

P. Grote and E. Ferrando-May. In vitro assay for the quantitation of apoptosis-induced alterations of nuclear permeability. *Nature Protocols*, 6:3034 – 40, 2006.

DV. Guryev, AN. Osipov, EY. Lizunova, NY. Vorobyeva, and OV. Boeva. Ionizing radiation-induced genomic instability in cho cells is followed by selection of radioresistant cell clones. *Bulletin of experimental biology and medicine*, 147(5):596–8, 2009.

EJ Hall and AJ Giaccia. *Radiobiology for the Radiologist*. Lippincott Williams & Wilkins, Philadelphia, 6th edition, 2006.

K. Hamasaki, Y. Kusunoki, E. Nakashima, N. Takahashi, K. Nakachi, N. Nakamura, and Y. Kodama. Clonally expanded t lymphocytes from atomic bomb survivors in vitro show no evidence of cytogenetic instability. *Radiation Research*, 172(2):234–243, 2009.

M. Hamasaki, ST. Shibutani, and T. Yoshimori. Up-to-date membrane biogenesis in the autophagosome formation. *Current Opinion in Cell Biology*, 25(4):455 – 460, 2013. ISSN 0955-0674. doi: http://dx.doi.org/10.1016/j.ceb.2013.03.004. URL `http://www.sciencedirect.com/science/article/pii/S0955067413000550`. ¡ce:title¿Cell organelles¡/ce:title¿.

W. Han, L. Wu, B. Hu, L. Zhang, S. Chen, L. Bao, Y. Zhao, A. Xu, and Z. Yu. The early and initiation processes of radiation-induced bystander effects involved in the induction of dna double strand breaks in non-irradiated cultures. *The British Journal of Radiology*, 80 Spec No 1:S7–12, 2007.

W. Han, S. Chen, KN. Yu, and L. Wu. Nitric oxide mediated dna double strand breaks induced in proliferating bystander cells after alpha-particle irradiation. *Mutation Research*, 684(1-2): 81–89, 2010.

TK. Hei. Cyclooxygenase-2 as a signaling molecule in radiation-induced bystander effect. *Molecular Carcinogenesis*, 45(6):455–460, 2006.

B. Henry, C. Mller, MT. Dimanche-Boitrel, E. Gulbins, and KA. Becker. Targeting the ceramide system in cancer. *Cancer Letters*, 332(2):286 – 94, 2013.

AW. Hickman, RJ. Jaramillo, JF. Lechner, and NF. Johnson. Alpha-particle-induced p53 protein expression in a rat lung epithelial cell strain. *Cancer Research*, 54(22):5797–5800, 1994.

E. Holtzman. *Lysosomes*. Cellular Organelles. Plenum Press, New York, 1989.

P. Horton, KJ. Park, T. Obayashi, N. Fujita, CJ. Harada, H.and Adams-Collier, and K. Nakai. Wolf psort: protein localization predictor. *Nucleic Acids Research*, pages 1 – 3, 2007. doi: doi:10.1093/nar/gkm259.

J. Huai, F. Nora Vogtle, L. Jockel, Y. Li, T. Kiefer, E. Ricci, and C. Borner. Tnf alpha-induced lysosomal membrane permeability (lmp) is downstream of momp and triggered by caspase-mediated p75 cleavage and ros formation. *Journal of Cell Science*, 126(Pt 17):4015 – 25, 2013.

F. Hutchison. Chemical changes produced in dna by ionizing radiation. *Progress in Nucleic Acid Research*, 32:115 – 154, 1985.

G. Iliakis, Y. Wang, J. Guan, and H. Wang. Dna damage checkpoint control in cells exposed to ionizing radiation. *Oncogene*, 22(37):5834–5847, 2003. DNA damage after IR.

S. Inoue, M. Tyrkus, Y. Ravindranath, and N. Gohle. A variant translocation between chromosomes 4 and 11 , t(4q;11p) in a child with acute leukemia. *The American journal of pediatric hematology/oncology*, 7(2):211–214, 1985.

SL. Irons, V. Serra, D. Bowler, K. Chapman, S. Militi, F. Lyng, and Kadhim M. The effect of genetic background and dose on non-targeted effects of radiation. *International Journal of Radtion Biology*, 88(10):735–42, 2012.

AC. Johansson, H. Appelqvist, C. Nilsson, K. Kagedal, K. Roberg, and K. Ollinger. Regulation of apoptosis-associated lysosomal membrane permeabilization. *Apoptosis*, 15(5):527 – 540, 2010.

M. Kadhim, S. Salomaa, E. Wright, G. Hildebrandt, OV. Belyakov, KM. Prise, and MP. Little.

Non-targeted effects of ionising radiation-implications for low dose risk. *Mutation Research*, 752(2):84 – 98, 2013.

MA. Kadhim, DA. Macdonald, DT. Goodhead, SA. Lorimore, SJ. Marsden, and EG. Wright. Transmission of chromosomal instability after plutonium alpha-particle irradiation. *Nature*, 355(6362):738–740, 1992.

MA. Kadhim, SA. Lorimore, MD. Hepburn, DT. Goodhead, VJ. Buckle, and EG. Wright. Alpha-particle-induced chromosomal instability in human bone marrow cells. *Lancet*, 344 (8928):987–988, 1994.

MA. Kadhim, SJ. Marsden, and EG. Wright. Radiation-induced chromosomal instability in human fibroblasts: temporal effects and the influence of radiation quality. *International Journal of Radiation Biology*, 73(2):143–148, 1998.

MA. Kadhim, SR. Moore, and EH. Goodwin. Interrelationships amongst radiation-induced genomic instability, bystander effects, and the adaptive response. *Mutation Research*, 568: 21–32, 2004.

MA. Kadhim, MA. Hill, and SR. Moore. Genomic instability and the role of radiation quality. *Radiation protection dosimetry*, 122(1-4):221–7, 2006.

V. Kaminskyy and BB. Zhivotovsky. Proteases in autophagy. *Biochimica Et Biophysica Acta*, 1824(1):44–50, 2012.

M. Kandouz and G. Batist. Gap junctions and connexins as therapeutic targets in cancer. *Expert Opinion on Therapeutic Targets*, 14(7):681 – 692, 2010.

M. Karlsson, T. Kurz, UT. Brunk, SE. Nilsson, and CI. Frennesson. What does the commonly used dcf test for oxidative stress really show? *The Biochemical Journal*, 428(2):183 – 90, 2010.

AV. Karotki and K. Baverstock. What mechanisms/processes underlie radiation-induced genomic instability? *Cellular and Molecular life sciences*, 69(20):3351–60, 2012.

G. Kashino, K. Prise, K. Suzuki, N. Matsuda, S. Kodama, M. Suzuki, K. Nagata, Y. Kinashi,

S. Masunaga, K. Ono, and M. Watanabe. Effective suppression of bystander effects by dmso treatment of irradiated cho cells. *Journal of Radiation Research*, 48(4):327–333, 2007.

GJ. Kim, K. Chandrasekaran, and WF. Morgan. Mitochondrial dysfunction, persistently elevated levels of reactive oxygen species and radiation-induced genomic instability: a review. *Mutagenesis*, 21(6):361 – 7, 2006.

M. Kimura, T. Yoshioka, M. Saio, Y. Banno, H. Nagaoka, and Y. Okano. Mitotic catastrophe and cell death induced by depletion of centrosomal proteins. *Cell Death and Disease*, 4:603 – 614, 2013.

Y. Kodama, K. Ohtaki, M. Nakano, K. Hamasaki, AA. Awa, F. Lagarde, and N. Nakamura. Clonally expanded t-cell populations in atomic bomb survivors do not show excess levels of chromosome instability. *Radiation Research*, 164(5):618–26, 2005.

S. Kosugi, M. Hasebe, M. Tomita, and H. Yanagawa. Systematic identification of yeast cell cycle-dependent nucleocytoplasmic shuttling proteins by prediction of composite motifs. *Proceedings of the Academy of Sciences of the United States of America*, 106:10171 – 6, 2009.

I. Koturbash, M. Baker, J. Loree, K. Kutanzi, Dl. Hudson, I. Pogribny, O. Sedelnikova, W. Bonner, and O. Kovalchuk. Epigenetic dysregulation underlies radiation-induced transgenerational genome instability in vivo. *International Journal of Radiation Oncology, Biology, Physics*, 66(2):327–330, 2006a.

I. Koturbash, RE. Rugo, CA. Hendricks, J. Loree, B. Thibault, K. Kutanzi, I. Pogribny, JC. Yanch, BP. Engelward, and O. Kovalchuk. Irradiation induces dna damage and modulates epigenetic effectors in distant bystander tissue in vivo. *Oncogene*, 25(31):4267–4275, 2006b.

I. Koturbash, K. Kutanzi, K. Hendrickson, R. Rodriguez-Juarez, D. Kogosov, and O. Kovalchuk. Radiation-induced bystander effects in vivo are sex specific. *Mutation Research*, 642(1 - 2): 28 – 36, 2008.

O. Kovalchuk and JE. Baulch. Epigenetic changes and nontargeted radiation effects–is there a link? *Environmental and Molecular Mutagenesis*, 49(1):16–25, 2008.

G. Kroemer, P. Galluzzi, L. Vandenabeele, and J. Abrams. Classi?cation of cell death: recommendations of the nomenclature committee on cell death 2009. *Cell Death and Differentiation*, 16:3 – 11, 2009.

T. Kurz, A. Leake, T. Von Zglinicki, and Brunk UT. Relocalized redox-active lysosomal iron is an important mediator of oxidative-stress-induced dna damage. *The Biochemical Journal*, 378(Pt 3):1039–45, 2004.

T. Kurz, JW. Eaton, and UT. Brunk. Redox activity within the lysosomal compartment: implications for aging and apoptosis. *Antioxidants & Redox Signaling*, 13(4):511 – 23, 2010.

J. Lacombe, G. Karsenty, and Ferron M. Regulation of lysosome biogenesis and functions in osteoclasts. *Cell Cycle*, 12(17), 2013.

PB. Lakshmanagowda, L. Viswanath, N. Thimmaiah, L. Dasappa, SS. Supe, and Kallur P. Abscopal effect in a patient with chronic lymphocytic leukemia during radiation therapy: a case report. *Cases journal*, 2, 2009.

S. Laufer, S. Gay, and K. Brune. *Inflammation and rheumatic diseases: the molecular basis of novel therapies*. Thieme, 2003.

YL. Law, TPW. Wong, and KN. Yu. Influence of catechins on bystander responses in cho cells induced by alpha-particle irradiation. *Applied Radiation and Isotopes: Including Data, Instrumentation and Methods for Use in Agriculture, Industry and Medicine*, 68(4-5):726–729, 2010.

T. Lbke, P. Lobel, and DE. Sleat. Proteomics of the lysosome. *Biochimica Et Biophysica Acta*, 1793(1793):625–635, 2009.

B. E. Lehnert and E. H. Goodwin. A new mechanism for dna alterations induced by alpha particles such as those emitted by radon and radon progeny. *Environmental Health Perspectives*, 105 Suppl 5:1095–1101, 1997.

BE. Lehnert, EH. Goodwin, and A. Deshpande. Extracellular factor(s) following exposure to

alpha particles can cause sister chromatid exchanges in normal human cells. *Cancer Research*, 57(11):2164–2171, 1997.

S. Lehnert. *Biomolecular Action of Ionizing Radiation*. Taylor & Francis, 2008.

R. Lev Bar-Or, R. Maya, LA. Segal, U. Alon, AJ. Levine, and M. Oren. Generation of oscillations by the p53-mdm2 feedback loop: a theoretical and experimental study. *Proceedings of the Academy of Sciences of the United States of America*, 97(21):11250–5, 2000.

B. Levine and J. Yuan. Autophagy in cell death: an innocent convict? *The Journal of Clinical Investigation*, 115(10):2679 – 2688, 2005.

N. Li, Y. Zheng, W. Chen, C. Wang, X. Liu, W. He, H. Xu, and X. Cao. Adaptor protein lapf recruits phosphorylated p53 to lysosomes and triggers lysosomal destabilization in apoptosis. *Cancer Research*, 67(23):11176 – 85, 2007.

CL. Limoli and E. Giedzinski. Induction of chromosomal instability by chronic oxidative stress. *Neoplasia (New York, N.Y.)*, 5(4):339–346, 2003.

Y. Lin, Epstein DL., and Liton P. Intralysosomal iron induces lysosomal membrane permeabilization and cathepsin dmediated cell death in trabecular meshwork cells exposed to oxidative stress. *Investigative Opthalmology & Visual Science*, 51(12):6483 – 95, 2010.

C. Lindholm, A. Acheva, and S. Salomaa. Clastogenic plasma factors: a short overview. *Radiation and Environmental Biophysics*, 49(2):133–138, 2010.

AM. Liu, WW. Qu, X. Liu, and CK. Qu. Chromosomal instability in in vitro cultured mouse hematopoietic cells associated with oxidative stress. *American Journal of Blood Research*, 2 (1):71–76, 2012.

B. Liu, J. Wang, KM. Chan, WM. Tjia, W. Deng, X. Guan, JD. Huang, KM. Li, PY. Chau, DJ. Chen, D. Pei, AM. Pendas, J. Cadianos, C. Lpez-Otn, HF. Tse, C. Hutchison, J. Chen, Y. Cao, KS. Cheah, K. Tryggvason, and Z. Zhou. Genomic instability in laminopathy-based premature aging. *Nature Medicine*, 11(7):780 – 5, 2005.

S. Lorimore, PJ. Coates, GE. Scobie, G. Milne, and EG. Wright. Inflammatory-type responses

after exposure to ionizing radiation in vivo: a mechanism for radiation-induced bystander effects? *Oncogene*, 20:7085 – 7095, 2001.

SA. Lorimore and EG. Wright. Radiation-induced genomic instability and bystander effects: related inflamatory type responses to radiation induced stess and injury? a review. *International Journal of Radiation Biology*, 79(1):15–25, 2003.

SA. Lorimore, MA. Kadhim, DA. Pocock, D. Papworth, DL. Stevens, DT. Goodhead, and EG. Wright. Chromosomal instability in the descendants of unirradiated surviving cells after alpha-particle irradiation. *Proceedings of the National Academy of Sciences of the United States of America*, 95(10):5730–5733, 1998.

SA. Lorimore, PJ. Coates, and EG. Wright. Radiation-induced genomic instability and bystander effects: inter-related nontargeted effects of exposure to ionizing radiation. *Oncogene*, 22(45):7058–7069, 2003.

PJ. Luzio, PR. Pryor, and NA. Bright. Lysosomes: fusion and function. *Nature Reviews. Molecular Cell Biology*, 8(8):622–632, 2007.

FM. Lyng, CB. Seymour, and C. Mothersill. Production of a signal by irradiated cells which leads to a response in unirradiated cells characteristic of initiation of apoptosis. *British Journal of Cancer*, 83(9):1223–1230, 2000.

FM. Lyng, OL. Howe, and B. McClean. Reactive oxygen species-induced release of signalling factors in irradiated cells triggers membrane signalling and calcium influx in bystander cells. *International Journal of Radiation Biology*, 87(7):683 – 95, 2011.

BL. Mahaney, K. Meek, and SP. Lees-Miller. Repair of ionizing radiation-induced dna double-strand breaks by non-homologous end-joining. *The Biochemical Journal*, 417(3):639–650, 2009.

M. Mancuso, E. Pasquali, S. Leonardi, M. Tanori, S. Rebessi, V. Di Majo, S. Pazzaglia, MP. Toni, M. Pimpinella, V. Covelli, and A. Saran. Oncogenic bystander radiation effects in patched heterozygous mouse cerebellum. *Proceedings of the National Academy of Sciences*, 105(34):12445–12450, 2008.

SJ. McMahon, KT. Butterworth, C. Trainor, CK. McGarry, JM. O'Sullivan, G. Schettino, AR. Hounsell, and Prise KM. A kinetic-based model of radiation-induced intercellular signalling. *PLoS One*, 8(1), 2013.

PL. McNeil. Repairing a torn cell surface: make way, lysosomes to the rescue. *Jornal of Cell Science*, 115:873 – 9, 2002.

M. Mehrpour, A. Esclatine, I. Beau, and P. Codogno. Autophagy in health and disease. 1. regulation and significance of autophagy: an overview. *American Journal of Physiology. Cell Physiology*, 298(4):C776–785, 2010.

AE. Meijer, AB. Saeidi, A. Zelenskaya, S. Czene, F. Granath, and M. Harms-Ringdahl. Influence of dose-rate, post-irradiation incubation time and growth factors on interphase cell death by apoptosis and clonogenic survival of human peripheral lymphocytes. *International journal of Radiation Biology*, 75(10):1265–73, 1999.

M. Merrifield and O. Kovalchuk. Epigenetics in radiation biology: a new research frontier. *frontiers in Genetics*, 4(40), 2013.

JA. Mindell. Lysosomal acidification mechanisms. *Annual review of Physiology*, 74:69–86, 2012.

RE. Mitchel. The bystander effect: recent developments and implications for understanding the dose response. *Nonlinearity in biology, toxicology, medicine*, 2(3):173 – 183, 2004.

W. Morgan, A. Hartmann, CL. Limoli, S. Nagar, and B. Ponnaiya. Bystander effects in radiation-induced genomic instability. *Mutation Research*, 504:91 – 100, 2002.

W. F. Morgan, J. P. Day, M. I. Kaplan, E. M. McGhee, and C. L. Limoli. Genomic instability induced by ionizing radiation. *Radiation Research*, 146(3):247–258, 1996.

WF. Morgan and M. Sowa. Non-targeted effects induced by ionizing radiation: Mechanisms and potential impact on radiation induced health effects. *Cancer Letters*, (0): –, 2013. ISSN 0304-3835. doi: http://dx.doi.org/10.1016/j.canlet.2013.09.009. URL `http://www.sciencedirect.com/science/article/pii/S0304383513006629`.

William F. Morgan. Non-targeted and delayed effects of exposure to ionizing radiation: I.

radiation-induced genomic instability and bystander effects in vitro. *Radiation Research*, 159 (5):567–580, 2003.

William F. Morgan and Marianne B. Sowa. Non-targeted effects of ionizing radiation: implications for risk assessment and the radiation dose response profile. *Health Physics*, 97(5): 426–432, 2009.

P. Mosesso, F. Palitti, J. Pepe, G. Piero, R. Bellacima, G. Ahnstrom, and AT. Natarajan. Relationship between chromatin structure, dna damage and repair following x-irradiation of human lymphocytes. *Mutation Research*, 701(1):86–91, 2010.

C. Mothersill and C. Seymour. Medium from irradiated human epithelial cells but not human fibroblasts reduces the clonogenic survival of unirradiated cells. *International Journal of Radiation Biology*, 71(4):421–427, 1997.

D. Mukherjee, PJ. Coates, SA. Lorimore, and EG. Wright. The in vivo expression of radiation-induced chromosomal instability has an inflammatory mechanism. *Radiation Research*, 177 (1):18–24, 2012.

C. Mullins and JS. Bonifacino. The molecular machinery for lysosome biogenesis. *BioEssays: News and Reviews in Molecular, Cellular and Developmental Biology*, 23(4):333–343, 2001.

K. Muraki, K. Nyhan, L. Han, and JP. Murnane. Mechanisms of telomere loss and their consequences for chromosome instability. *Frontiers in Oncology*, 2(135), 2012.

JM. Murray, T. Stiff, and PA. Jeggo. Dna double strand break repair within heterochromatic regions. *Biochemical Society Transactions*, 40(1):173–8, 2012.

S. Nagar, L. Smith, and WF. Morgan. Mechanisms of cell death associated with death-inducing factors from genomically unstable cell lines. *Mutagenesis*, 18(6):549–60, 2003a.

S. Nagar, LE. Smith, and WF. Morgan. Characterization of a novel epigenetic effect of ionizing radiation: the death-inducing effect. *Cancer Research*, 63(2):324–8, 2003b.

P. Nagaria, C. Robert, and FV. Rassool. Dna double strand break response in stem cells:

mechanisms ti maintain genomic integrity. *Biochimica Et Biophysica Acta*, 1839(2):2345 – 53, 2013.

H. Nagasawa and JB. Little. Induction of sister chromatid exchanges by extremely low doses of alpha-particles. *Cancer Research*, 52(22):6394–6396, 1992.

H. Nagasawa, A. Cremesti, R. Kolesnick, Z. Fuks, and JB. Little. Involvement of membrane signaling in the bystander effect in irradiated cells. *Cancer Research*, 62(9):2531 – 2534, 2002.

Y. Nakagami, M. Ito, T. Hara, T. Inoue, and S. Matsubara. Nuclear translocation of dnase ii and acid phosphatase during radiation-induced apoptosis in hl60 cells. *Acta Oncologica*, 42 (3):227–236, 2003.

C. Nicolini, A. Belmont, S. Parodi, S. Lessin, and S. Abraham. Mass action and acridine orange staining: static and ?ow cyto?uorometry. *Journal of Histochemistry and Cytochemistry*, 27: 102 – 113, 1979.

PJ. O'Connor, Manning. FC., AT. Gordon, MA. Billett, DP. Cooper, RH. Elder, and Margison GP. Dna repair: kinetics and thresholds. *Toxicologic Pathology*, 28(3):375–81, 2000.

EA. Oczypok, TD. Oury, and CT. Chu. It's a cell-eat-cell world: autophagy and phagocytosis. *The American Journal of Pathology*, 182(3):612–22, 2013.

A. Ottolenghi, F. Ballarini, and M. Merzagora. Modelling radiation-induced biological lesions: from initial energy depositions to chromosome aberrations. *Radiation and Environmental Biophysics*, 38(1):1–13, 1999.

K. Ozaki and WJ. Leonard. Cytokine and cytokine receptor pleiotropy and redundancy. *The Journal of biological chemistry*, 277(33):29355–8, 2002.

U.S. Dept of Energy Pacific Northwest National Laboratory. Frequently asked questions about health effects of low doses of radiation, October 2012. URL `http://lowdose.energy.gov/faqs.aspx`.

F. Paris, Z. Fuks, A. Kang, P. Capodieci, G. Juan, D. Ehleiter, A. Haimovitz-Friedman,

C. Cordon-Cardo, and RE. Kolesnick. Endothelial apoptosis as the primary lesion initiating intestinal radiation damage in mice. *Science*, 293:293–97, 2001.

E. Pastwa and J. Blasiak. Non-homologous dna end joining. *Acta Biochimica Polonica*, 50(4): 891–908, 2003.

E. Pastwa and M. Malinowski. Non-homologous dna end joining in anticancer therapy. *Current Cancer Drug Targets*, 7(3):243–50, 2007.

AA. Peden, V. Oorschot, BA. Hesser, CD. Austin, RH. Scheller, and J. Klumperman. Localization of the ap-3 adaptor complex defines a novel endosomal exit site for lysosomal membrane proteins. *The Journal of Cell Biology*, 164(7):1065–1076, 2004.

LA. Pena, Z. Fuks, and RN. Kolesnick. Radiation-induced apoptosis of endothelial cells in the murine central nervous system: protection by fibroblast growth factor and sphingomyelinase deficiency. *Cancer Research*, 60:321 – 327, 2000.

R. Persaud, H. Zhou, SE. Baker, TK. Hei, and EJ. Hall. Assessment of low linear energy transfer radiation-induced bystander mutagenesis in a three-dimensional culture model. *Cancer Research*, 65(21):9876–9882, 2005.

HL. Persson. Iron-dependent lysosomal destabilization initiates silica-induced apoptosis in murine macrophages. *Toxicology Letters*, 159(2):124–33, 2005.

RL. Pisoni. *Subcellular Biochemistry: Volume 27 Biology of the Lysosome*, volume 27. Plenum Press, 1996.

Dennis Pitt. *Lysosomes and Cell Function.* Intergrated Themes in Biology. Longman, New York, 1975.

I. Pogribny, I. Koturbash, D. Tryndyak, V. Hudson, SM. Stevenson, O. Sedelnikova, W. Bonner, and Kovalchuk O. Fractionated low-dose radiation exposure leads to accumulation of dna damage and profound alterations in dna and histone methylation in the murine thymus. *Molecular Cancer Research*, 3(10):553–61, 2005.

K. Polyak, Y. Xia, JL. Zweier, KW. Kinzler, and B. Vogelstein. A model for p53-induced apoptosis. *Nature*, 389(6648):300 – 5, 1997.

B. Ponnaiya, M. Suzuki, C. Tsuruoka, Y. Uchihori, Y. Wei, and TK. Hei. Detection of chromosomal instability in bystander cells after si490-ion irradiation. *Radiation Research*, 176(3): 280–90, 2011.

RJ. Preston. Radiation biology: concepts for radiation protection. *Health Physics*, 87(1):3–14, 2004.

KM. Prise, M. Folkard, and BD. Michael. A review of the bystander effect and its implications for low-dose exposure. *Radiation Protection Dosimetry*, 104(4):347–355, 2003.

S. Prithivirajsingh, MD. Story, SH. Bergh, FB. Gera, KK. Ang, SM. Ismail, CW. Stevens, TA. Buchholz, and WA. Brock. Accumulation of the common mitochondrial dna deletion induced by ionizing radiation. *FEBS Letters*, 571:227 – 232, 2004.

L. Qiang, C. Wu, M. Ming, B. Viollet, and YY. He. Autophagy controls p38 activation to promote cell survival under genotoxic stress. *The Journal of Biological Chemistry*, 288(3): 1603 – 11, 2013.

S. Rajendran, SH. Harrison, RA. Thomas, and JD. Tucker. The role of mitochondria in the radiation-induced bystander effect in human lymphoblastoid cells. *Radiation Research*, 175 (2):159 – 71, 2011.

S. Rashi-Elkeles, R. Elkon, S. Shavit, Y. Lerenthal, C. Linhart, A. Kupershtein, N. Amariglio, G. Rechavi, R. Shamir, and Y. Shiloh. Transcriptional modulation induced by ionizing radiation: p53 remains a central player. *Molecular Oncology*, 5(4):336–48, 2011.

JL. Redpath and M. Gutierrez. Kinetics of induction of reactive oxygen species during the post-irradiation expression of neoplastic transformation in vitro. *International Journal of Radiation Biology*, 77(11):1081–10185, 2001.

AB. Robertson, A. Klungland, T. Rognes, and I. Leiros. Dna repair in mammalian cells: Base

excision repair: the long and short of it. *Cellular and Molecular Life Sciences : CMLS*, 66 (6):981–93, 2009.

R. Roots and S. Okada. Estimation of life ttime and diffusion distances of radicals involved in x-ray-induced dna sstrand breaks of killing of mammalian cells. *Radiation Research*, 64: 306–320, 1975.

JS. Roth, J. Bukovsky, and HJ. Eichel. The effect of whole-body x-irradiation on the activity of some acid hydrolases in homogenates and subcellular fractions of rat spleen. *Radiation Research*, 16:27–36, 1962.

I. Rundquist, M. Olsson, and U. Brunk. Cyto?uorometric quantitation of acridine orange uptake by cultured cells. *Acta Pathologica Microbiologica et Immunologica Scandinavica*, 92:303 – 9, 1984.

SW. Ryter, HP. Kim, A. Hoetzel, JW. Park, K. Nakahira, X. Wang, and AM. Choi. Mechanisms of cell death in oxidative stress. *Antioxidants and Redox Signalling*, 9(1):49–89, 2007.

J. Rzeszowska-Wolny, WM. Przybyszewski, and M. Widel. Ionizing radiation-induced bystander effects, potential targets for modulation of radiotherapy. *European Journal of Pharmacology*, 625(1-3):156–164, 2009.

P. Saftig. *Lysosomes*. Springer, 2005.

A. Sallmyr, J. Fan, and FV. Rassool. Genomic instability in myeloid malignancies: increased reactive oxygen species (ros), dna double strand breaks (dsbs) and error-prone repair. *Cancer Letters*, 270(1):1–9, 2008.

R. Saroya, R. Smith, C. Seymour, and C. Mothersill. Injection of resperpine into zebrafish, prevents fish to fish communication of radiation-induced bystander signals: confirmation in vivo of a role for serotonin in the mechanism. *Dose Response*, 8(3):317 – 30, 2009.

JR. Savage. Update on target theory as applied to chromosomal aberrations. *Environmental and Molecular Mutagenesis*, 22(4):198–207, 1993.

P. Schafer, IA. Cymerman, JM. Bujnicki, and G. Meiss. Human lysosomal dnase ii? contains

two requisite pld-signature (hxk) motifs: Evidence for a pseudodimeric structure of the active enzyme species. *Protein Science*, 16(1):82 – 91, 2009.

D. Schaue, EL. Kachikwu, and WH. McBride. Cytokines in radiobiological responses: a review. *Radiation Research*, 178(6):505–23, 2012.

R. Scully and A. Xie. Double strand break repair functions of histone h2ax. *Mutation Research*, 5107(13), 2013.

C. Settembre, A. Fraldi, DL. Medina, and A. Ballabio. Signals from the lysosome: a control centre for cellular clearance and energy metabolism. *Nature reviews: Molecular Cell Biology*, 14(5):283 – 96, 2013.

CB. Seymour and C. Mothersill. Relative contribution of bystander and targeted cell killing to the low-dose region of the radiation dose-response curve. *Radiation Research*, 153(5 Pt 1): 508–511, 2000.

V. Shahin, Y. Ludwig, C. Schafer, D. Nikova, and H. Oberleithner. Glucocorticoids remodel nuclear envelope structure and permeability. *Journal of Cell Science*, 118:2881 – 2889, 2005.

B. Shankar, R. Pandy, and K. Sainis. Radiation-induced bystander effects and adaptive response in murine lymphocytes. *International Journal of Radiation Biology*, 82(8):537–548, 2006.

C. Shao, M. Folkard, BD. Michael, and KM. Prise. Targeted cytoplasmic irradiation induces bystander responses. *Proceedings of the National Academy of Sciences of the United States of America*, 101(37):13495 – 13500, 2004.

HM. Shen and P. Codogno. Autophagic cell death: Loch ness monster or endangered species? *Autophagy*, 7(5):457 – 465, 2011.

S. Shimizu, T. Kanaseki, N. Mizushima, T. Mizuta, S. Arakawa-Kobayashi, CB. Thompson, and Y. Tsujimoto. Role of bcl-2 family proteins in a non-apoptotic programmed cell death dependent on autophagy genes. *Nature cell biology*, 6(12):1221 – 1228, 2004.

RE. Shore. Low-dose radiation epidemiology studies: status and issues. *Health Physics*, 97(5): 481–486, 2009.

P. Simpson, T. Morris, J. Savage, and J. Thacker. High-resolution cytogenetic analysis of x-ray induced mutations of the hprt gene of primary human fibroblasts. *Cytogenetics and Cell Genetics*, 64(1):39 – 45, 1993.

DE. Sleat, MC. Della Valle, H. Zheng, DF. Moore, and P. Lobel. The mannose 6-phosphate glycoprotein proteome. *Journal of Proteome Research*, 7(7):3010–3021, 2008.

LB. Smilenov, EJ. Hall, WM. Bonner, and OA. Sedelnikova. A microbeam study of dna double-strand breaks in bystander primary human fibroblasts. *Radiation Protection Dosimetry*, 122 (1-4):256–259, 2006.

SL. Snyder and SK. Eklund. Radiation-induced alterations in the distribution of lysosomal hydrolases in rat spleen homogenates. *Radiation Research*, 75(1):91–97, 1978.

MV. Sokolov, LB. Smilenov, EJ. Hall, IG. Panyutin, WM. Bonner, and OA. Sedelnikova. Ionizing radiation induces dna double-strand breaks in bystander primary human fibroblasts. *Oncogene*, 24(49):7257–7265, 2005.

MB. Sowa, W. Goetz, JE. Baulch, DN. Pyles, J. Dziegielewski, S. Yovino, AR. Snyder, SM. de Toledo, EI. Azzam, and WF. Morgan. Lack of evidence for low-let radiation induced bystander response in normal human fibroblasts and colon carcinoma cells. *International Journal of Radiation Biology*, 86(2):102–113, 2010.

C. Strasser, P. Grote, K. Schuble, M. Ganz, and E. Ferrando-May. Regulation of nuclear envelope permeability in cell death and survival. *Nucleus*, 3(6):540 – 51, 2012.

K. Tanaka, A. Kohda, T. Toyokawa, K. Ichinohe, and Y. Oghiso. Chromosome aberration frequencies and chromosome instability in mice after long-term exposure to low-dose-rate gamma-irradiation. *Mutation Research*, 657(1):19–25, 2008.

S. Tapio and V. Jacob. Radioadaptive response revisited. *Radiation and Environmental Biophysics*, 46(1):1–12, 2007.

IR. Telford and CF. Bridgman. *Introduction to functional histology.* Harper Collins College Publishers, 1995.

J. Temme and G. Bauer. Low-dose gamma irradiation enhances superoxide anion production by nonirradiated cells through tgf-?1-dependent bystander signaling. *Radiation Research*, 179 (4):422–32, 2013.

J. Thacker, EW. Fleck, T. Morris, BJF. Rossiter, and TL. Morgan. Localization of deletion points in radiation-induced mutants of the hprt gene in hamster cells. *Mutation Research*, 232:163 – 70, 1990.

KA. Toops and A. Lakkaraju. Let's play a game of chutes and ladders: Lysosome fusion with the epithelial plasma membrane. *Communicative & intergrative biology*, 6(4):e24474, 2013.

T. Tsukada, M. Watanabe, and T. Yamashima. Implications of cad and dnase ii in ischemic neuronal necrosis specific for the primate hippocampus. *Journal of Neurochemistry*, 79:1196 – 1206, 2001.

K. Valerie, A. Yacoub, MP. Hagan, DT. Curiel, PB. Fisher, S. Grant, and P. Dent. Radiation-induced cell signaling: inside-out and outside-in. *Molecular Cancer Therapeutics*, 6(3):789–801, 2007a.

K. Valerie, A. Yacoub, MP. Hagan, DT. Curiel, PB. Fisher, S. Grant, and P. Dent. Radiation-induced cell signalling: inside-out and outside-in. *Molecular Cancer Therapeutics*, 6(3):789 – 801, 2007b.

M. Valko, CJ. Rhodes, J. Moncol, M. Izakovic, and M. Mazur. Free radicals, metals and antioxidants in oxidative stress-induced cancer. *Chemico-Biological Interactions*, 160(1):1 – 40, 2006.

RS. Vasireddy, CN. Sprung, NL. Cempaka, M. Chao, and MJ. McKay. H2ax phosphorylation screen of cells from radiosensitive cancer patients reveals a novel dna double-strand break repair cellular phenotype. *British Journal of Cancer*, 102(10):1511–1518, 2010.

J. Veeraraghavan, M. Natarajan, S. Aravindan, TS. Herman, and N. Aravindan. Radiation-triggered tumor necrosis factor (tnf) alpha-nfkappab cross-signaling favors survival advantage in human neuroblastoma cells. *The Journal of Biological Chemistry*, 286(24):21588 – 600, 2011.

GE. Villalpando Rodriguez and A. Torriglia. Calpain 1 induce lysosomal permeabilization by cleavage of lysosomal associated membrane protein 2. *Biochimica Et Biophysica Acta*, 1833 (10):2244 – 53, 2013.

R. Wakeford. The cancer epidemiiology of radiation. *Oncogene*, 23(38):6404 – 6428, 2004.

SU. Walkley. Pathogenic mechanisms in lysosomal disease: a reappraisal of the role of the lysosome. *Acta Paediatrica*, 96:26–32, 2007.

G. E. Watson, S. A. Lorimore, S. M. Clutton, M. A. Kadhim, and E. G. Wright. Genetic factors influencing alpha-particle-induced chromosomal instability. *International Journal of Radiation Biology*, 71(5):497–503, 1997.

G. E. Watson, S. A. Lorimore, D. A. Macdonald, and E. G. Wright. Chromosomal instability in unirradiated cells induced in vivo by a bystander effect of ionizing radiation. *Cancer Research*, 60(20):5608–5611, 2000.

GE. Watson, SA. Lorimore, and EG. Wright. Long-term in vivo transmission of alpha-particle-induced chromosomal instability in murine haemopoietic cells. *International Journal of Radiation Biology*, 69(2):175–182, 1996.

GE Watson, DA Pocock, D Papworth, SA Lorimore, and EG Wright. In vivo chromosomal instability and transmissible aberrations in the progeny of haemopoietic stem cells induced by high- and low-let radiations. *International Journal of Radiation Biology*, 77:409–417, 2001.

H. Wei, SJ. Kim, Z. Zhang, PC. Tsai, KE. Wisniewski, and AB. Mukherjee. Er and oxidative stresses are common mediators of apoptosis in both neurodegenerative and non-neurodegenerative lysosomal storage disorders and are alleviated by chemical chaperones. *Human Molecular Genetics*, 17(4):469–477, 2008.

G. Weissman, H. Kaiser, and AW. Bernheimer. Studies on lysosomes iii. the effect of streptolysins o and s on the release of acid hydrolases from a granular fraction of rabbit liver. *Journal of Experimental Medicine*, 118:205, 1963.

N. Werneburg, ME. Guicciardi, XM. Yin, and GJ. Gores. Tnf-alpha-mediated lysosomal per-

meabilization is fan and caspase 8/bid dependent. *American Journal of Physiology. Gastrointestinal and Liver Physiology*, 287(2):G436–, 2004.

E. White and RS. DiPaola. The double-edged sword of autophagy modulation in cancer. *Clinical Cancer Research*, 15(17):5308 – 16, 2009.

D. Williams. Radiation carcinogenesis: lessons from chernobyl. *Oncogene*, 27 Suppl 2:S9–18, 2008.

LJ. Wu, G. Randers-Pehrson, A. Xu, CA. Waldren, CR. Geard, Z. Yu, and TK. Hei. Targeted cytoplasmic irradiation with alpha particles induces mutations in mammalian cells. *Proceedings of the National Academy of Sciences of the United States of America*, 96(9):4959–4964, 1999.

J. Xu, KA. Toops, F. Diaz, JM. Carvajal-Gonzalez, D. Gravotta, F. Mazzoni, R. Schreiner, E. Rodriguez-Boulan, and A. Lakkaraju. Mechanism of polarized lysosome exocytosis in epithelial cells. *Journal of Cell Science*, 125(Pt 24):5937 – 43, 2012.

T. Yamashima, TC. Saido, M. Takita, A. Miyazawa, J. Yamano, A. Miyakawa, H. Nishijyo, J. Yamashita, S. Kawashima, T. Ono, and T. Yoshioka. Transient brain ischaemia provokes ca2+, pip2 and calpain responses prior to delayed neuronal death in monkeys. *The European Journal of Neuroscience*, 8(9):1932 – 1944, 1996.

T. Yasuda, D. Nadano, S. Awazu, and K. Kishi. Human urine deoxyribonuclease ii (dnase ii) isoenzymes: a novel immunoaffinity purification, biochemical multiplicity, genetic heterogeneity and broad distribution among tissues and body fluids. *Biochimica Et Biophysica Acta*, 1119(2):185 – 93, 1992.

T. Yoshida, S. Goto, M. Kawakatsu, Y. Urata, and TS. Li. Mitochondrial dysfunction, a probable cause of persistent oxidative stress after exposure to ionizing radiation. *Free Radical Research*, 46(2):147 – 53, 2012.

M. Younes, M. Albrecht, and CP. Siegers. Interrelation between lipid peroxidation and lysosomal enzyme release in the presence of carbon tetrachloride, cumene hydroperoxide or thioac-

etamide. *Research Communications in Chemical Pathology and Pharmacology*, 40(1):121–132, 1983.

L. Yu, A. Alva, H. Su, P. Dutt, E. Freundt, S. Welsh, EH. Baehrecke, and MJ. Lenardo. Regulation of an atg7-beclin 1 program of autophagic cell death by caspase-8. *Science*, 304 (5676):1502 – 1502, 2004.

X. Zhang, S. Chen, S. Yoo, S. Chakrabarti, T. Zhang, T. Ke, C. Oberti, SL. Yong, F. Fang, L. Li, R. de la Fuente, L. Wang, Q. Chen, and QK. Wang. Mutation in nuclear pore component nup155 leads to atrial fibrillation and early sudden cardiac death. *Cell*, 135(6):1017 – 27, 2008.

H. Zhou, G. Randers-Pehrson, CA. Waldren, D. Vannais, EJ. Hall, and TK. Hei. Induction of a bystander mutagenic effect of alpha particles in mammalian cells. *Proceedings of the National Academy of Sciences of the United States of America*, 97(5):2099–2104, 2000.

H. Zhou, M. Suzuki, G. Randers-Pehrson, D. Vannais, G. Chen, JE. Trosko, CA. Waldren, and TK. Hei. Radiation risk to low fluences of alpha particles may be greater than we thought. *Proceedings of the National Academy of Sciences of the United States of America*, 98(25): 14410–14415, 2001.

H. Zhou, I. Vladimir, G. Joseph, CR. Geard, SA. Amundson, DJ. Brenner, Z Yu, HB. Lieberman, and TK. Hei. Mechanism of radiation-induced bystander effect: role of the cyclooxygenase-2 signaling pathway. *Proceedings of the National Academy of Sciences of the United States of America*, 102(41):14641–14646, 2005.

H. Zhou, VN. Ivanov, Y. Lien, M. Davidson, and TK. Hei. Mitochondrial function and nuclear factor-kappab-mediated signaling in radiation-induced bystander effects. *Cancer Research*, 68(7):2233–2240, 2008.